University of Stavanger

FACULTY OF SCIENCE AND TECHNOLOGY

MASTER'S THESIS

Study programme/specialisation: Petroleum Engineering/Natural gas	Spring semester, 2020 ~~Open~~ / Confidential
Author: Hans Christian Walker	Hans Ch. Walker (signature of author)
Faculty supervisor: Assoc. Prof. Anton Shchipanov (UiS) External supervisor: Harald Selseng (Lundin)	
Title of master's thesis: **Study of Well Communication from Analysis of Pressure Transients**	
Credits: 30	
Keywords: Interference analysis Time-lapse PTA Multiple wells analysis Reservoir characterization	Number of pages…67… Stavanger. 15 July 2020

Summary

On 5th October 2019, one of the largest oil fields discovered in recent years on the Norwegian continental shelf started its production from the Utsira high formation. The field is called Johan Sverdrup and is considered pivotal not just for the partners involved, but for the whole Norwegian petroleum industry when it comes to creating jobs and revenue. Since the field has just started to produce and because of its geological structure and size, there are some uncertainties regarding sand thickness and permeability. Papers published on the field reported permeability ranged from 1 to 70 Darcy because the rock is made up of unconsolidated sand. It is important to estimate these two properties applying different methods because they are important for evaluating how much hydrocarbons the field will produce in the future. Seismic data from the field indicate there are many faults present in the reservoir, yet there has been observation of communication between faults. Drill Stem Tests (DST) from exploration wells may also indicate communication across the faults. One way to estimate properties of the reservoir along with identifying characteristics of the faults is by analysing all pressure transient data available for the field. This includes initial well tests such as DSTs, specially designed and performed well interference tests during production and reviewing the variety of pressure transient data available for production and shut-in periods as measured by Permanent Downhole Gauges. Pressure Transient Analysis (PTA) is the tool to address all the data.

The purpose of this thesis is to investigate what values of permeability and sand thickness we can obtain by interpreting different pressure transients. In our study, the interference test interpretation is the starting point providing base-line values for permeability and pay thickness as well as cross-fault leakage. DST interpretation is used for verifying these values and time-lapse PTA is employed to see the applicability of these values in reproducing the whole history of production, where well interference becomes the driving factor for pressure transient responses. In addition, these PTA methods are used to identify boundaries like faults dividing the field into compartments, and their flowing conditions (sealing or conductive faults). It was observed in the thesis that neighboring wells had an impact on the interference tests and had to be taken into account in the analyses. Furthermore, geological data are integrated into the analysis to see if the results obtained are sensible in relation to reported data. Observation from the interference analysis and time-lapse PTA indicates that the area of interest has a sand thickness around 29-30 meters and a range of permeability from 27D to 34D. A leakage factor for the fault in focus at 0.25 was identified with interference tests. The time-lapse PTA with a numerical reservoir model with multiple wells was able to match most of the transient periods

of the wells. This indicates that there is communication between the wells and the reservoir model integrates major reservoir features like faults in the area of interest. However, the model is only limited to the northern part of the reservoir providing some mismatch of the observations. A further study with added wells from south is recommended. Finally, two compressibility values were looked into to see which one best matched the pressure responses along with being aligned with other geological data sources.

Acknowledgments

List of Figures

List of Tables

Nomenclature

B= formation volume factor

c= compressibility

C_s= wellbore storage constant

C_t= total compressibility

d_D= dimensionless distance

D= diffusivity ratio

h= sand thickness

k= permeability

k_H= horizontal permeability

k_s= permeability of the skin area

k_V= vertical permeability

L= fracture half-length

L_h= length of horizontal observation well

m= value of slope

M= mobility ratio

$\vec{n}$= direction of pressure diffusion

p= pressure

p_i= initial pressure

p_{wf}= pressure inside wellbore

p_{BU}= shut-in pressure

p_{DD}= flowing pressure

q= flowrate

q_S= flow rate at surface level

q_{SF}= flow rate at sand face

r= radius

r_d= ratio of the distance between source well and observation well against length of observation well.

r_s= the radius of the skin area

r_w= radius of well

r_D= dimensionless radial

S= Skin

S_w= wellbore mechanical skin

S_z= partial penetration effect

S_{zT}= pressure drop due to convergence of flow lines

t= time

t_p= production time

t_D= dimensionless time

V= wellbore volume

z_w= well location in formation thickness

μ= viscosity

ρ= density

ϕ= porosity

Abbreviations

BU= Build up

DD= Drawdown

DST= Drill Stem Test

kh= permeability thickness product

PTA= Pressure Transient Analysis

WBS= Wellbore storage

Table of content

Chapter 1   Introduction

In this chapter, I will first introduce what Pressure Transient Analysis (PTA) is and why it is important to conduct this sort of analysis. Then the thesis objective will be introduced and finally an outline will be presented.

1.1   What is PTA?

Pressure transient analysis is a way to characterize and estimate the parameters of a reservoir by analyzing the pressure behavior from the bottom of the well. In addition, it is also used for estimating well damage / stimulation or skin factor. When looking into the pressure and the pressure derivative, we use certain equations or apply different models to match the trend of pressure and the derivative. It is a parameter estimation technique where one or more parameters of a differential equation are calculated from a measured solution (Stewart, 2011). Previously, the way to acquire pressure data was to use wireline tools and record the pressure while producing at a rate. This was a costly and a lengthy process because to take a test, it required the production well to shut-in and lower down tools into the well. Now days using modern methods, it is more common today to have permanent pressure gauges down at the bottom hole to acquire the data. There is thus no need to stop the production and lowering down wireline for taking a test. Another modern technique to acquire pressure data is by drill stem testing. Pressure and rates are recorded while drilling a new well. This is very common to do when companies are apprising a reservoir they recently have discovered.

1.2   Why do we need PTA?

PTA is a very useful analysis when looking into the dynamic part of a reservoir. As mention above in regard to characteristics, it is important to have an indication on what boundaries / restrictions exist, and how high the permeability and sand thickness of the reservoir is. When a case is identified and it matches with recorded geological data, then the company can begin to deduct how the flow pattern behaves in the reservoir and create an optimal drainage strategy. Furthermore, PTA during the production stage helps to identify and calculate skin or identify completion-related damage or effect from previous stimulation, thereby, helping the decision makers to optimize well stimulation and performance (Chaudhry, 2004).

1.3   Objective

The objective of this thesis is to apply PTA interpretation techniques on an oil field in the Norwegian continental shelf. The goals of the PTA can be summarized as follows :

- Analysis of field case: wells in focus.
- Analysis of time-lapse pressure transients from horizontal wells.
- Segment simulations and history matching of the segment history, testing of concepts on different reservoir features.
- Integration of the PTA results into a 3D reservoir simulation.

First, the interference tests from production wells will be analysed. Then the results will be compared with a couple of DSTs and time-lapse PTA. Why this is done is because it is important to have an overview of what range of values we get from the results with properties ,and to clarify what boundaries are in the reservoir. The time-lapse PTA will only be done with the horizontal production wells. Both analytical and numerical models where created to achieve results that was realistic representation of the investigated area, but only final results will be presented. All this is done to achieve two main goals, what is the property values at a certain part of the reservoir. What type boundaries are most likely to be present there.

1.4   Outline

First the thesis will go through basic theory of PTA. The thesis will explain the fundamentals of pressure build up, flowing and interference analysis, how they are applied, which differential equation is used, and their strengths and weaknesses.

Then the results from the analysis will be presented and there some description on observations, what results where relevant and comparisons. Then in the next chapter there will be discussions about the methodology of the analysis, its results in an overall context and how applicable this work is. Finally, a conclusion will be presented.

Chapter 2   Theory

When analyzing pressure transients in wells, there are usually two important measurements of interest. The pressure increase / decrease from the initial pressure to the end of defined time and the pressure derivative (how the pressure changes during the period). These two measurements provide an indication and valuable information about the reservoir. In PTA, certain analysis for particular well completion and reservoir features has its own differential equations and form of visualizing (for example special plots like semi-log). In addition, a pressure shut-in response is analysed differently from a pressure flowing response. A such, it needs its own set of equations, both for calculating and visualizing the pressure responses and estimating different characteristics.

Throughout the years of well testing, many differential equations have been developed and used to identify pressure responses. However, the thesis will go through the basic and the most general differential equations for pressure buildups, flowing and interference testing. In *Figure 1*, we can see two of the main pressure transient analysis techniques, flowing and shut-in.
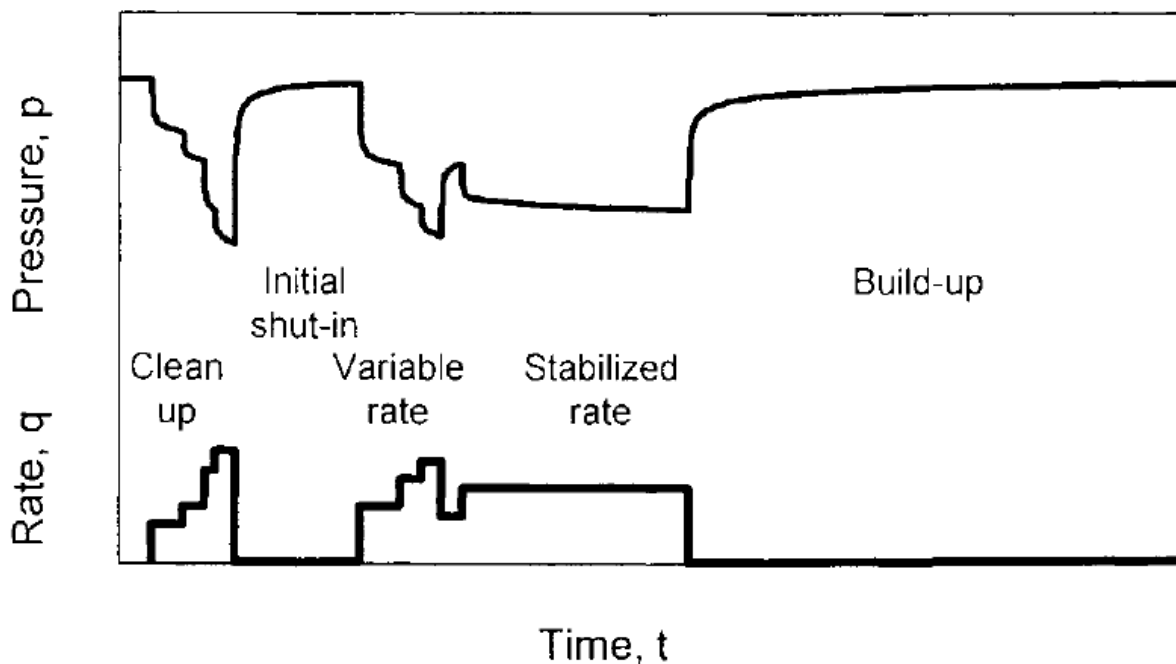
Figure 1 Illustration on bottom hole pressure response on different (Bourdet, 2002).

2.1 Basic flow equations

One of the fundamental parts in PTA is the diffusivity equation. Most of the derived differential equations in PTA comes from this equation. Diffusivity equation simply explains how the pressure reacts in time as a function of the local pressure gradient in the rock (kappa book). Assumptions for this equation are (Houzé, Viturat, & Fjaere, 2011):

- Homogenous reservoir and isotropic
- Single phase and slightly compressible fluid
- Gravity effects are ignored
- Darcy law
- Reservoir and fluid properties are independent of pressure, except for porosity. A reference porosity (porosity value at a certain pressure) is used in calculations.

By combining the principle of conservation of mass, darcy's law, slightly compressible fluid equations and isothermal flow, we derive the nonlinear diffusive equation for an infinite acting radial flow (Chaudhry, 2004):

$$\frac{1}{r}\frac{\partial}{\partial r}\left(\frac{k\rho}{\mu}r\frac{\partial p}{\partial r}\right) = \phi c\rho \frac{\partial p}{\partial t} \dots\dots\dots\dots\dots\dots\dots\dots\dots\dots\dots\dots\dots\dots\dots (1)$$

where r is the radius, p is pressure k is permeability, ρ is density, c is compressibility, t is time and ϕ is porosity at reference pressure. By linearizing it, the derivation gives:

$$\frac{\partial^2 p}{\partial r^2} + \frac{1}{r}\frac{\partial p}{\partial r} = \frac{\phi\mu C_t}{0.000355k} \cdot \frac{\partial p}{\partial t} \dots\dots\dots\dots\dots\dots\dots\dots\dots\dots\dots\dots\dots\dots (2)$$

where $\frac{\phi\mu C_t}{0.000355k}$ is the hydraulic diffusivity, μ is fluid viscosity and C_t is total compressibility of the fluid and pore volume.

When calculating the equation, it is important to define initial conditions, well conditions (inner conditions) and outer boundary conditions (Houzé, Viturat, & Fjaere, 2011). Setting up initial conditions usually starts with a reference time zero and the reservoir is in a uniform pressure (p_i) state. In numerical simulations however, there is the possibility to make the initial conditions with a dynamic pressure to simulate. With well conditions, the simplest form of set up is using darcy's law at the sand face (Houzé, Viturat, & Fjaere, 2011):

$$\left[r\frac{\partial p}{\partial r}\right]_{r_w,t} = 18.66\frac{qB\mu}{kh} \dots\dots\dots\dots\dots\dots\dots\dots\dots\dots\dots\dots\dots\dots (3)$$

q is the flowrate, B is the formation volume factor, and h is sand thickness. For more complex modeling a PVT equation is required to calculate their dynamic properties. In addition, wellbore storage and skin factor are also important properties in the well condition. This is explained in detail later in the chapter. With some modifications, the darcy's equation can also correspond to other complex well geometries like fractured or horizontal wells.

The last and important conditions are the boundaries. It is important to accurately identify these conditions to be able to correctly estimate the properties of a reservoir. The simplest form of boundary condition is infinite reservoir (no boundary (Houzé, Viturat, & Fjaere, 2011):

$$\lim[p(r,t)]_{r\to\infty} \dots\dots\dots\dots\dots\dots\dots\dots\dots\dots\dots\dots\dots\dots\dots\dots\dots\dots\dots\dots \text{(4)}$$

The infinite reservoir assumption has however limited applications due to the fact that faults and aquifer are usually present in a reservoir and act as boundaries. So, it is important to identify with geological data what is present in the reservoir. Depending on what form of boundaries are acting on the flow, different versions of the diffusivity equation will be used, or be relevant for well and reservoir features. The most common deviations from the radial flow equation are (Chaudhry, 2004):

- Linear flow: $\frac{\partial^2 p}{\partial x^2} = \frac{\phi \mu C_t}{0.00035k} \cdot \frac{\partial p}{\partial t}$ $\dots\dots\dots\dots\dots\dots\dots\dots\dots\dots\dots\dots$ (5)

- Radial flow: $\frac{1}{r}\frac{\partial}{\partial r}\left(r\frac{\partial p}{\partial r}\right) = \frac{\phi \mu C_t}{0.00035k}\frac{\partial p}{\partial t}$ $\dots\dots\dots\dots\dots\dots\dots\dots\dots\dots\dots$ (6)

- Spherical flow: $\frac{1}{r^2}\frac{\partial}{\partial r}\left(r^2\frac{\partial p}{\partial r}\right) = \frac{\phi \mu C_t}{0.00035k}\frac{\partial p}{\partial t}$ $\dots\dots\dots\dots\dots\dots\dots\dots\dots\dots$ (7)

Therefore, it is important to identify what boundaries are most likely present, to be able to conduct the right form of equation on the flow type.

2.1.1 Wellbore storage

Whenever a well is under producing or injecting fluids, the valve that controls the well is normally not at sand face level (Houzé, Viturat, & Fjaere, 2011). In fact, the control valve is frequently at the surface level. When the valve is closing or adjusting, the flow of fluids in the well are reacting first and before the fluid flow in the sand face. In the case of opening a closed well, the decompressed fluid in the well is producing first before the fluid in the reservoir. Both situations create a time lag (transition time) between the surface and the sand face (Houzé, Viturat, & Fjaere, 2011). This is called wellbore storage. The expansion factor for fluids in the well is described by (Stewart, 2011):

$$C_s = cV \dots\dots\dots\dots\dots\dots\dots\dots\dots\dots\dots\dots\dots\dots\dots\dots\dots\dots\dots\dots\dots\dots\dots \text{(8)}$$

where C_s is wellbore storage constant, c is fluid compressibility and V is the wellbore volume. With the constant wellbore storage, we can derive an equation that describes the flow at sand face level by the rate at surface plus the C_s factor (Stewart G. , 2011):

$$q_{SF} = q_S B + C_s \frac{dp_{wf}}{dt} \dots\dots\dots\dots\dots\dots\dots\dots\dots\dots\dots\dots\dots\dots\dots\dots\dots\dots (9)$$

where q_{SF} is the flow rate at sand face, q_S is flow rate at surface level, B is volume factor of liquid and p_{wf} is pressure inside the wellbore. It should be mentioned that this equation is valid in situations where the wellbore fluids do not experience drastic changes because of compressibility. If there is a situation where the wellbore fluids have a dynamic compressibility like in a gas well or an oil well below the bubble point, then a different approach has to be taken, by using time related PVT correction or a numerical pressure dependent storage model to account for the dynamic wellbore storage (Houzé, Viturat, & Fjaere, 2011).

2.1.2 Skin

Skin effect is a parameter to account for the difference of well performance in an ideal case and actual well performance which has changed due to near wellbore damage or stimulation (Houzé, Viturat, & Fjaere, 2011). Main causes for positive skin (well damage) are (Schlumberger, 2002):

- Flow convergence near the wellbore.
- Visco-inertial flow.
- Blocking of pores and fracturs that occurs under production and drilling.

Positive skin creates an additional pressure drop while negative skin enhances flow, thereby increasing the pressure at the well foot. ***Figure 2*** shows us how the skin effects the pressure based on distance from well.

Non damaged skin = 0   Damaged Skin > 0   Stimulated Skin < 0
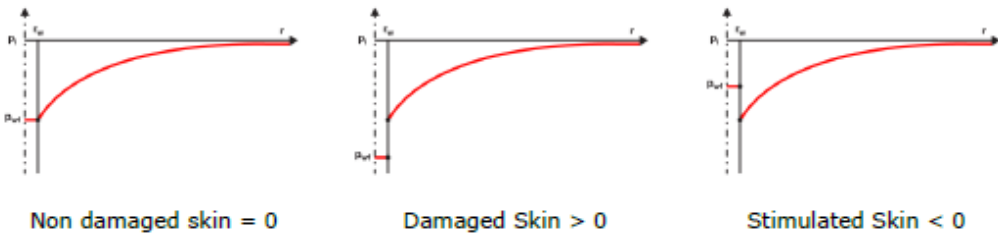
Figure 2 Illustration on the effect of skin (Bourdt, 2002).

The equation for describing the pressure drop in a reservoir due to skin (Larson, 2010)

$$\Delta p_{Skin} = 18.66 \frac{q\mu}{kh} S \dots\dots\dots\dots\dots\dots\dots\dots\dots\dots\dots\dots\dots\dots\dots\dots\dots\dots (10)$$

where S in this equation represent skin. To model the positive skin effect in the reservoir, an equivalent composite reservoir equation is proposed (Bourdet, 2002) :

$$S = \left(\frac{k}{k_s} - 1\right) \ln \left(\frac{r_s}{r_w}\right) \dots\dots\dots\dots\dots\dots\dots\dots\dots\dots\dots\dots\dots\dots\dots\dots\dots\dots\dots\dots \text{ (11)}$$

where r_w is the radius of the well, k_s is the permeability of the skin area and r_s is the radius of the skin area.

2.2 Pressure flowing

Pressure flowing analysis refers to reservoir response during a production period. The idea is that in an ideal situation the well operator manages to produce at a constant rate for a lengthy time period, the responses in the derivative and in the flowing (pressure decrease) data gives an accurate estimation of reservoir properties, along with identification of boundaries. It is considered that the initial production period of a well is the best source of data and particularly flowing data (Stewart, 2011). *Figure 3* shows an ideal pressure flowing test.
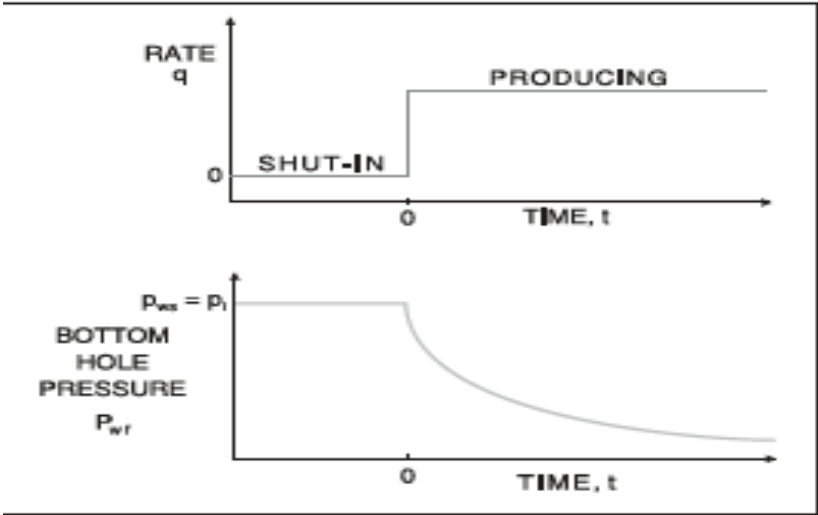
Figure 3 Illustration of a pressure flowing (Stewart, 2011).

One of the challenges with the pressure flowing analysis is getting a constant rate of production during a long period. Normally that is very rare to achieve because several factors can lead to unstable rates. Therefore, whenever it is possible flowing data should be collected. One main advantage of flowing analysis however, is it can estimate the reservoir volumes with no loss in production (Stewart G. , 2011).

The equation for bottom hole pressure during a constant production period in an infinite acting reservoir (Bourdet, 2002):

$$p_{wf} = p_i - \frac{21.5qB\mu}{kh} * \left[\log(\Delta t) + \log\left(\frac{k}{\varphi\mu c_t r_w^2}\right) - 3.10 + 0.87S\right] \dots\dots\dots\dots\dots\dots\dots\dots \text{ (12)}$$

Where p_i is the initial pressure of the reservoir, and S represents skin factor and wellbore storage. This equation changes as different boundaries occur.

2.3 Pressure shut-in

One of the most widely used forms of PTA is the pressure shut-in analysis (Stewart, 2011). Originally, groundwater hydrologists were the first one to introduce this form of testing, but it is now used extensively in the oil industry. The idea is to shut-in an appraisal / production well after a production period, and then record the pressure shut-in from the moment the well is shut. *Figure 4* illustrates an ideal pressure shut-in test.
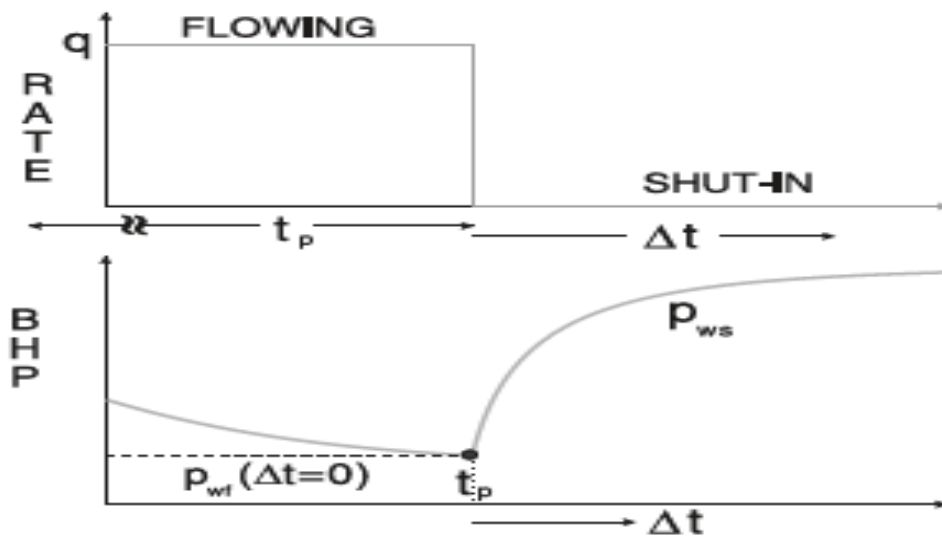
Figure 4 Illustration of pressure shut-in test (Stewart, 2011).

Prior to the shut-in, it is important that the flow rate is stabilized. If there is large variation before the shut-in, the shut-in analysis will be disturbed, and the estimated values of the analysis will be inaccurate.

One of the most popular methods for analyzing pressure shut-ins is the Horner method (Bourdet, 2002):

$$p_{wf} = p_i - \frac{21.5qB\mu}{kh} * \left(log\left(\frac{t_p\Delta t}{t_p+\Delta t}\right) + log\left(\frac{kt}{\varphi\mu c_t r_w^2}\right) \text{-3.10+0.87S}\right) \dots\dots\dots\dots\dots\dots\dots\dots (13)$$

where the $\frac{t_p\Delta t}{t_p+\Delta t}$ is superposition of time. t_p is production time and Δt is running shut-in time.

Usually, this analysis is very robust when it comes to estimate kh and skin as long as there is no interference. However, much like flowing this equation would change in the presence of reservoir boundaries (like faults of aquifers).

2.3.1 Superposition in time

The diffusivity equation in radial flow theory is based on an idealized case of a single well operating on a constant rate in infinite (Stewart, 2011). However, the assumption is questionable because the reservoir system usually has several wells operating at different rates. A more general approach is required. Since the diffusivity equation is linear, we can apply the principals of superposition in time to handle disturbance with varying rates from the well and other wells. One of the main principles is "*If a linear combination of solutions honors the diffusion equation and the different flux and boundary conditions at any time, then it is THE solution of the problem.*" (Houzé, Viturat, & Fjaere, 2011). The superposition is used in pressure build up analysis for converting the diffusivity equation that is meant for flowing to shut-ins. The superposition time becomes as in equation 13: $\frac{t_p \Delta t}{t_p + \Delta t}$. Overall, the difference between the last flowing pressure and current pressure at shut-in becomes (Bourdet, 2002):

$$\Delta p_{BU}(\Delta t) = \Delta p_{DD}(t_p) + \Delta p_{DD}(\Delta t) - \Delta p_{DD}(t_p + \Delta t) \dots\dots\dots\dots\dots\dots\dots\dots (14)$$

where p_{BU} is the shut-in pressure and p_{DD} is flowing pressure.

2.4   Interference

Interference testing is a form in multiple well analysis and it is used to identify if two wells are in pressure communication (Chaudhry, 2004). It is considered as one of the oldest and simplest forms of well testing analysis (Houzé, Viturat, & Fjaere, 2011). It requires minimum of two wells where one of them is an observation well and the other an active well. However, it is possible to have several wells in an interference testing scenario (kappa book), but at least one well has to be an observation point. The idea is that both well are in a long production period with stabilized pressures. Then the active well is changing its rate and creates a disturbance with the observation well (Schlumberger, 2002). This disturbance of the observation will provide valuable information about the reservoir. To present the data from the interference, a line source equation is used (Larson, 2010):

$$p(r,t) = p_i - \frac{18.66qB\mu}{kh} p_D(r_D, t_D)] \dots\dots\dots\dots\dots\dots\dots\dots\dots\dots\dots\dots\dots\dots\dots (15)$$

r_D is the dimensionless radial distance to the second well and t_D is time of production in dimensionless form. One thing to be aware in an interference is that there is a time delay for the observation when the active well is changing its rate. Determining the time lag are the parameters; $\frac{\phi \mu c_t}{k}$. These are called the *diffusivity coefficient.* For the pressure amplitude, these

parameters are the dominant factors; $\frac{kh}{\mu}$. These are called the *transmissivity or flow capacity* (Houzé, Viturat, & Fjaere, 2011).

The equation above is ideal for vertical wells, but horizontal wells presents more difficulties. When doing an interference test with vertical wells, the observation point is at the end point where pressure diffuses to. However, for horizontal wells the observation point might vary because of the horizontal length of the well. In addition, location and orientation of the well could also have an impact on the interference analysis. To make the equation above applicable to horizontal wells, the distance between the wells must be large enough so that the wells are considered as points. The minimum distance for an accurate well interference has to have the r_d ratio larger than 3 (Al-Khamis, Ozkan, & Raghavan, 2005) and the equation is as follows:

$$r_d = \frac{2r}{L_h} \dots\dots\dots\dots\dots\dots\dots\dots\dots\dots\dots\dots\dots\dots\dots\dots\dots\dots\dots\dots\dots\dots\dots\dots\dots\dots (16)$$

where the r is the radial distance between the wells, and L_h is the length of the horizontal observation well.

2.5 Boundaries

As mentioned earlier in basic flow theory, boundaries are an important factor in PTA. One of the main goals of well testing is to identify what boundaries are present in the reservoir. Since there are numerous and different forms of boundaries, this subchapter only focuses on the boundaries that are observed in the field case.

2.5.1 Sealing fault (no flow boundary)

The physical definition of a no flow boundary is that no fluids manage to pass through the boundary. Typical examples of such a boundary is when a fault is happening, and it fills/smear the rock next to it as it moves, making it seal off a part of the reservoir. Another is when a large throw happens and there is shale on top. The shale gets repositioned between two areas of sand and creates a barrier between them. In terms of mathematics, the boundary condition is described as (Houzé, Viturat, & Fjaere, 2011):

$$[\frac{\partial p}{\partial \vec{n}}]_\Sigma = 0 \dots\dots\dots\dots\dots\dots\dots\dots\dots\dots\dots\dots\dots\dots\dots\dots\dots\dots\dots\dots\dots\dots\dots\dots\dots\dots (17)$$

where $\vec{n}$ is the direction of pressure diffusion. The equation tells us that when the pressure diffuses to the no flow boundary orthogonality, pressure profile flattens (Houzé, Viturat, & Fjaere, 2011). In a loglog plot, the derivative starts to have an increase when the pressure

disturbance hits the fault and then it stabilizes on a new level. ***Figure 5*** show us in an ideal setting of such a situation.
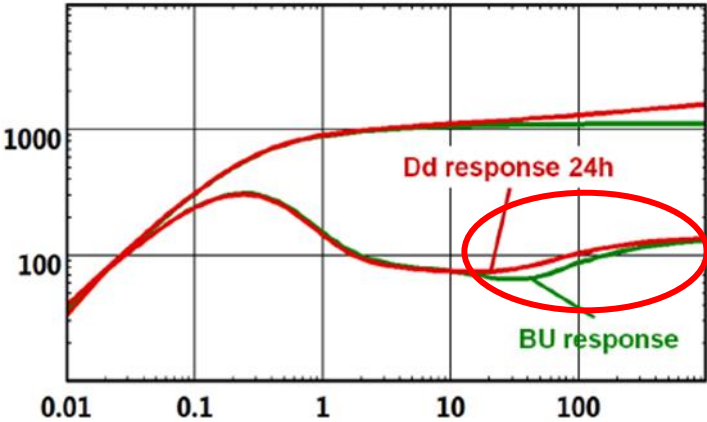
Figure 5 A visualization on a sealing fault response on the pressure derivative (Houzé, Viturat, & Fjaere, 1988).

An interesting note, one can see that the pressure shut-in response has a much sharper incline then the flowing when the pressure changes hits at contact with the fault. The derivative equations that quantifies the effect on bottom hole pressure is by (Larson, 2010):

$$\Delta p = \frac{18.66qB\mu}{kh}[p_d(r_{1D}, t_D) + p_d(r_{2D}, t_D)] \dots\dots\dots\dots\dots\dots\dots\dots\dots\dots\dots\dots (18)$$

r_D in this situation is the distance to fault in a dimensionless form. In the equation, a second imaginative well is defined to be able to capture the effect from a no flow boundary. (Larson, 2010)

2.5.2 Constant pressure boundaries

A constant pressure boundary is an area where there is ample amount of pressure support that keeps the pressure around the boundary constant (Houzé, Viturat, & Fjaere, 2011). Normally the boundaries hold the pressure to the initial reservoir pressure and the equation that describe this is (Houzé, Viturat, & Fjaere, 2011):

$$[p]_\Sigma = p_i \dots\dots\dots\dots\dots\dots\dots\dots\dots\dots\dots\dots\dots\dots\dots\dots\dots\dots\dots\dots\dots\dots (20)$$

The typical constant pressure boundaries are aquifers on the sides of the reservoirs, but gas caps and large underlying aquifers can also act as a constant pressure boundary (Stewart, 2011). For the loglog plot, the signature of a constant pressure boundary is that the derivative makes a dip at the end. This goes for both pressure flowing and shut-in. The speed of the dip depends on the

geometry of the boundary (Houzé, Viturat, & Fjaere, 2011). *Figure 6* and *Figure 7* illustrates how constant pressure boundaries affects the derivative in flowing and the shut-in.
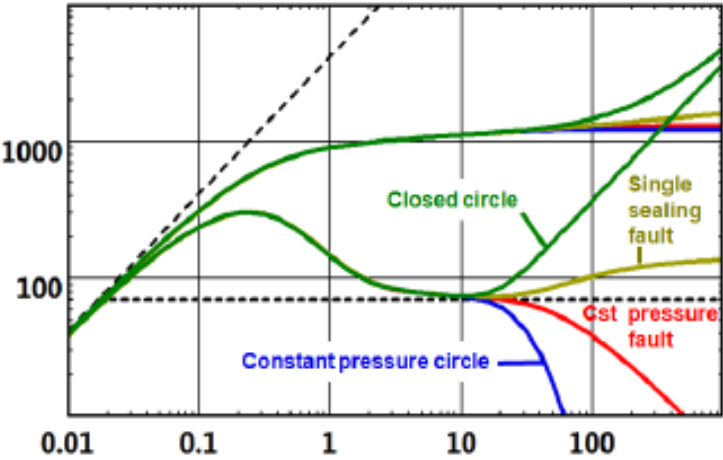
Figure 6 Pressure flowing responses to different boundaries (Houzé, Viturat, & Fjaere, 1988).
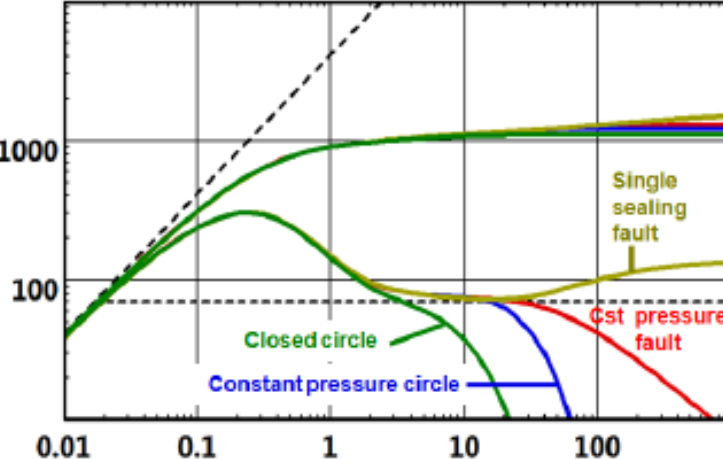
Figure 7 Pressure shut-in responses to different boundaries (Houzé, Viturat, & Fjaere, 1988).

As one can observe in *Figure 7*, the derivative for a shut-in will fall when a closed circular boundaries or a constant pressure boundaries is present. While the flowing in the derivative increases when there is a closed system present and decreases when it is a constant pressure circle instead. In one of the papers by (Shchipanov, Berenblyum, & Kollbotn, 2014), they too noted the importance of looking into both shut-ins and flowing data for a producer, and the fall-offs and injections data by an injector . By comparing both forms of analysis one can obtain a more complete picture of boundaries around the well and a more accurate estimate on reservoir parameters (Shchipanov, Berenblyum, & Kollbotn, 2014). In *Figure 8,* we see a case from an

injector where the fall-off data shows presence of boundary at late stage, while the injection data does not indicate any boundary.
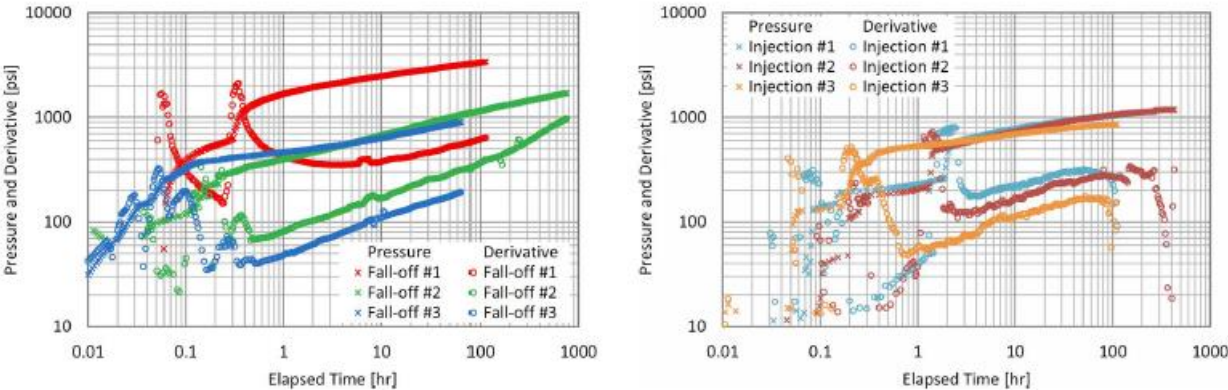
Figure 8 Comparison of fall-off and injection data from an injector (Shchipanov, Berenblyum, & Kollbotn, 2014).

This is an important observation because it shows when there is supposition of a constant boundary in the reservoir, it is important to look at both the flowing and the shut-in test to see if there is constant pressure or if there is a closed boundary instead. In one of the wells in the field case, such a comparison was possible because of good flowing data. The equation for constant pressure boundary (Larson, 2010):

$$p_{wf} = p_i - \frac{m}{1.151}(S + \ln 2d_D - \frac{d_D^2}{t_D}) \quad \text{......................} \quad (21)$$

$$\frac{d_D^2}{t_D} = (-\frac{d_D^2}{t_D})\frac{d}{dlnt_d} \quad \text{.................................} \quad (22)$$

m is the value of the slope and d_D is the dimensional distance to the boundary

2.5.3 Conductivity boundaries

Conductive boundaries are considered as faults or a skin zone area where the reservoir properties are different on either side. Yet, the two sides are still in pressure communicating with each other. Depending on what values are on either side of the fault, the pressure derivative will increase or decrease as the properties change from on area to another. The equations to describe this transition are (Houzé, Viturat, & Fjaere, 2011):

$$M = \frac{(k/\mu)_{Well\,side}}{(k/\mu)_{Other\,side}} \dots\dots\dots\dots\dots\dots\dots\dots\dots\dots\dots\dots\dots\dots\dots\dots\dots\dots\dots\dots.. \quad (23)$$

which is the mobility ratio and:

$$D = \frac{(k/\varphi\mu c_t)_{Well\,side}}{(k/\varphi\mu c_t)_{Other\,side}} \dots\dots\dots\dots\dots\dots\dots\dots\dots\dots\dots\dots\dots\dots\dots\dots\dots\dots\dots\dots. \quad (24)$$

which is the diffusivity ratio.

It should be noted that in practice, a reservoir can contain several different types of boundaries. As such, when doing an analysis, we combine several of these equations for each boundary into the model to capture the responses of the derivative. In numerical, the model is based on one equation that considers all boundaries present in a finite volume. It is important to understand how different boundaries affect the derivative, both in pressure flowing and shut-in so a realistic model can be provided. It is also important to compare not only flowing and shut-ins with each other, but also with other geological data to strengthen the case that is proposed.

2.6 Radius of investigation

Radius of investigation is the relation between time and distance for the pressure disturbance at a given mobility. The general equation for this relationship is (Bourdet, 2002):

$$r_i = 0.029\sqrt{\frac{kt}{\varphi\mu c_t}} \dots\dots\dots\dots\dots\dots\dots\dots\dots\dots\dots\dots\dots\dots\dots\dots\dots\dots\dots\dots.\dots \quad (25)$$

However, flowings and pressure shut-ins have their own radius of investigation equations, but with minor tweaks. They are overall the same. By combining radius of investigation with external geographical and geological data, we can have a rough idea what form of boundaries are impacting on the bottom hole pressure. In addition, by using the boundary distances as a reference point, we can estimate what the permeability must be to comply with the distances. However, one should approach this relationship with caution (Houzé, Viturat, & Fjaere, 2011).If the reservoir is heterogeneous and/or the reservoir is complex, then the equation will

be inaccurate. Accordingly, it is important to use this relationship for a reservoir system where there is not so high complexity.

2.7 Horizontal wells

With advances in drilling and completion technology, the horizontal well design is considered as one of the most preferable choice when it comes to reservoir development, largely because of its higher sweep efficiency and recovery factor than vertical wells (Shchipanov, Kollbotn, & Prosvirnov, 2017). However, horizontal wells prove challenging for PTA interpretation since several flow regimes are happening during a pressure development. In addition, many horizontal well are usually longer than the inter-well spacing, which will prevent late radial flow because of disturbance of nearby wells (Shchipanov, Kollbotn, & Prosvirnov, 2017).

In most cases, a horizontal well has an upper and lower sealing boundary nearby. When a flowing or shut-in is occurring for a horizontal production well, the upper and lower boundary affects the flow line geometry along with other boundaries horizontally of the well. In an infinite system, a horizontal well will produce three flow regimes in the following order at the start of an pressure development (Bourdet, 2002):

- Radial flow in a vertical plane
- Linear flow
- Radial flow in a horizontal plane

Figure 9 shows an illustration how the flow patterns develops for a horizontal well in an infinite system.
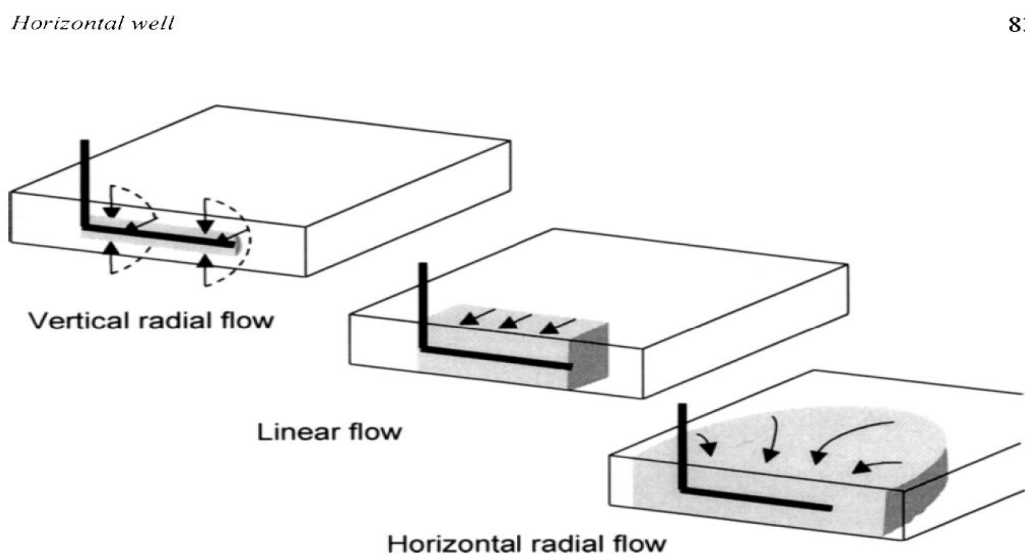
Figure 9 Illustration of flow patterns for a horizontal well (Bourdet, 2002).

One thing to be aware of however, is that horizontal wells have a large wellbore storage effect. This may mask the first flow regime in a pressure development (Bourdet, 2002). As a result of being horizontal and three flow regimes occurring during pressure development, new equations are implemented to capture all the effects in the flow regimes (Bourdet, 2002):

Radial flow in vertical plane:

$$\Delta p = \frac{21.49qB\mu}{2\sqrt{k_V k_H}L} * [\log\left(\frac{\sqrt{k_V k_H}\Delta t}{\varphi\mu c_t r_w^2}\right) \text{-}3.10 + 0.87S_w - 2log\frac{1}{2}\left(\sqrt[4]{\frac{k_V}{k_H}} + \sqrt[4]{\frac{k_H}{k_V}}\right)]\dots\dots\dots\dots\text{ (26)}$$

Linear flow:

$$\Delta p = \frac{1.246qB}{2Lh} * \sqrt{\frac{\mu\Delta t}{\varphi c_t k_H}} + \frac{18.66qB\mu}{2\sqrt{k_V k_H}L}S_w + \frac{18.66qB\mu}{k_H h}S_z\dots\dots\dots\dots\dots\dots\dots\dots\dots\dots\dots\text{ (27)}$$

Horizontal radial flow:

$$\Delta p = \frac{21.49qB\mu}{k_H h}[log\frac{k_H\Delta t}{\varphi\mu c_t L^2}\text{-}2.40] + \frac{18.66qB\mu}{2\sqrt{k_V k_H}L}S_w + \frac{18.66qB\mu}{k_H h}S_{zT}\dots\dots\dots\dots\dots\dots\text{ (28)}$$

Where S_{zT} is:

$$S_{zT} = S_z - 0.5\frac{k_H}{k_V}\frac{h^2}{L^2}(\frac{1}{3} - \frac{z_w}{h} + \frac{z_w^2}{h^2})\dots\dots\dots\dots\dots\dots\dots\dots\dots\dots\dots\dots\dots\dots\dots\text{ (29)}$$

k_V is vertical permeability, k_H is horizontal permeability, S_w is the wellbore mechanical skin factor, S_z is the partial penetration effect, S_{zT} describes the pressure drop due to convergence of flow lines before reaching the well (Bourdet, 2002) ,L is fracture half-length and z_w is well location in formation thickness.

Chapter 3 Field Case

The Johan Sverdrup field is located out in the North Sea about 150 km west of Stavanger. It is considered to be one of the largest fields ever discovered on the Norwegian continental shelf. The first persons to write about the field using PTA where (Ludvigsen & Le, 2015) and (Sætrom, Selseng, MacDonald, Kjølseth, & Kolbjørnsen, 2016). Both papers only examined the DST data sets because the field was not starting to produce before 5th of October 2019. In this thesis, two DST's were reviewed along with some of the production and injection wells. *Figure 10* gives us a geographical map of the field with observed faults and location of the production wells, injectors, and DSTs. Only the wells with their callsign showing were used in the analysis of the field. The D-wells are the produces, the E-wells are the injectors and the four other wells with the long callsign are the DSTs. The thin blue line going around the field is the aquifer boundary. In addition, there is also an aquifer present in the middle of the field (round thin blue line).
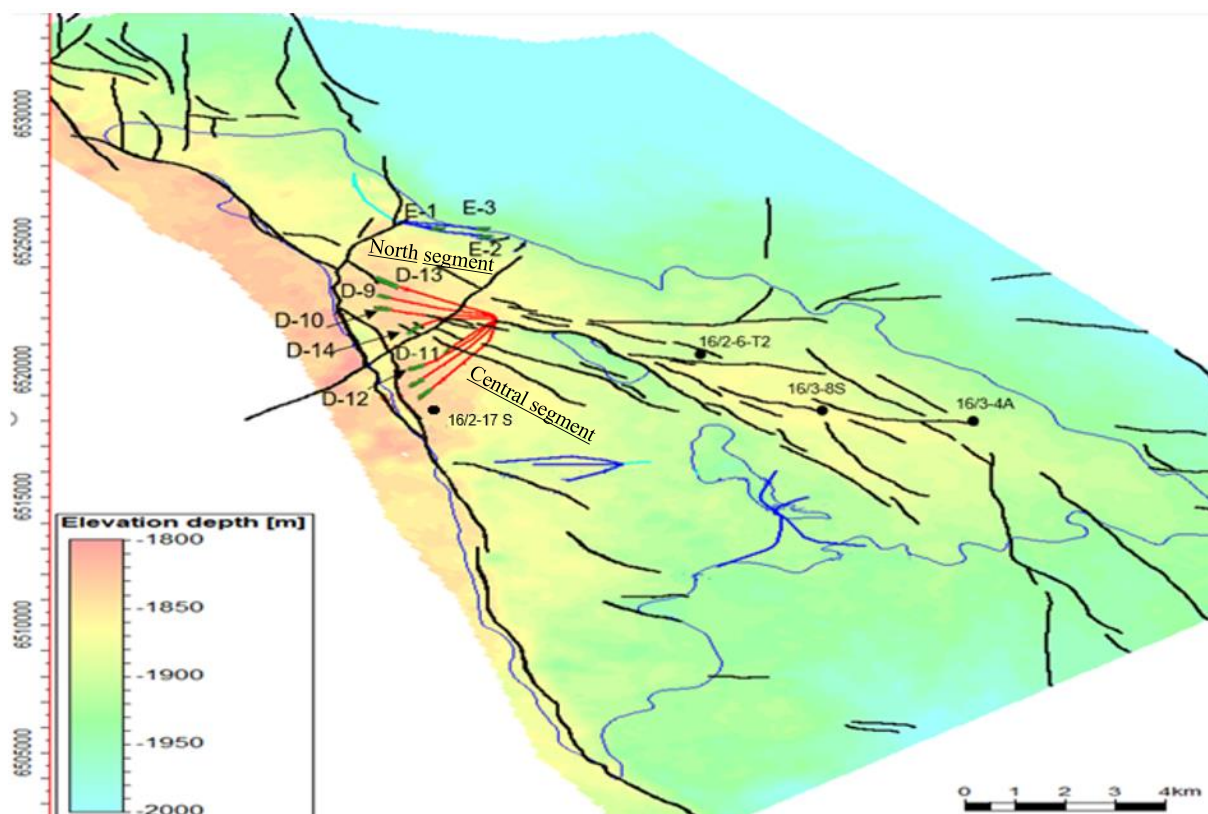
Figure 10 An overview the field with faults and aquifer present along with the production wells, injectors, and some of the DSTs.

The reservoir is mainly unconsolidated sandstone from the Jurassic and Triassic age. In *Table 1* a quick summary of the data over the entire field is shown. The reservoir is mainly homogenous and has high permeability ranging from 1 to 70 D and largely contains

17

undersaturated oil with moderate viscosity and density values. The gas-oil ratio is relatively low, formation volume factor is around 1.139 and the bubble point pressure is around 78 Bara.

Properties	Values	Properties	Values
Reservoir apex	~1800	Oil viscosity	~2 cp
Water depth	~110-120 m	Permeability	1-70 D
OWC	1921-1935	Thickness	4-146 m (well data)
Pressure	Hydrostatic	Reservoir fluid	Undersaturated oil
Max Dip	2 degrees	Area	200 km^2
Age	Early to late Jurassic	Recoverable	260-460 MSm^3
GOR	~40 Sm^3/ Sm^3	Oil Density	~800 kg/ m^3

Table 1 Parameter values from geological data (Ludvigsen & Le, 2015).

3.1 Challenges with the field

One of the challenges with the field is that there are many faults present in both the Triassic and Jurassic layers. Most faults tend to create a seal between two areas of the reservoir in the way that was discussed in subchapter 2.5.1. However, the only information about the faults obtained from the seismic interpretation was their geometry. What we do not see is if they are sealing or conductive.

In the evaluation of the field, there is some uncertainty about communication through the faults. There are indications of sand overlapping across the faults and communications between wells in different fault blocks. *Figure 10* shows us all the faults that are present in the reservoir. *Figure 11, Figure 12*, *Figure 13* and *Figure 14* illustrate the cross section of the reservoir at different locations. In addition, two of the last cross plots also shows grouping of areas where the production wells are. They are divided into three groups, North, Central and South. What is certain with the cross plots are that there is a strong indication of a sealing fault to the west of the reservoir. *Figure 12* and *Figure 13* indicates this. By looking into the pressure development, the effect from the faults may be identified. This makes the DST's, well interference and PTA interpretation crucial because they can indicate which faults can be sealing or conductive.

Another challenge with so many faults present and in such juxtaposition is the variability of sand thickness. Fault creates throws in areas thereby redistributing the sand in an area. This creates uneven sand thickness across the reservoir. PTA is a very useful tool for obtaining indications on how high the sand thickness is around the well.
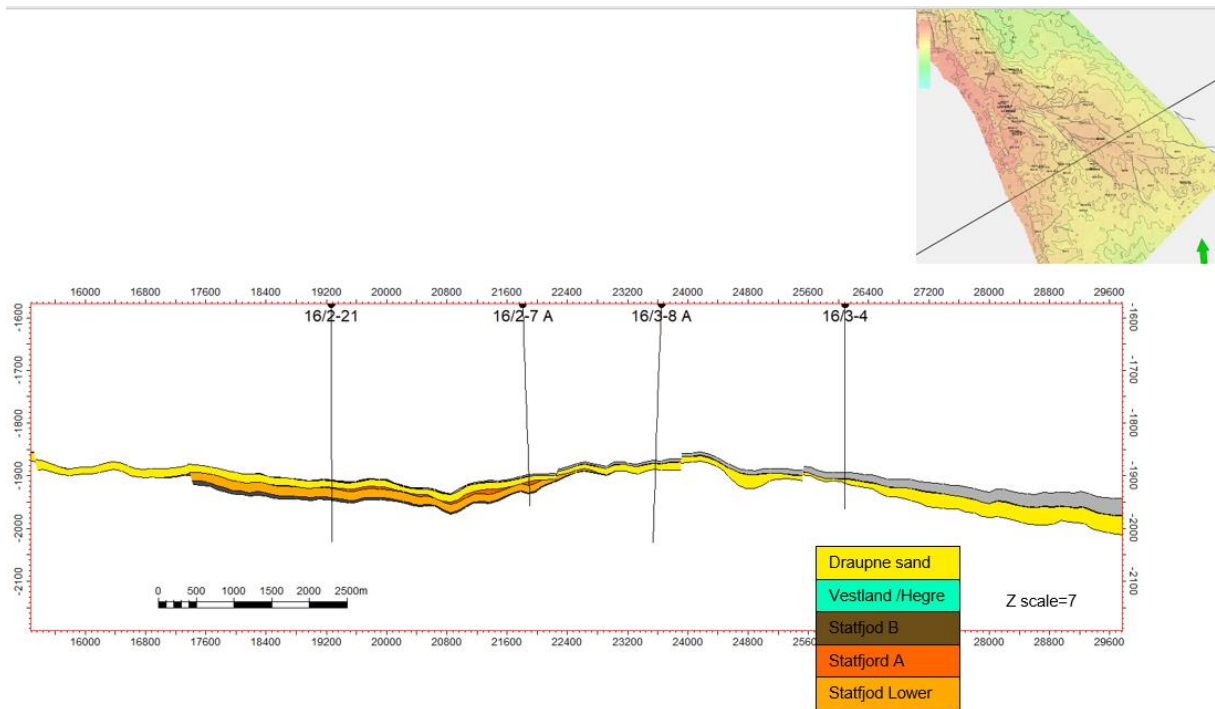
Figure 11 Cross section plot from west to east taken from a southern part of the reservoir.
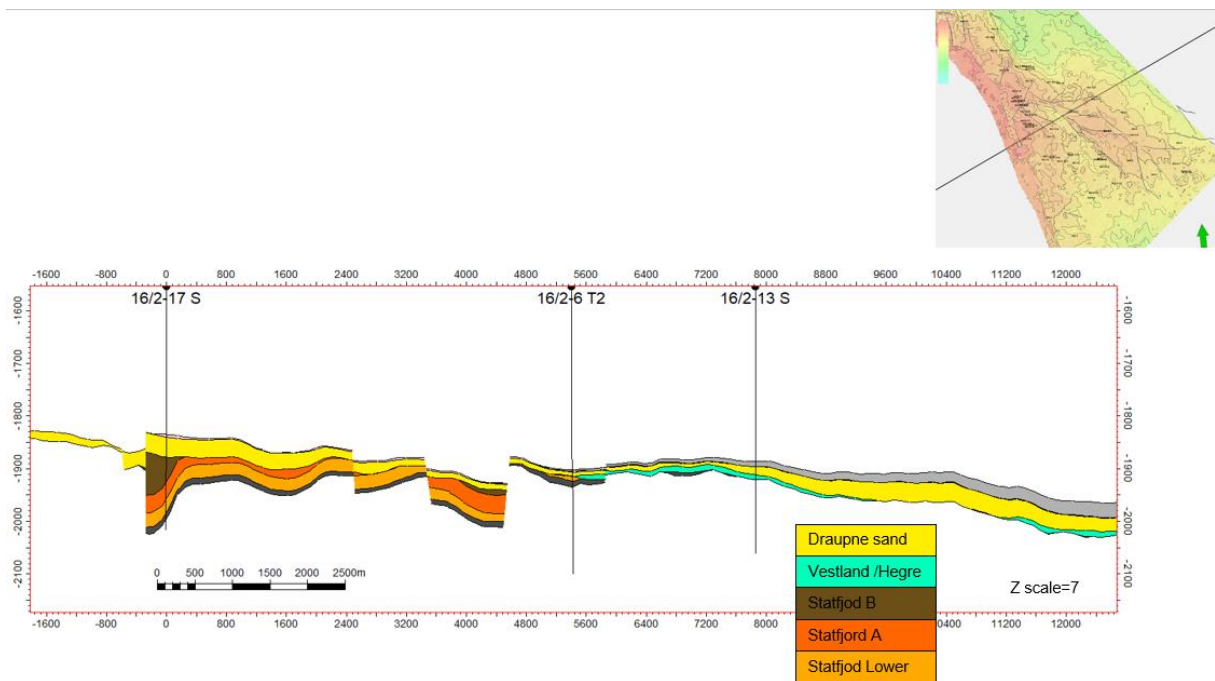
Figure 12 Second cross section of the reservoir from west to east little further north.
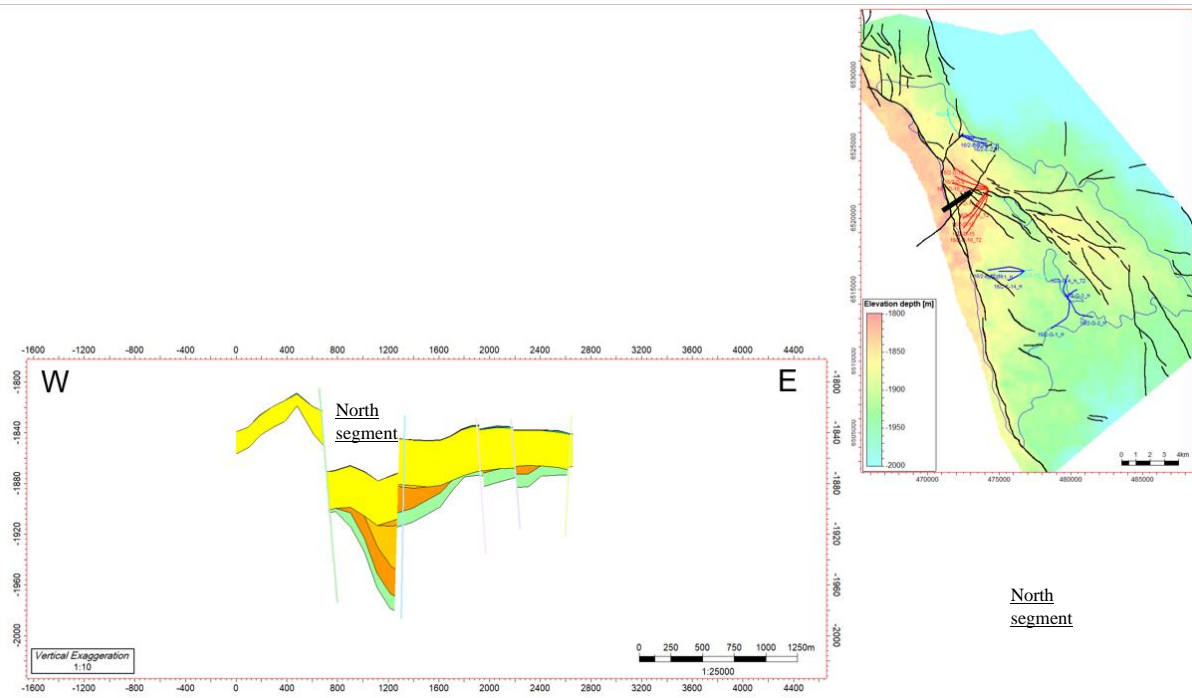
Figure 13 Third cross section of the reservoir where the producers are.
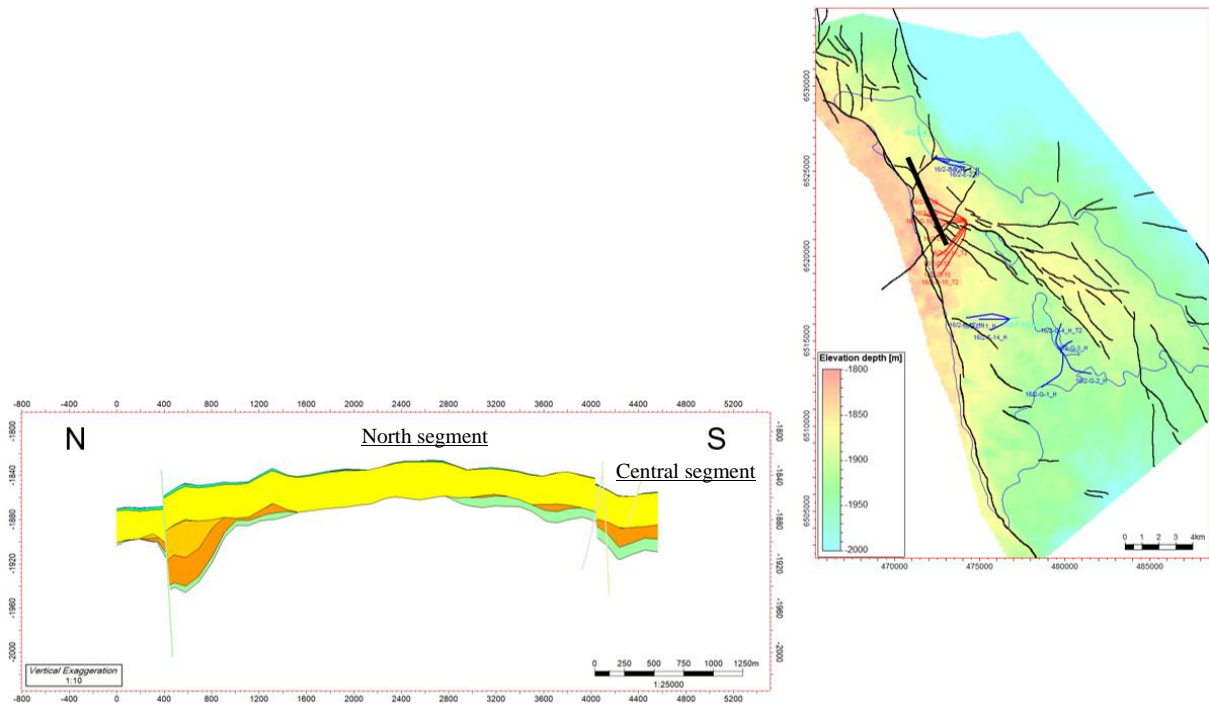
Figure 14 Last cross section from north to south taken between the production wells and the injectors.

3.2   Production uncertainties

When conducting time-lapse PTA all the liquid rates from the producers and injectors were averaged so the software could simulate a field with a large group of wells. This could however lead to some uncertainties because original rates usually gives more accurate description on pressure responses. Although this is true, when comparing pressure responses from original rates with average rates, there is no significant deviation between the plots. Hence, we can assume that the average rates give an accurate description of pressure responses. *Figure 15* shows the results.
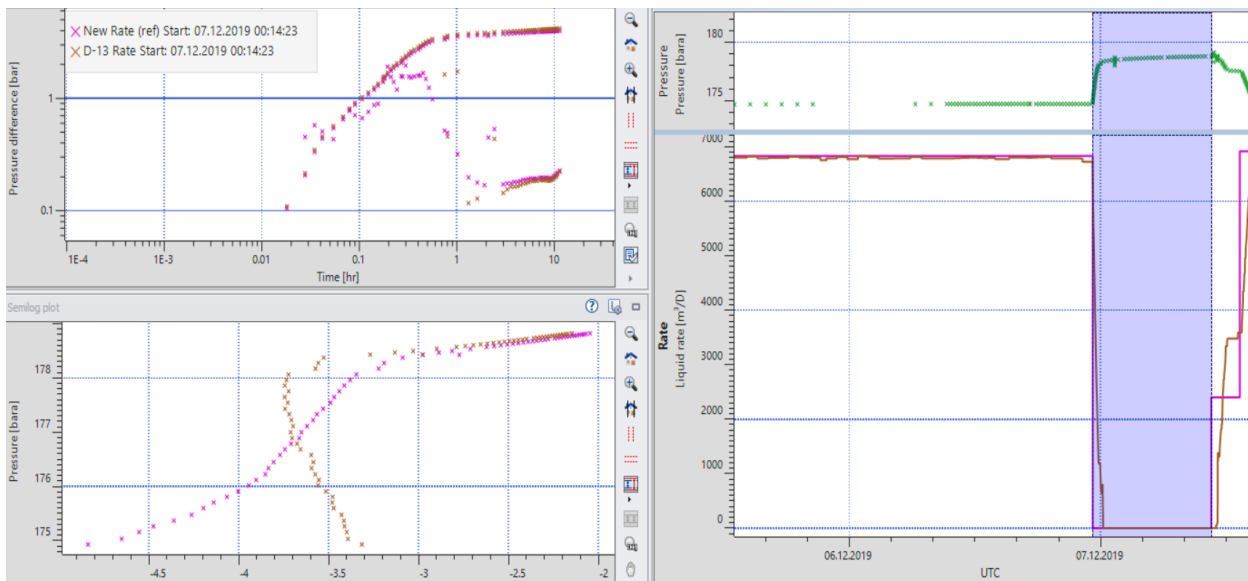
Figure 15 A pressure shut-in with original rates and average rates

In *Figure 16* a simple sketch of a production well highlighting the important equipment and their positions when conducting PTA. The reason why the locations of these instruments are important is because the distance between them can explain the wellbore storage effect and skin factor in a well. According to the well document, the multiphase meter and the master valve was on top of the well. The pressure gauges are roughly 3000 meters below them in measured depth and distance from the gauges to the open hole is around 250 meters.

Multiphase meter on top
of the well

Master valve

Pressure and temperature gauges

Open hole area with sand
screens (liquid flowing in)
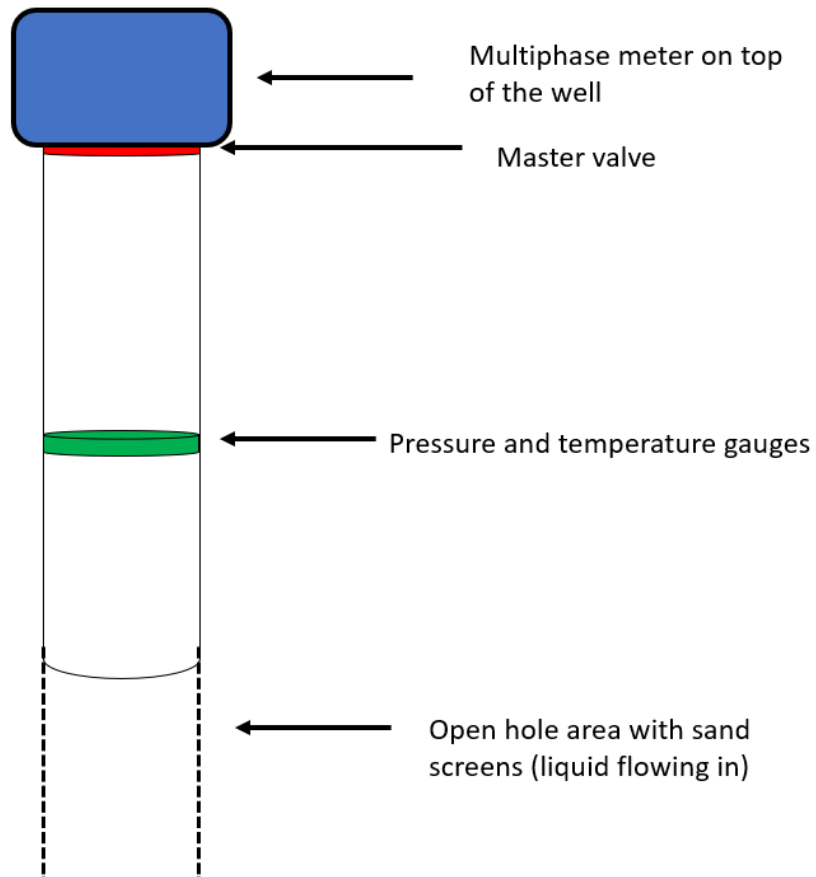
Figure 16 Simple sketch of a production well with the locations of rate measurement, gauges, and valve.

Chapter 4 Results

When conducting the analysis for the thesis, it was decided that the north segment with D-9, D-10, D-13 and D.14 plus the three injectors in further north would be the main focus area of the thesis. In addition to the study of the North segment, communication with the Central segment is explored including wells D-11 and D-12. *Figure 17* show us a picture of these wells. The reasoning behind this selection was that they had the best interference data compared to the two other wells south of D-12. As such, they provided a better and clearer analysis for the scope of the thesis. Furthermore, in time-lapse PTA these wells also had longer periods for shut-in which was an important factor for good interpretations.
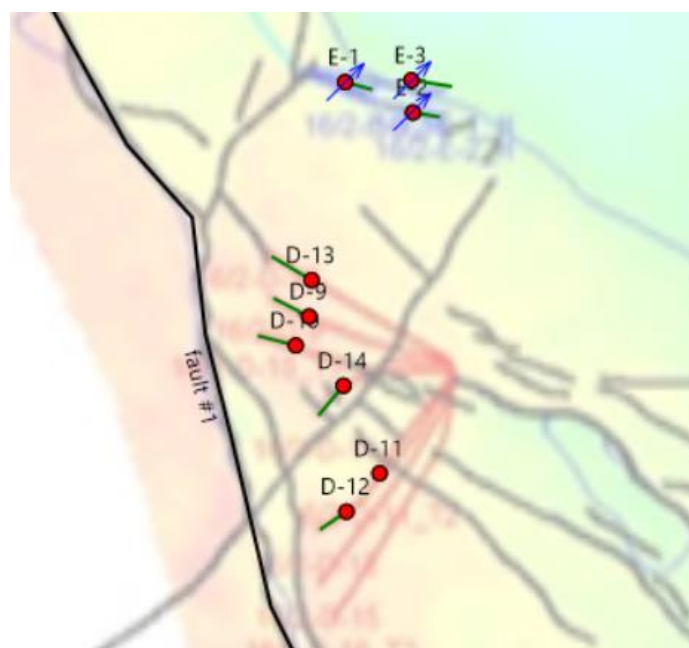
Figure 17 Picture of the area of interest with the wells.

When analyzing the pressure data for the field, certain parameters were kept constant because laboratory experiments indicated that these values are quite certain. The parameters that were kept constant throughout the analysis were:

- Porosity at 0.26
- Viscosity at 2.04 cp
- Formation volume factor at 1.139 m^3/stm^3

In addition, according to the company's geological data the sand thickness was not higher than 30 meter in the area of interest.

In addition to looking into finding sand thickness, permeability, and boundaries the company was also interested in checking whether certain total compressibility values gave better

matches. The reason for this interest was because of uncertainty of the values of rock (pore volume) compressibility as interpreted from the laboratory experiments. Total compressibility is the sum of fluid compressibility (in our case mainly oil due to the reservoir saturation), which is quite certain from PVT experiments and rock compressibility, which has some uncertainty as mentioned above The models were therefore run with two separate total compressibility values provided by the company to see what differences could be observed, and which compressibility had a better match with the pressure transient data. The two values of total compressibility are:

1. $C_{t1}=1.729E\text{-}4\ bar^{-1}$
2. $C_{t2}=2.350E\text{-}4\ bar^{-1}$

The first total compressibility is the primary, and initial presentations of the results are based on this value. The software that was used to analyse these pressure responses is called Kappa Saphir. Limited DST data sets were also provided by the company to determine whether the results from interference tests or time-lapse PTA showed a similar match with these pressure responses.

4.1   Interference test

The first analysis that was conducted was the interference between the production wells. As mentioned in subchapter 2.4, in order to properly analyse interference with horizontal wells, the ratio between the diameter of a pressure pulse and the length of the observation well had to be greater or equal too three. Otherwise there was a certain risk of estimating wrong values for the parameters because the observation point might be wrongly located. All the analyses presented in the thesis fulfill this requirement. *Figure 18* show us an ideal interference response with 30 Darcy in permeability and 30 meters of sand thickness.
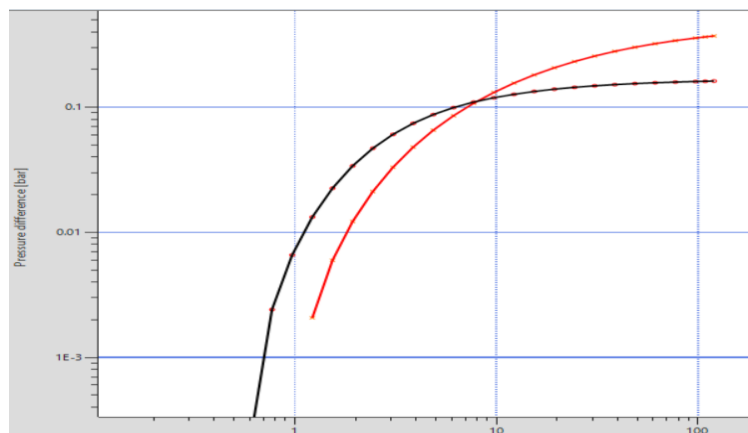
Figure 18 An ideal case for interference response.

The way the interference test was analysed was by setting up the sealing fault to the west and then simply changing the permeability and sand thickness until the model was able to match the cross section between the pressure derivative and the pressure curve. This is viable because as mentioned in the start of this chapter, porosity, viscosity, and compressibility were considered constant in the analysis. Therefor the *diffusivity coefficient* (which controlled the lag time) simplifies into: $\frac{1}{k}$, and the flow capacity (which controls the pressure amplitude) simplifies into: kh. Furthermore, by adjusting the sand thickness or permeability it should be able to line up at the cross section. **Figure 19** illustrates from an ideal case how change in permeability or thickness affects the pressure profile. Notice how the change in permeability moves the pressure profile horizontally and vertically, while changing the thickness only changes it vertically.
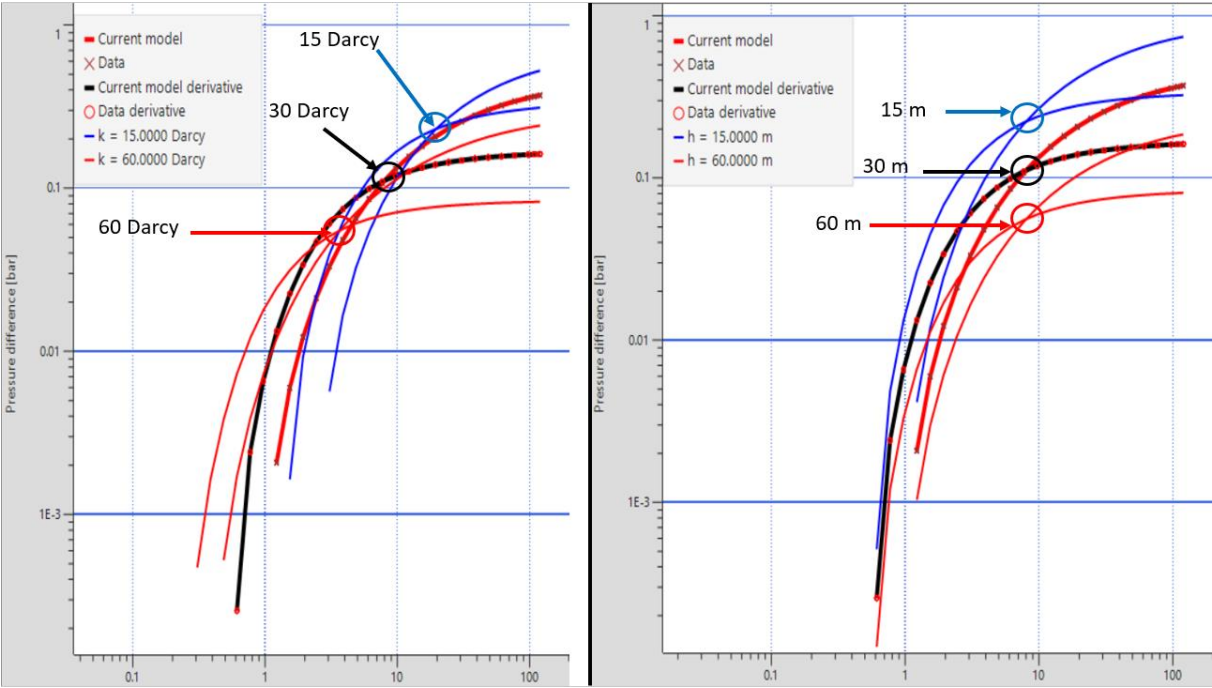
Figure 19 Illustration on how change in permeability or thickness affect pressure analysis in an interference test.

All interference tests were initially analysed with only two wells, but some of the values from these analyses were too high in comparison to what well logs and core measurements suggested around the area of interest. This led to some curiosity as to whether the presence of nearby wells had any impact on the pressure response. The interference tests were analysed again with additional wells. The interpretation was done first by only analyzing the communicating producers. It was observed in some cases that adding other production wells had a significant impact on the pressure interference, while in other cases there was no impact. Then the injectors

were implemented into the analysis because if the producers have an impact, there is the possibility that the injectors impact too. However, no significant change was observed in any cases. In the end, two interference analyses were significantly impacted when adding other wells in their analysis.

In the next subchapters, results from different interference tests are displayed. The reason why these interference tests are shown is because they cover the area on interest. By analyzing several of these interferences we achieve a better understanding of what values of permeability and sand thickness exist around the area.

4.1.1 Interference analysis to clarify conductivity.

When first performing the interference analysis, it was important to establish early on how conductive the fault between the producers D-14, D-11 and D-12 is. The location of this fault is shown in *Figure 10*. It was discovered early by just looking at the pressure of the wells that there is communication across the fault. Analysis of this fault was important for further investigations on other interference tests.

4.1.1.1   D-14 interfering D-11

The first test that was looked into was the interference on D-11 by D-14. *Figure 20* shows us the initial stages of the investigation where only the two wells were implemented in the model in combination with the sealing fault, neglecting the fault between the production wells. The distance to the sealing fault to the west is around 1500m.

Parameters	
Boundary	Infinite
Total compressibility	1.729E-4 bar^{-1}
Permeability	20D
Sand thickness	40m
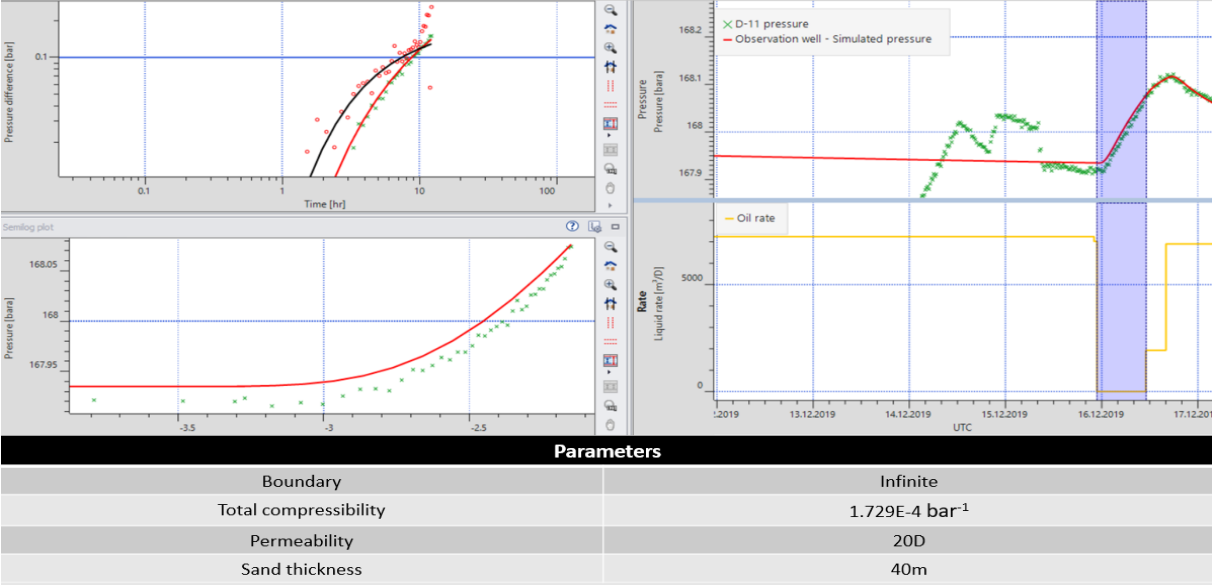
Figure 20 Image of an analytical model of an infinite reservoir containing the wells D-14 and D-11.

We can see that with given information from the geological data, it is not possible to match without going over 30m of sand thickness (which was given as the maximum limit). Additionally, we see in the log-log plot that the model crosses a little too early than what the data shows. A second attempt with the model was made to see if it was possible to get a match with 30 meters of sand thickness. This is shown in *Figure 21*.

Parameters	
Boundary	Infinite
Total compressibility	1.729E-4 bar^{-1}
Permeability	25D
Sand thickness	30m
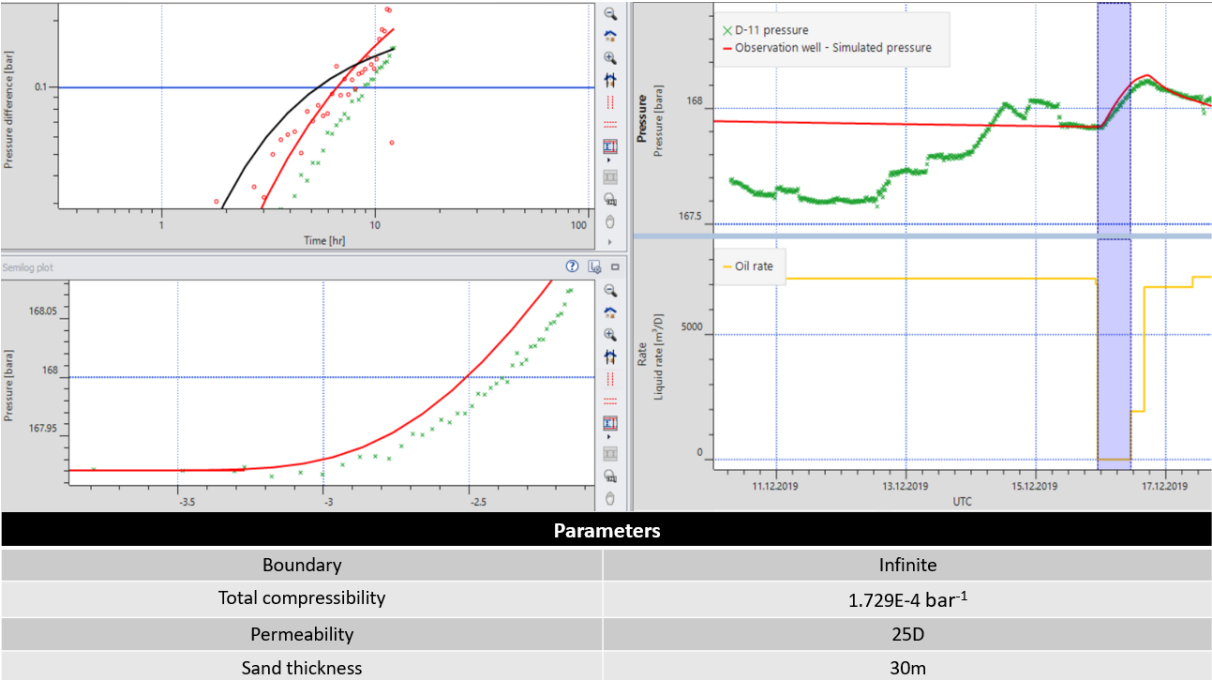
Figure 21 Second model to identify if other values can match the data.

A numerical model was then set up with a leaky fault between these two producers illustrated in *Figure 22*.

Figure 22 Setup of the numerical model. D-14 is the active well and D-11 is the observation well.

The end result was a model that matched well with the derivative and the pressure profile, shown in *Figure 23*. The values from the model did not contradict what the well logs and core data showed. An analysis with multiple wells was also conducted to see if there were any impact from nearby wells. It did not change the outcome. *Figure 24* shows the results.

Parameters	
Total compressibility	$1.729E\text{-}4 \text{ bar}^{-1}$
Permeability	21D
Sand thickness	30m
Leakage factor (Fault #2)	0.25
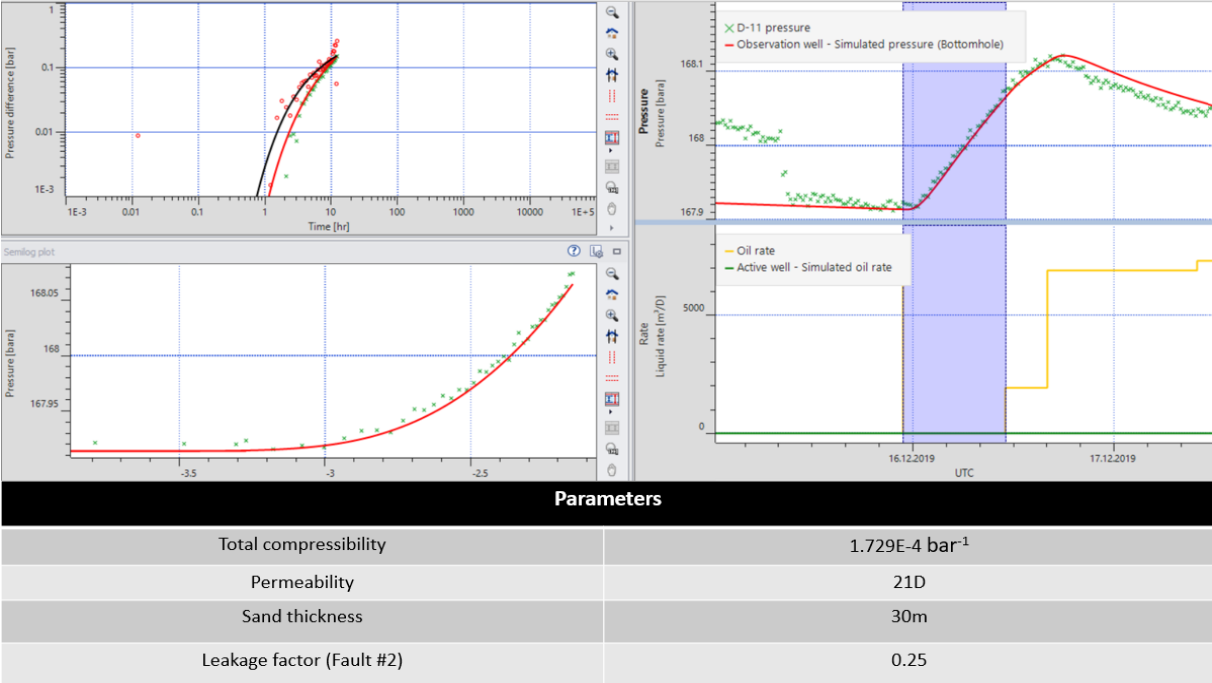
Figure 23 Numerical model of interference test between well D-14 and D-11 with the leaky fault in between them.

Parameters	
Total compressibility	$1.729E\text{-}4 \text{ bar}^{-1}$
Permeability	21D
Sand thickness	30m
Leakage factor (Fault #2)	0.25
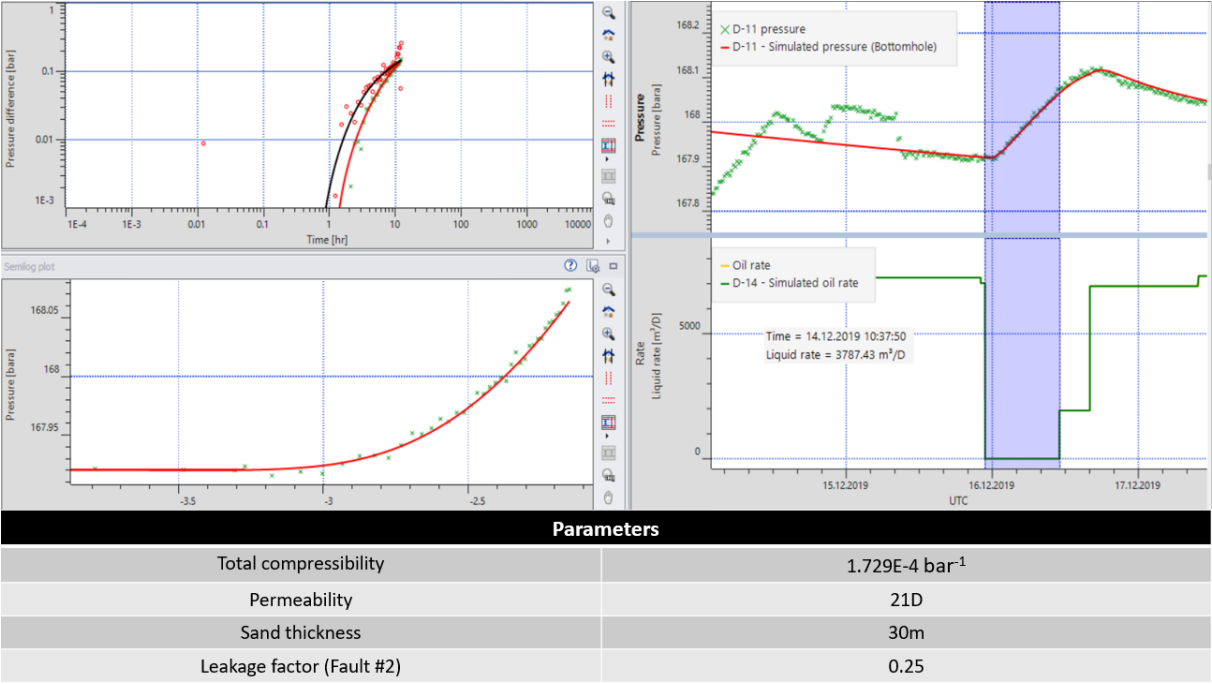
Figure 24 Another analysis with multiple wells.

28

A sensitivity analysis on the leakage factor was done just to show how it impacted the results. The sensitivity is displayed in *Figure 25*. It turned out that a leakage of about 0.25 gave us the best match with the pressure response.
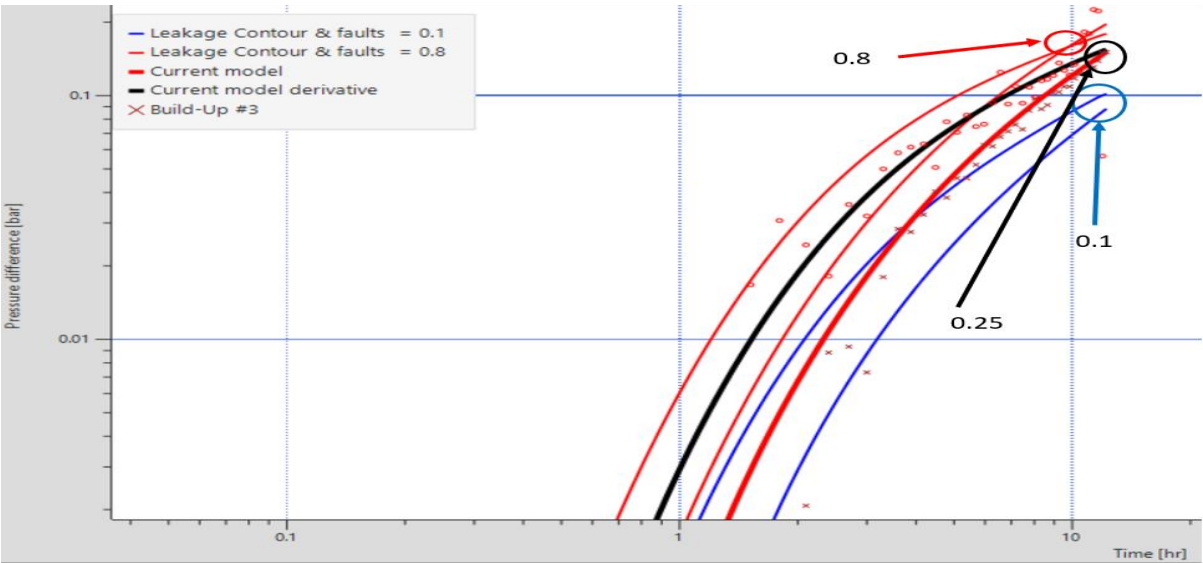
Figure 25 Sensitivity to the leakage value.

4.1.1.2   D-14 interfering D-12

To validate that the fault between these wells could have a leakage factor around 0.25, a second interference analysis was conducted between D-14 and D-12. Illustrated in *Figure 26*, the leakage value, sand thickness and permeability are the same as D-11 and D-14 interference analysis. This gives us validation that the model and estimation of leakage factor is a possibility.

Parameters	
Total compressibility	1.729E-4 bar^{-1}
Permeability	21D
Sand thickness	30m
Leakage factor (Fault #2)	0.25
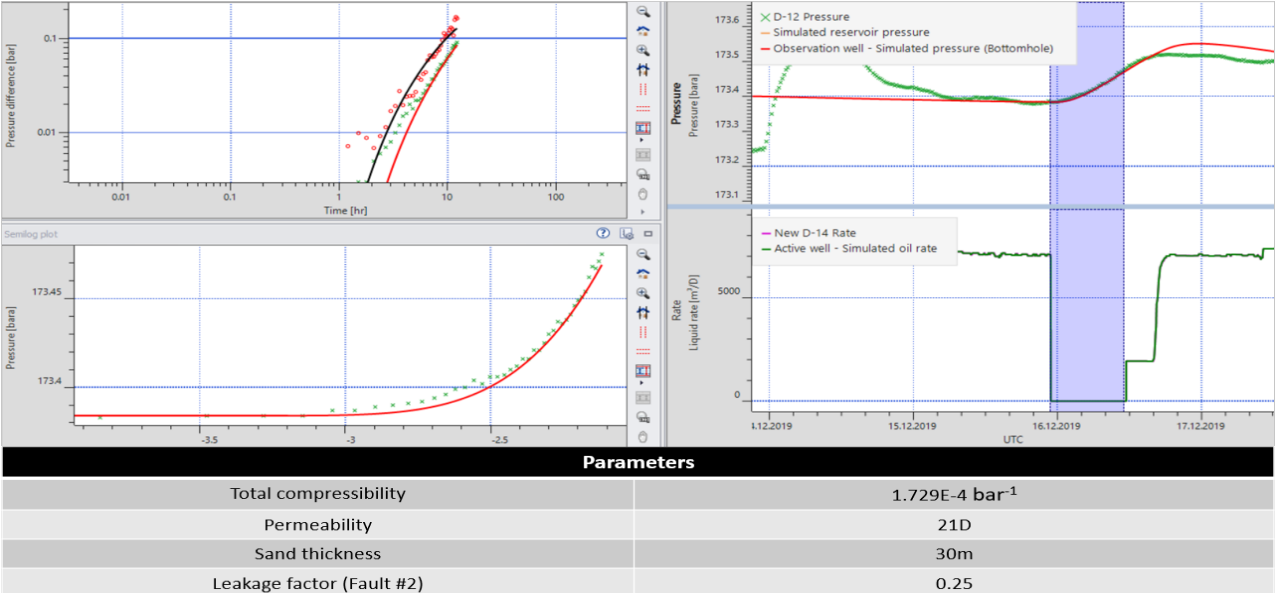
Figure 26 Analysis of interference between D-14 and D-12.

An analysis with multiple wells was also conducted, but the results were no different than simply having two wells.

4.1.2 Rest of the interference analysis.

Analytical model results showed that there is a need to add a flow restriction between the wells D-14, D-11 and D-12 to match the observed interference response. Introducing leaking fault helped to match the observations better. After establishing the value of fault leakage, the factor was further used in the other interference analysis in numerical models
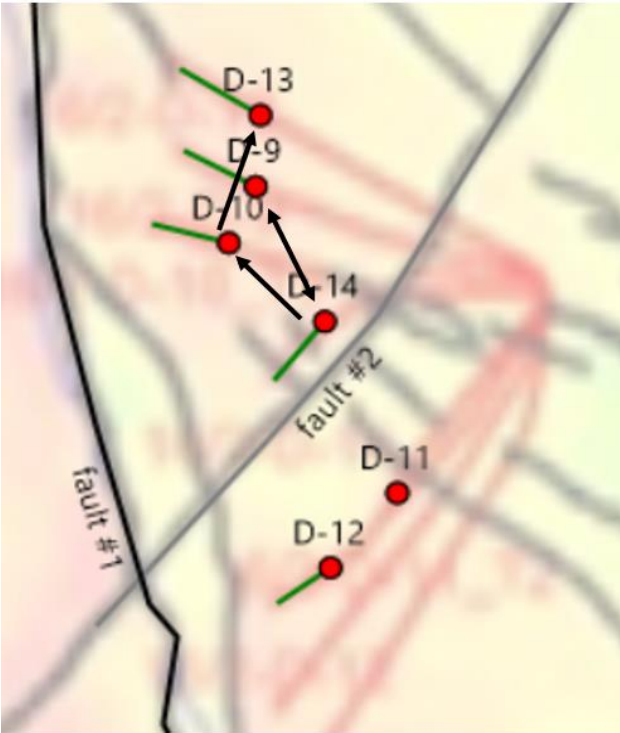
Figure 27 Picture of displacement of the production wells and which interference between wells were analysed. The black arrows show which wells interfered the other.

Figure 27 shows us which other wells were conducted with interference analysis and it also shows all the production wells that were added for multi well interference. Since the period of these interference were never longer than 20 hours, other boundary effects were not considered. These faults were too far away, or the pressure responses did not indicate additional faults than what was discovered. As the figure displays, the models had a sealing fault due west that was approximately 1000-1500 meters away depending on the position of the active well and the leaky fault to the south. Further interference analyses with this model was conducted to look into what values of permeability and sand thickness do we observe from the area on interest.

4.1.2.1 D-14 interfering D-10

An analysis of interference between D-14 and D-10 was first reviewed starting with only these wells. *Figure 28* shows the results and the values of permeability and sans thickness correlates with core measurements and well logs. Multi well interference (all nearby well) was conducted on this well, but the results remained the same.

Parameters	
Total compressibility	1.729E-4 bar^{-1}
Permeability	35D
Sand thickness	29m
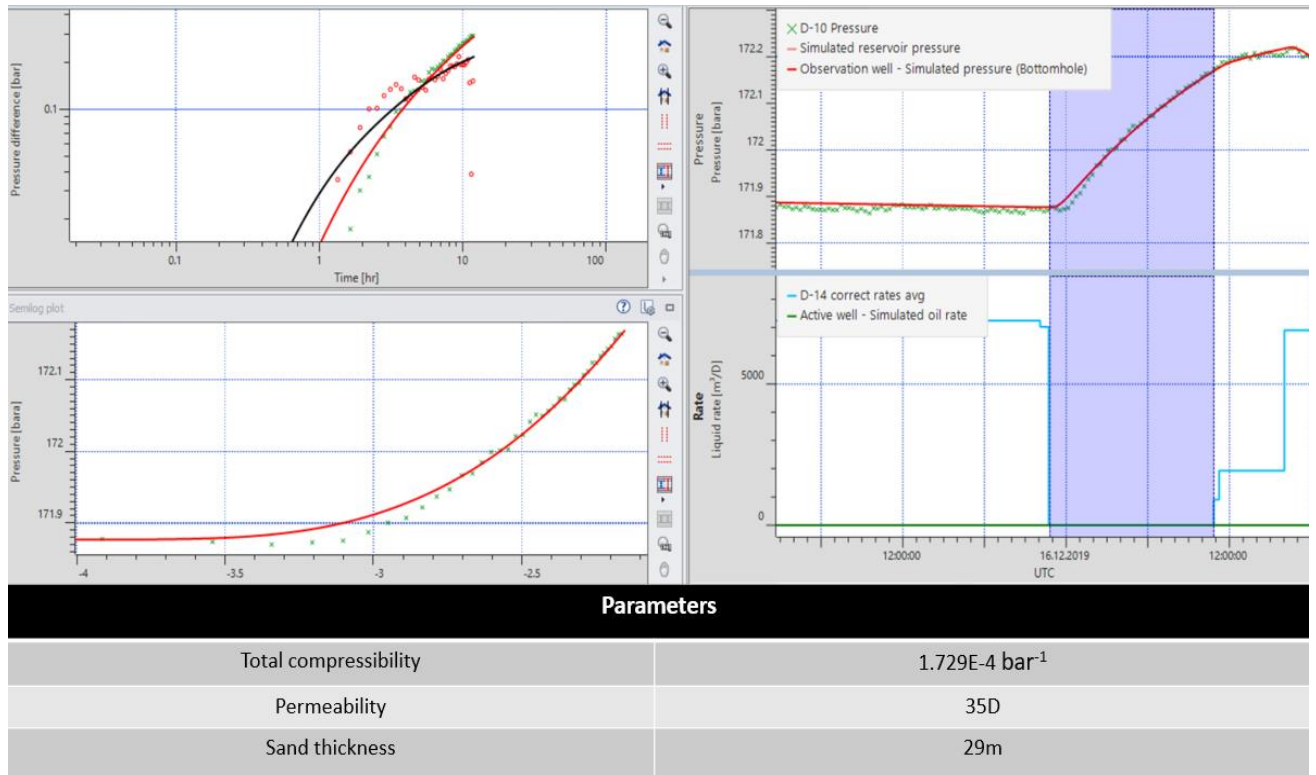
Figure 28 Numerical model between D-14 and D-10.

4.1.2.2 D-14 interfering D-9

The second interference test that was analysed was between the D-14 and D-9 wells. Only these wells were selected because additional wells did not provide any different results. Interesting observation from this test is that the sand thickness is the same as the other test, but the permeability is much higher. *Figure 29* displays the results from the analysis.
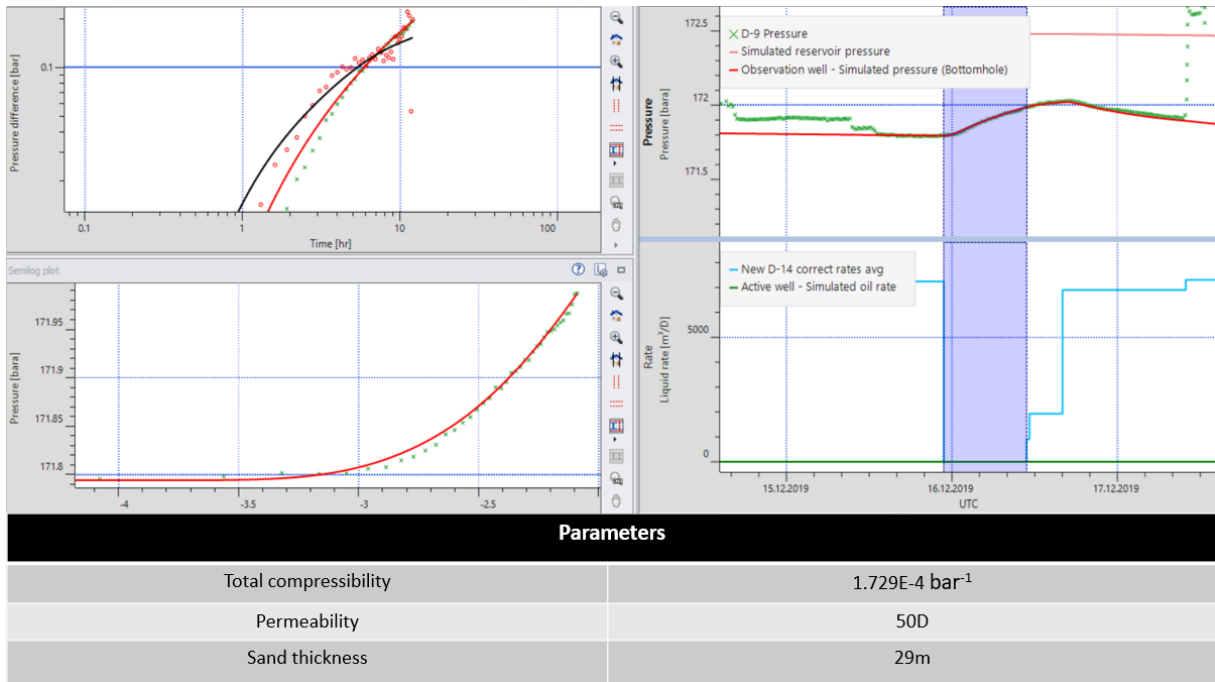
Figure 29 Numerical model between D-14 and D-9.

4.1.2.3   D-9 interfering D-14

It was also observed that production well D-9 interfered with well D-14. Therefore, an analysis with only these two wells was conducted first. *Figure 30* shows the results and in this test the permeability value is also very high compared to the other tests. However, it is close to the same value as in D-14 interfering D-9 test.
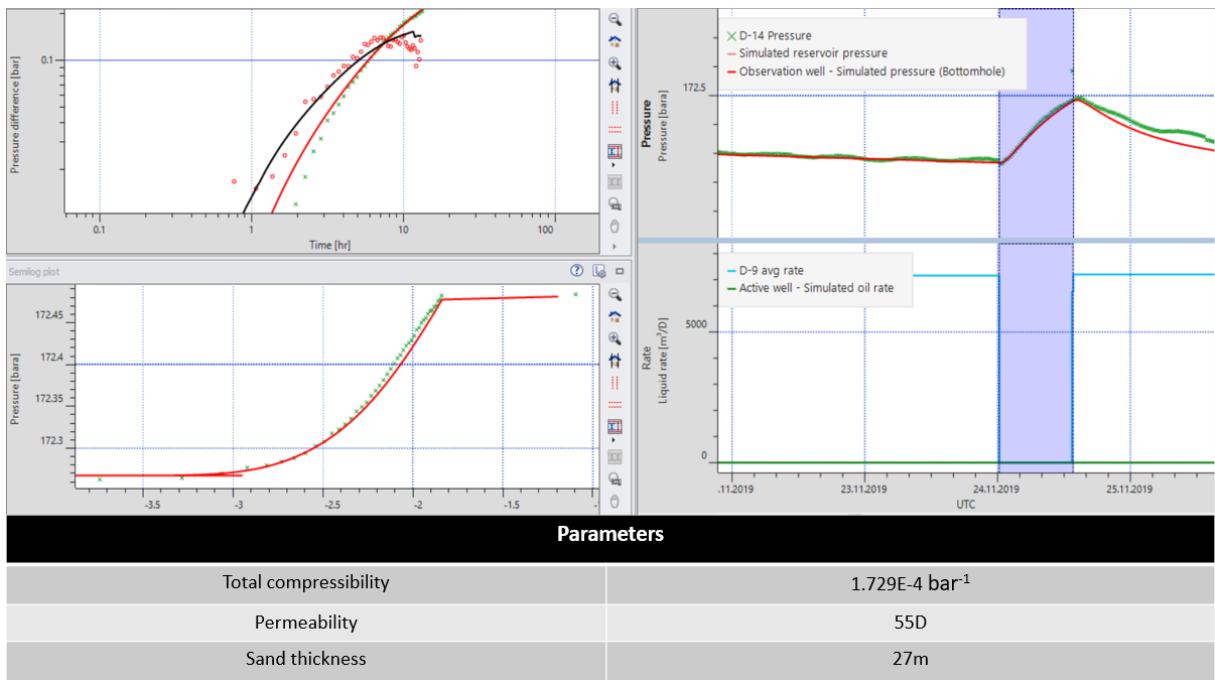
Figure 30 Numerical model between D-9 and D-14.

The result from interference test D-9 on D-14 shows that the permeability is high compared to most other interference tests. After the first result of this interference test, a second analysis with multiple wells was done, where it was observed that neighboring wells had an impact on the analysis. *Figure 31* displays the results showing the permeability value was reduced with 10 Darcy. This is still high when compared to the other results. Sand thickness remained constant.

Parameters	
Total compressibility	1.729E-4 bar^{-1}
Permeability	45D
Sand thickness	27m
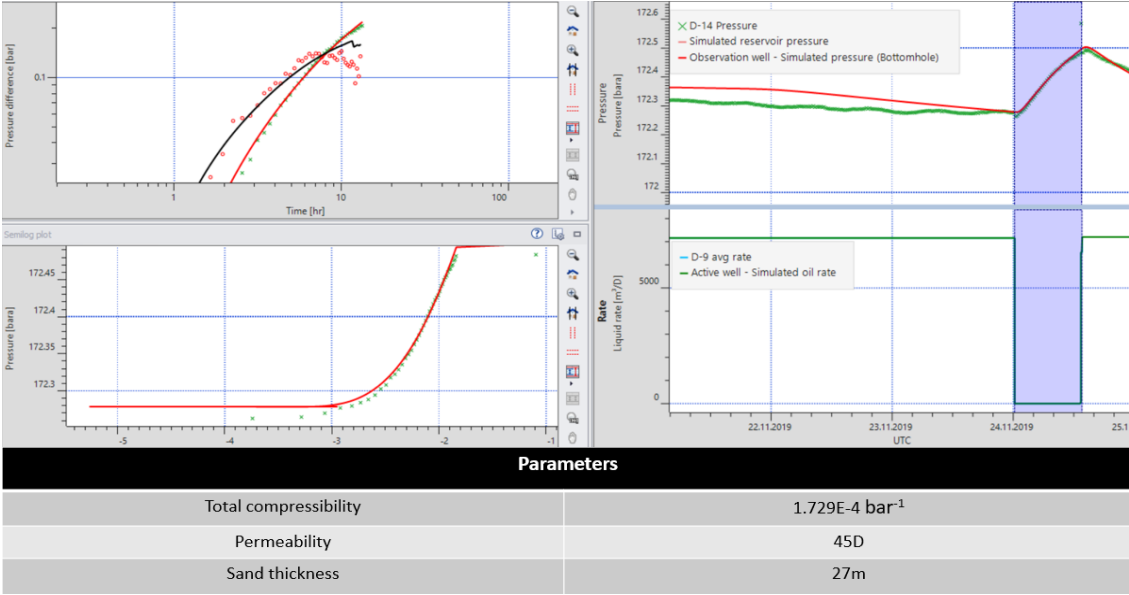
Figure 31 Numerical model of interference between D-9 and D-14 with neighboring wells.

4.1.2.4 D-10 interfering D-13

The last interference that was looked into was between D-10 and D-13. *Figure 32* shows us the results when only these two wells are present.

Parameters	
Total compressibility	1.729E-4 bar^{-1}
Permeability	40D
Sand thickness	30m
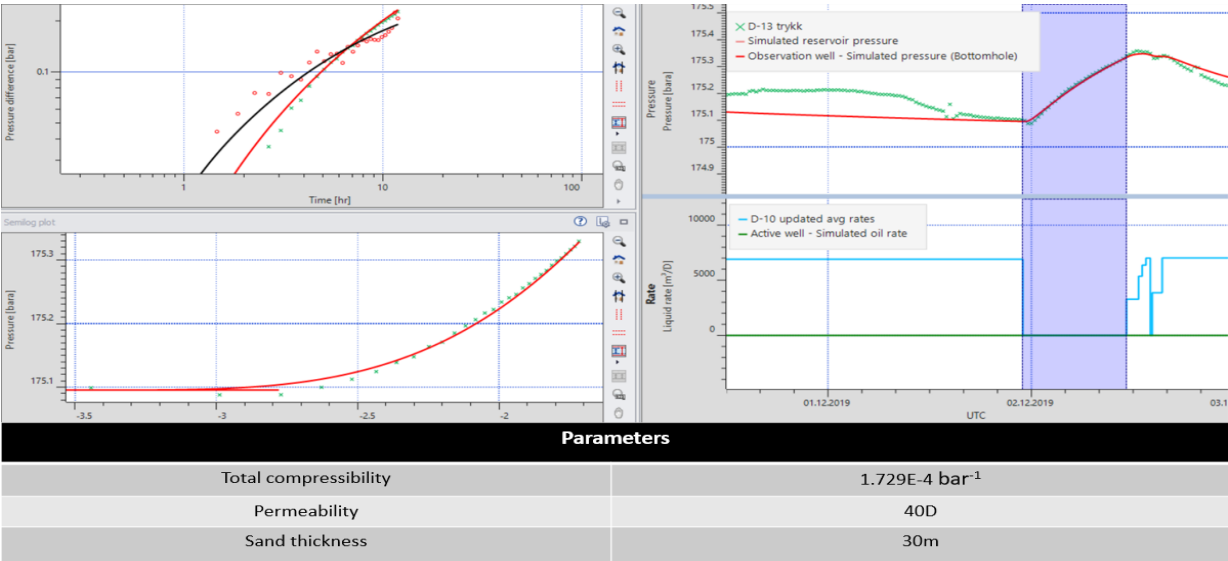
Figure 32 Numerical model between D-10 and D-13.

The permeability was considered slightly too high, so it was looked into if additional wells made a more realistic result. In *Figure 33* we see from the analysis that the permeability value was reduced and the sand thickness increased when adding neighboring wells. The values from the result were considered more realistic when compared with core measurements and well logs, but the sand thickness was considered marginally too high. Nevertheless, it is an interesting observation that the interference tests with wells close by the source well (active well) were significantly impacted by the production from nearby wells, while the other interference tests that did not have any close neighboring wells were not impacted.

Parameters	
Total compressibility	1.729E-4 bar^{-1}
Permeability	35D
Sand thickness	32.5m
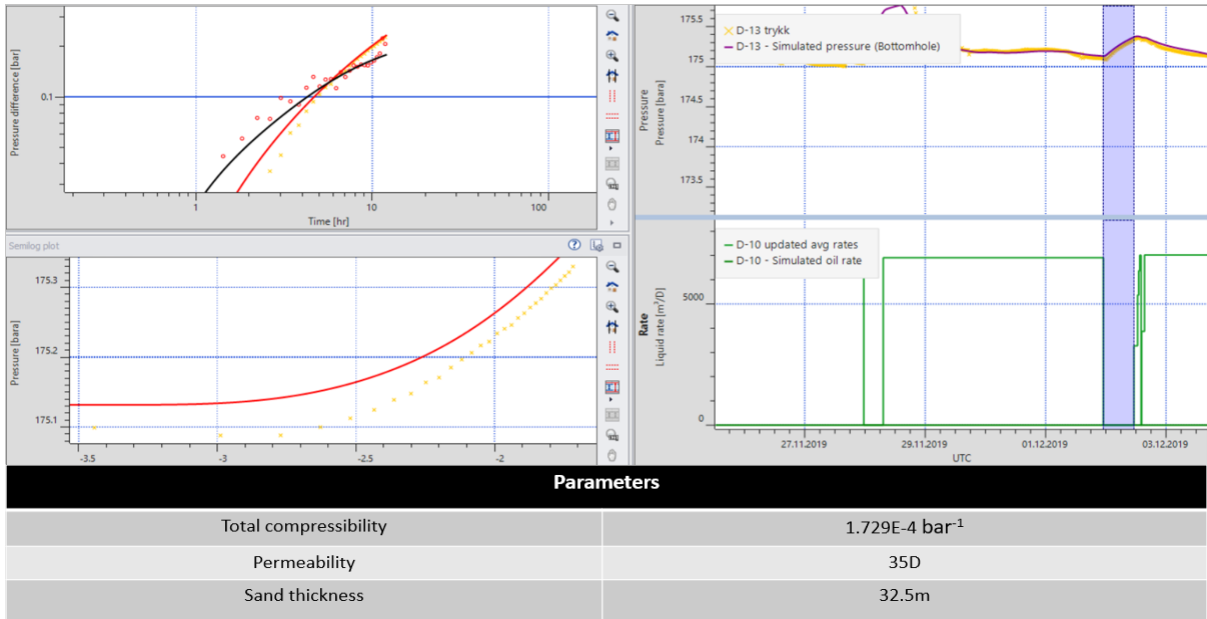
Figure 33 Numerical model of interference between D-10 and D-13 with neighboring wells.

4.1.3 Change in compressibility

An interesting observation with the interference test is that when the compressibility changed most analysis responded the same. They all had to increase their permeability values by around 10 and decrease the sand thickness by around 8-9. However, the interference analysis between the leaky fault (D-14 interfering D-11 and D-14 interfering D-12) showed that the leakage percentage went up from 0.25 to 0.6 as the compressibility increased. *Figure 34* shows us how total compressibility impacts the interference test
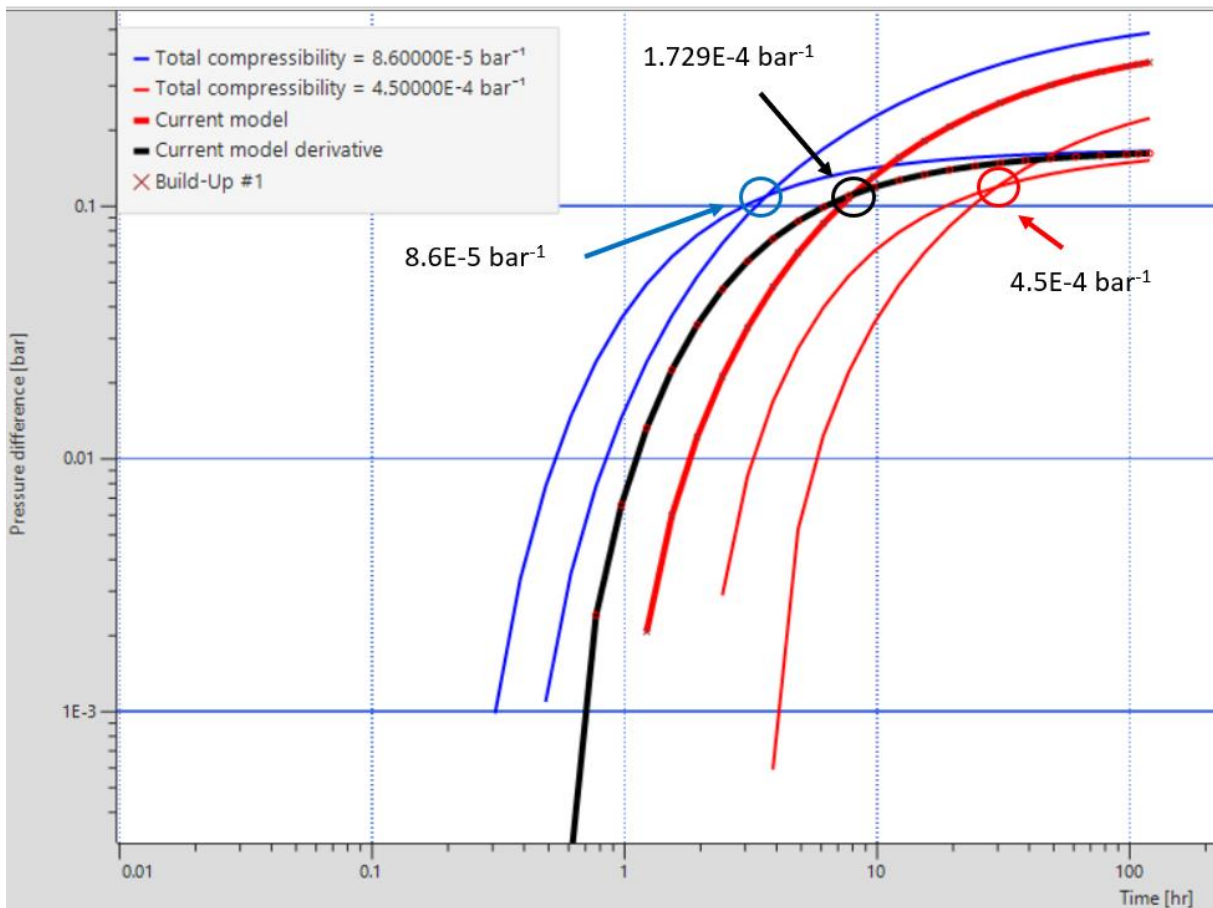
Figure 34 Sensitivity of total compressibility in an ideal case.

Below are a couple of pictures from these tests with changed compressibility. By comparing *Figure 26* and *Figure 28* with *Figure 35* and *Figure 36* we see how change in total compressibility effected the permeability, sand thickness and leakage.
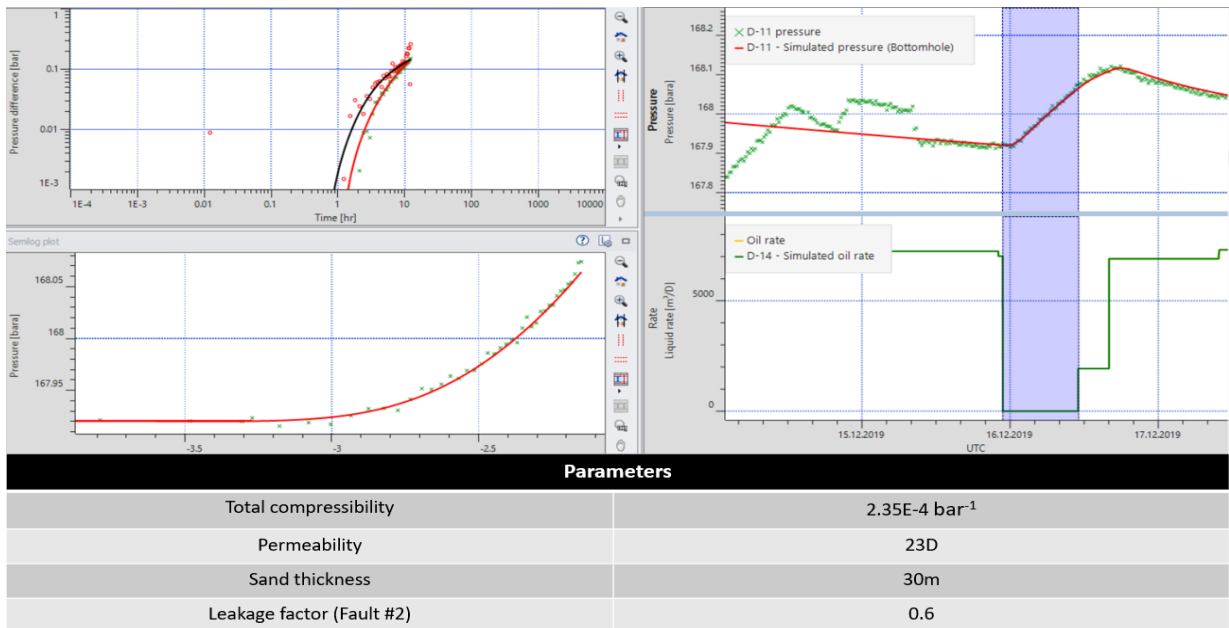
Figure 35 Interference test between D-14 and D-11.

Parameters	
Total compressibility	2.35E-4 bar^{-1}
Permeability	23D
Sand thickness	30m
Leakage factor (Fault #2)	0.6
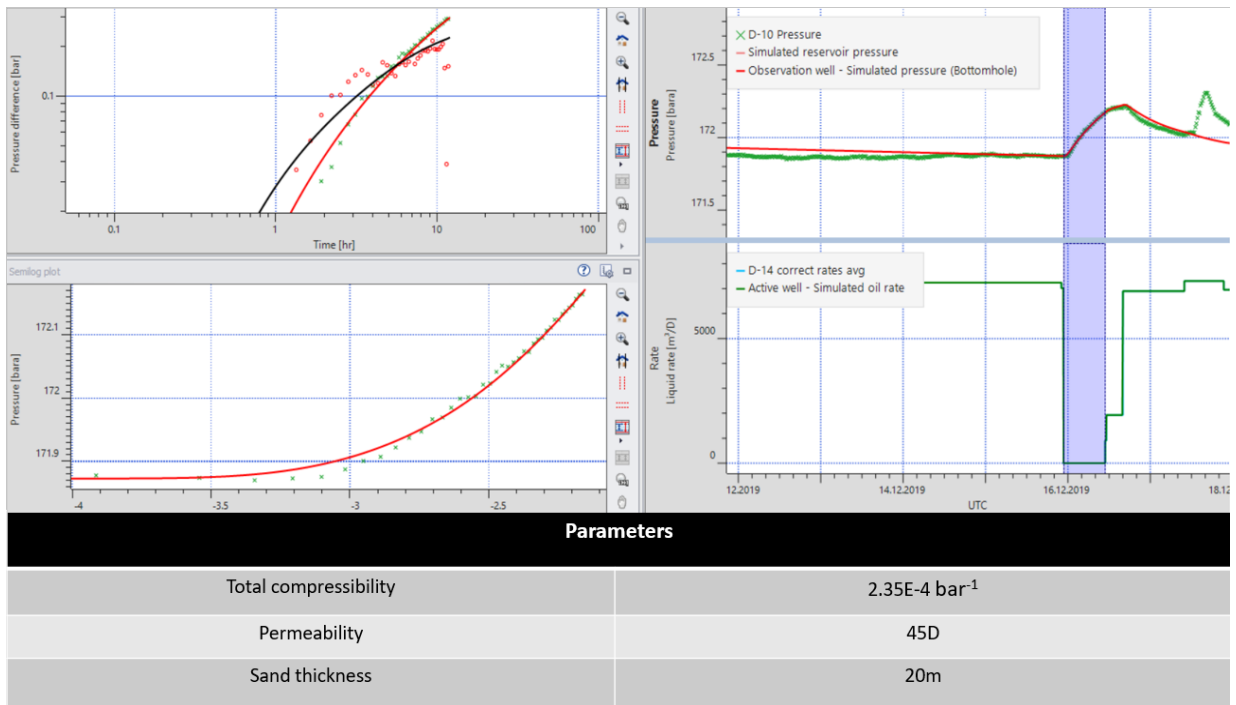
Figure 36 Interference test between D-14 and D-10.

Parameters	
Total compressibility	2.35E-4 bar^{-1}
Permeability	45D
Sand thickness	20m

A summary of all final results from all analyses are displayed in ***Table*** 2. By averaging the four first well to well results plus the two results from the analyses with multiple wells, we get an average around 34D and 29m. This was considered the average value for permeability and sand thickness around the area of interest.

	Well to well	Multiple wells	Compressibility change
D-14 and D-11	21D 30m	-	23D 30m
D-14 and D-12	21D 30m	-	-
D-14 and D-10	35D 29m	-	45D 20m
D-14 and D-9	50D 29m	-	-
D-9 and D-14	55D 29m	45D 29m	-
D-10 and D-13	40D 30m	35D 32.5m	-

Table 2 Summary of final results from all interference analysis. Each cell shows the permeability and sand thickness values.

4.2   DSTs

After analysing the interference tests, the results were compared to two DSTs that were closest to the area of interest. This comparison was done to verify that the values from the analysis made sense with the pressure response from these exploration wells. The DSTs data were taken two years before production start and some analysis had already been undertaken on them. It should be noted that these DST's are a distance away from the production area and have a slightly different geology. Therefore, these DST's are indirect analogs. Furthermore, the values from formation volume factor and viscosity in previous analyses are brought into these analyses since a different stage separator was used for the exploration wells.

4.2.1   Well 16/2-17S

The first exploration well that was reviewed was well 16/2-17S which is located south of the production wells. ***Figure 37*** bellow shows us the initial observations with the average values from the interference test using some default parameter values from previous analysis.
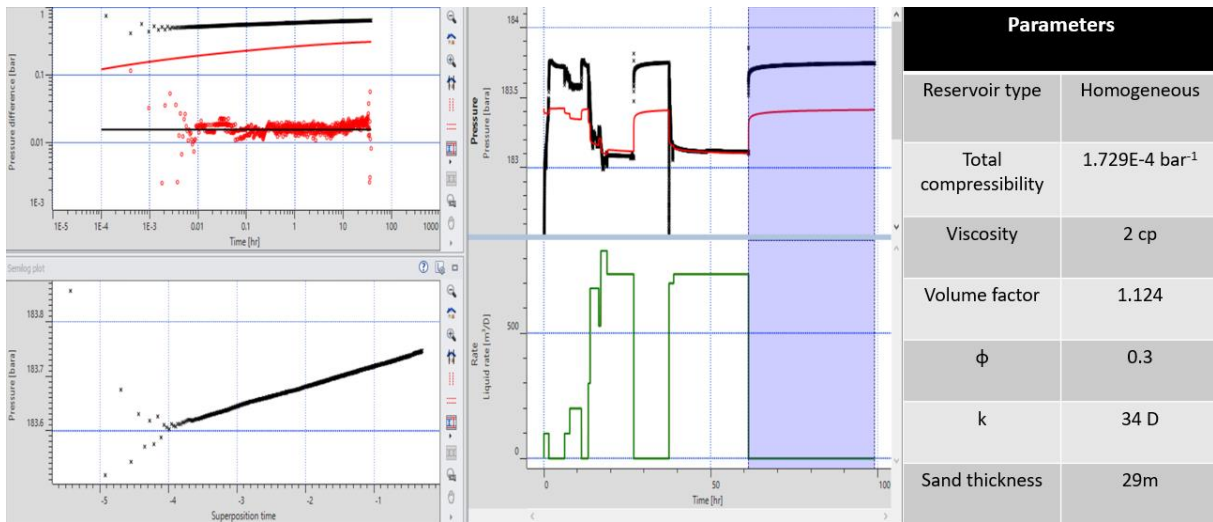
Figure 37 Initial test of the of the permeability and sand thickness values with default values.

We see that the model matches the radial flow regime closely with 34D and 29m. This is a good indication that the average values from the interference tests could be correct.

Since the model was able to match the kh, it was investigated whether the model could match with the sealing fault that is furthest to the west. A single fault at 1300 meters plus 10 in skin was therefore added to the model. *Figure 38* display the results.
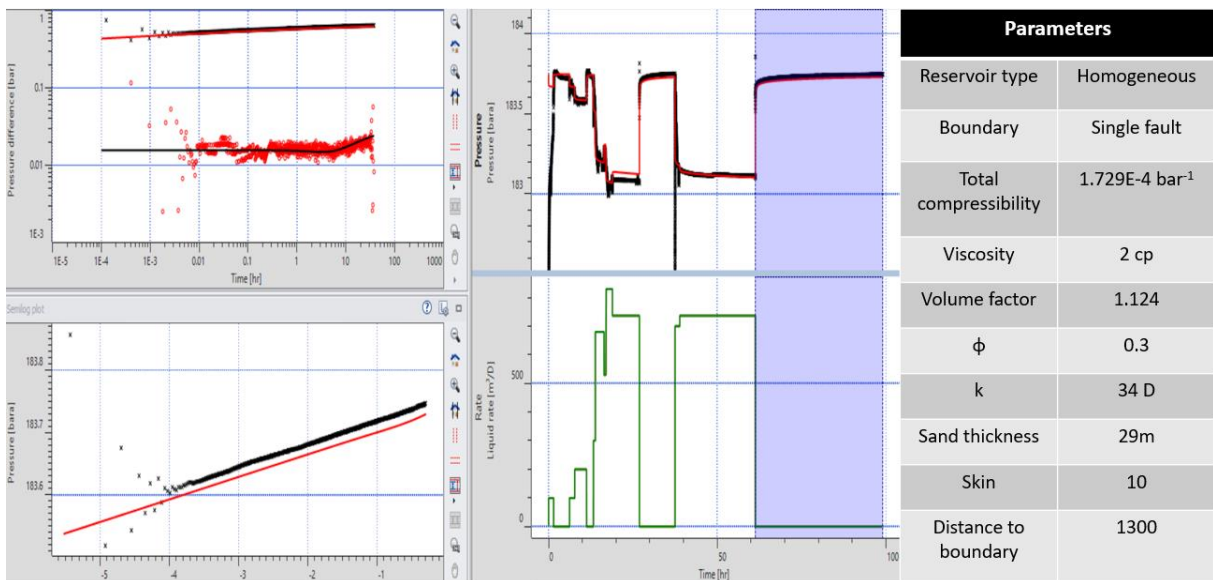
Figure 38 Same previous model, but with a sealing fault 1100 meters from the well.

We see a very good match is achieved, but the distance to the westmost fault do not correlate with the map (*Figure 10*). According to the map the fault is supposed to be 1100 meters from the well. A second analysis was done to see if the other compressibility gives a more correct

length. *Figure 39* display the results and the distance to the fault complied more with the map. This is an interesting observation for the compressibility analysis, since the second compressibility gives a more correct length then the first one. Another observation from this analysis is that kh is not affect by change in compressibility. Only the distance to the sealing fault and skin are affected.

Parameters	
Reservoir type	Homogeneous
Boundary	Single fault
Total compressibility	2.50E-4 bar^{-1}
Viscosity	2.0 cp
Volume factor	1.139
ϕ	0.26
k	34 D
Sand thickness	29m
Skin	10
Distance to boundary	1100
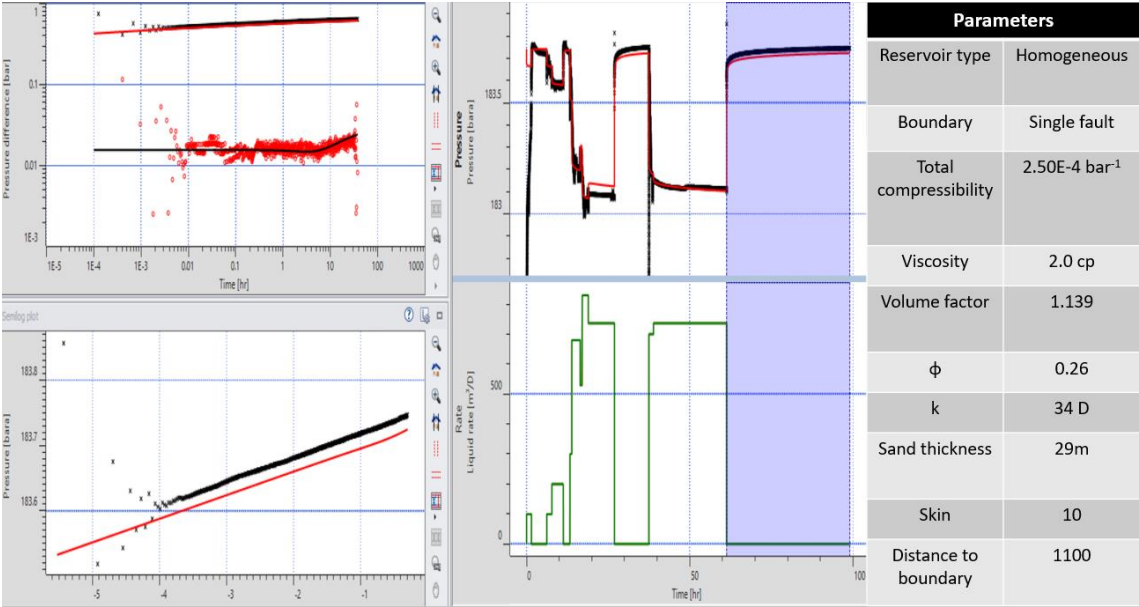
Figure 39 A second model with the parameter values run in the interference test.

4.2.2 Well 16/2-6T2

A second DST was then examined with the average values from the interference test. What was observed was that the sand thickness in the DST did not conform to the observed value in the interference. The thickness was much lower, but the permeability was approximately the same. If we look at *Figure 40* we see that the average permeability value from the interference tests is almost able to match the initial part of the derivative. Core experiments from this exploration well suggested that the value of permeability is around 38D.

Parameters	
Reservoir type	Homogenous
Boundary	Infinite
Compressebility	1.729E-4
φ	0.273
k	34 D
Thickness	6.0 m
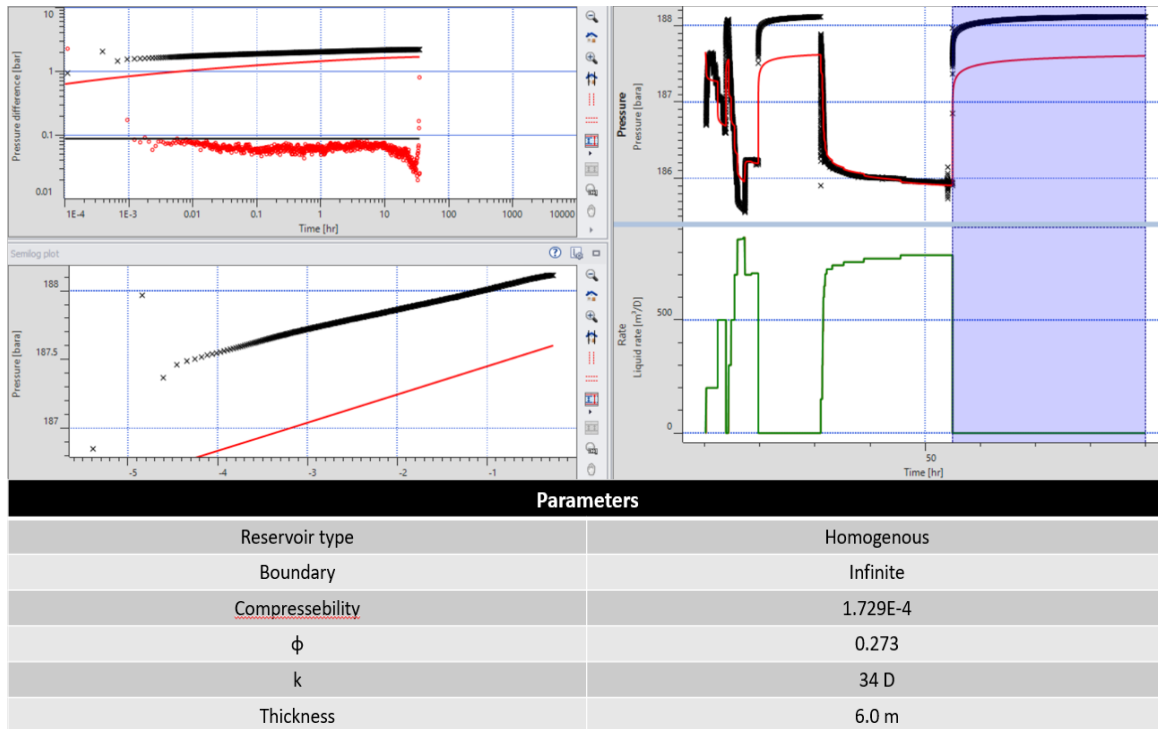
Figure 40 Pressure response from a DST with a model.

If we look at the end part of the derivative, we see that there is a strong dip in it. The dip effect was explained by Sætrom, Selseng, MacDonald, Kjølseth, & Kolbjørnsen in 2016 (appendix A goes through their observations). A test was conducted to discover whether the parameters from the interference test could give a match that made sense with the map from *Figure 10*. By having total compressibility at 1.729E-4 bar[-1] and higher permeability we are able to have a relatively good match with a constant pressure boundary at 1800 meters. These seems reasonable when comparing to the map, but there could be other effects that influences this dip. *Figure 41* shows the results. Other analyses were done with a compressibility at 2.35E-4 bar[-1]. It did not provided a results that comply with the map (*Figure 10*) or match the dip.

Parameters	
Reservoir type	Homogenous
Boundary	Infinite
Total compressibility	1.729E-4
Viscosity	2.04 cp
Volume factor	1.139
Skin	7.5
ϕ	0.273
k	46 D
Thickness	6 m
Constant pressure distance	1800 m
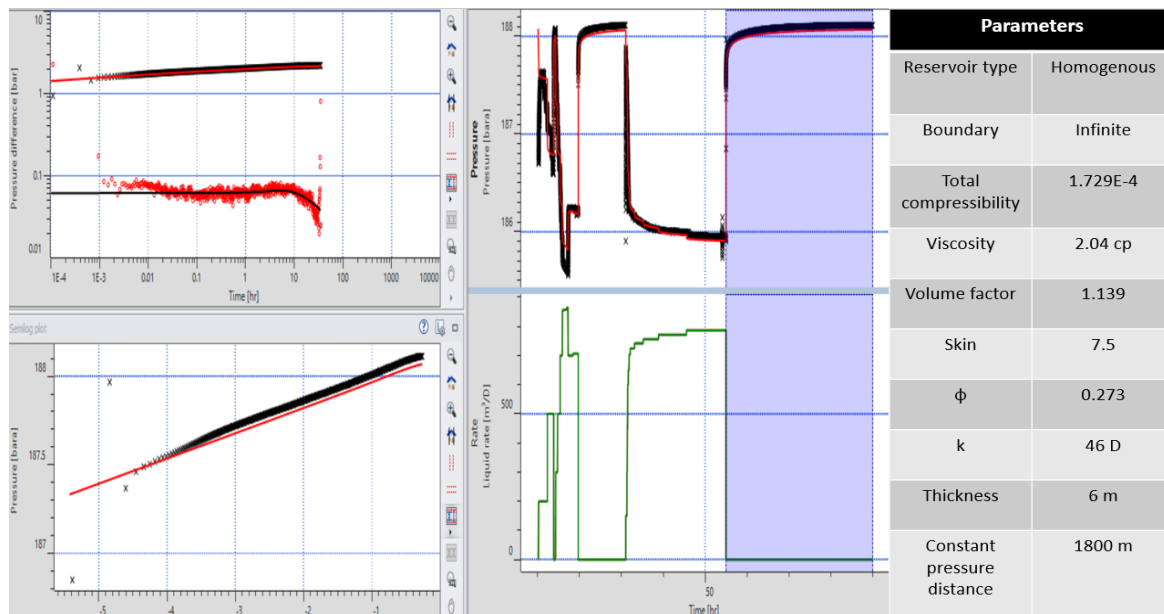
Figure 41 Modified model where parameters values from the interference test were applied and a constant pressure boundary.

4.3 Time-lapse PTA

After the interference tests were conducted, each production well was looked into for finding the periods shut-ins and the flowing that were not to overly affected by noise and lasted for a long time. The reason for looking into the flowing periods is because it is important to look at both types of pressure responses as mentioned in the theory chapter above. Furthermore flowing periods are usually longer and can tell us more about the reservoir further out.

In an ideal pressure response of a shut-in or flowing period for a horizontal well, we should see early radial flow at the start. Then it will transition to linear flow for a short time because of the upper and lower boundaries before, it will again transition to a second radial flow once the flow is further out. In *Figure 42* this is illustrated as the black line that is going straight after the linear flow period. A second case is also illustrated in *Figure 42* (the green line), which illustrates how the sealing fault impacts the pressure response.
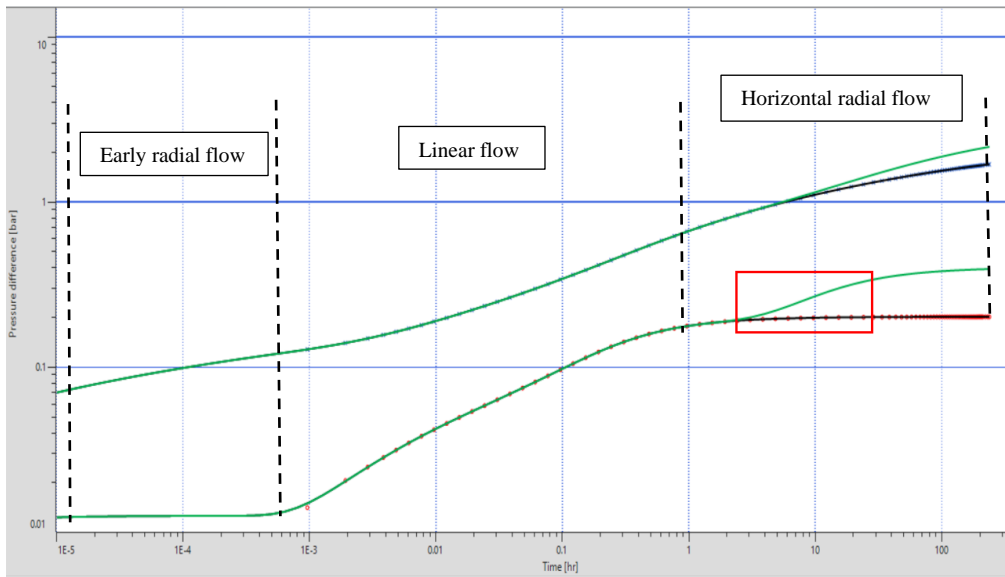
Figure 42 Ideal case of a pressure response of a shut-in or flowing period with a case where there is infinite acting radial flow response and a second case where there is a sealing fault 1000 meters from the well.

In practice, real pressure responses are not as clear because other unforeseen events impact the response. *Figure 43* illustrates selected periods from each production well that had a time-lapse PTA conducted. It was decided that the wells D-9, D-13, and D-14 were most suitable for this form of analysis because the others had either too short transients (production) periods or noisy data set. We see in *Figure 43* that none of them behave like the ideal case.
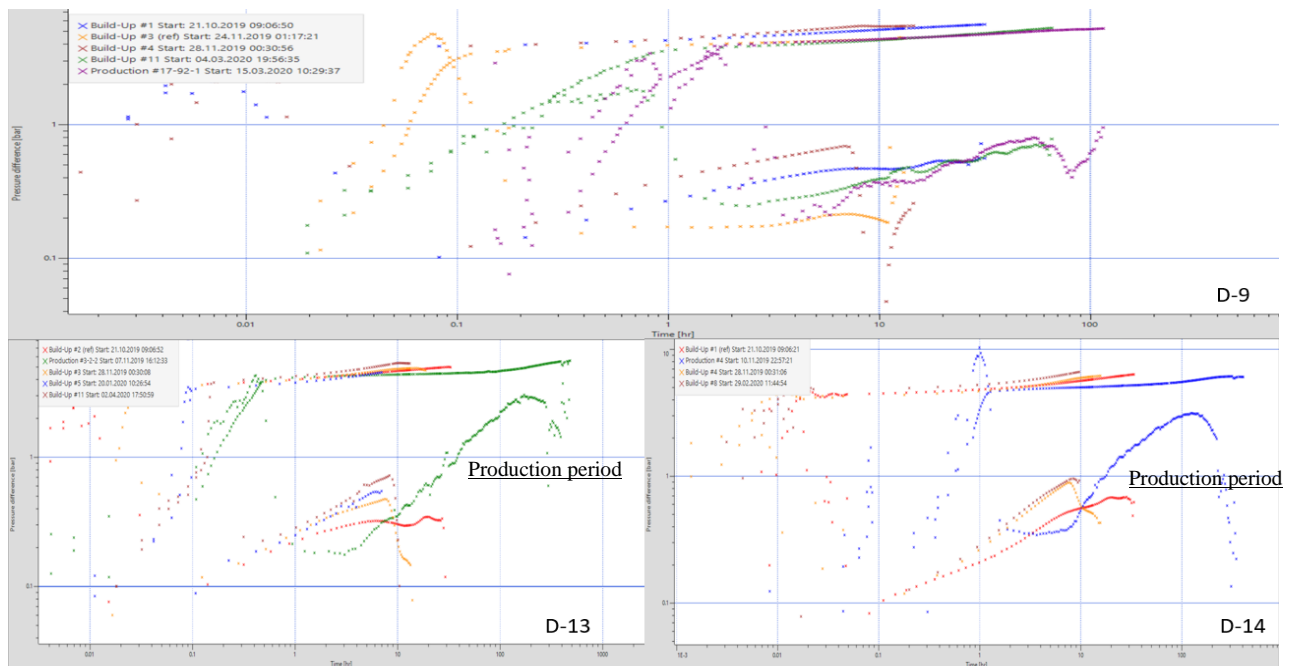
Figure 43 Shut-in and flowing periods from the wells that did time-lapse PTA.

4.3.1 Time-lapse PTA interpretation

In the time-lapse PTA all wells of interest were added to the analysis because it was identified that the presence of other wells had the major impact on the time-lapse pressure shut-in and flowing. First, analytical models were used to look into the periods. This however did not lead to any matches that made sense with core measurement and well logs. The analytical models also deviated a bit from the average values of interference tests. A numerical model was then created with a sealing fault to the west and a leaky fault between D-14, D-11 and D-12 with a 0.25 leakage factor. The model is illustrated in *Figure 44*.
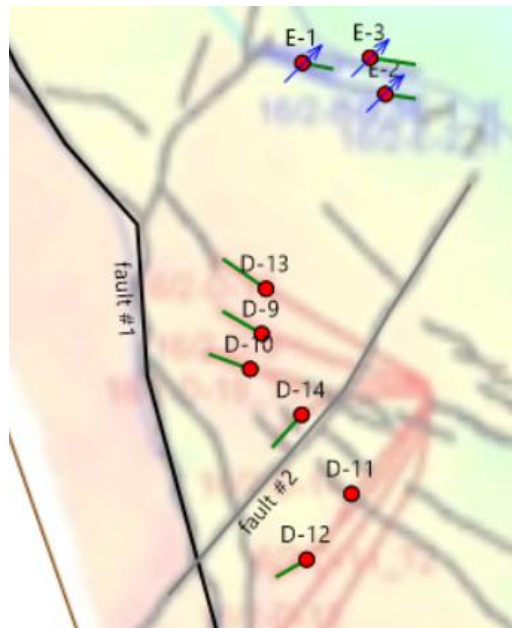
Figure 44 Model set up for time-lapse PTA.

When conducting this analysis, there was a challenge in finding kh for the shut-in or flowing periods. Early radial flow was not visible in any of the periods and second radial flow was difficult to find because of obscureness from nearby wells. In addition, some shut-in or flowing periods did not last long enough for a second radial flow to establish due to well interference. It was also observed when looking at the positions of these production wells that the development of flow regimes does not develop in the way one would expect. *Figure 45* illustrates how flow regimes (drainage area) develop when a well starts to produce accounting for the reservoir boundaries and well locations.
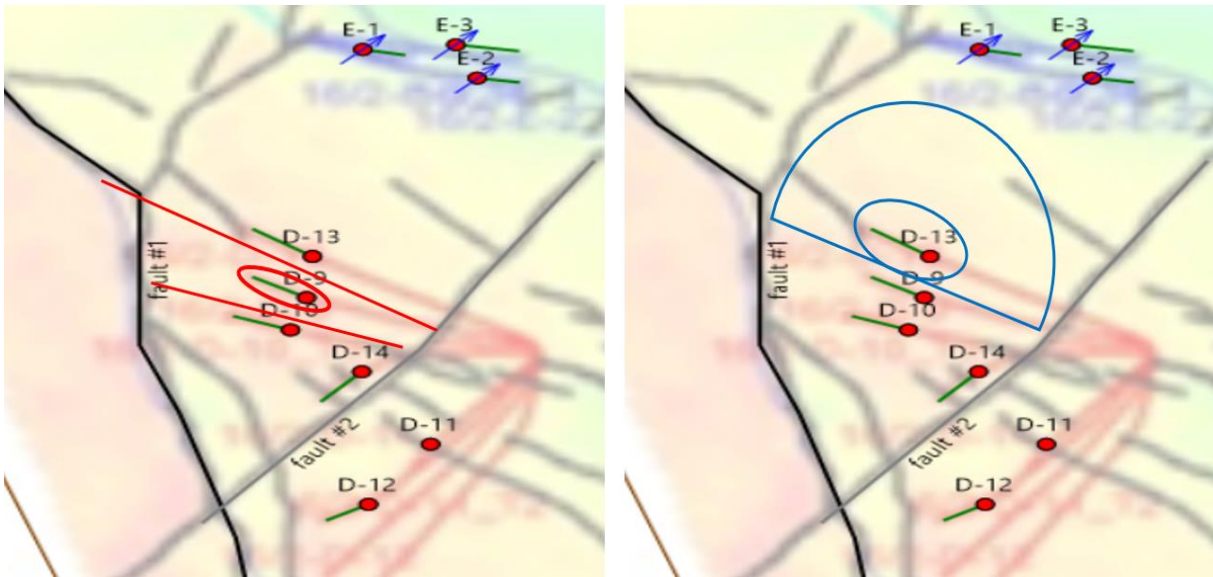
Figure 45 Development of effective drainage area for well D-9 and D.13. Left picture is well D-9 and right picture is well D-13.

On the left side of the figure, we see the development of flow regimes for production well D-9. On the right side of the figure we see the development of flow regimes for production well D-13. Because of the production wells presence, a second radial flow regime is difficult to observe from these periods. This is because neighboring wells act as boundaries for each other, and when they change the rate simultaneously, they interfere with each other. This proves a challenge because in order to find kh there must be presence of a radial flow. It would have been possible to find permeability and sand thickness with a hemi-radial flow in well D-13 (right-hand picture displayed in *Figure 45*. By finding the kh value for the hemi radial flow and dividing it in half we get real permeability and sand thickness. Unfortunately, no second radial flow was observed in D-13 transient periods. However, a shut-in period in the D-9 well shows a close to a second-radial flow regime (elliptical shaped). Therefore, it was decided that this shut-in period was suitable as the initial starting point for time-lapse PTA

When initially conducting time-lapse PTA, the average values of permeability and thickness from the interference tests were applied. The reason for using these values initially was to see if the values from interference tests matched with pressure transient responses in the production wells. In addition, the shut-in period shows a radial flow, but no linear flow beforehand. This makes it challenging to identify what permeability and sand thickness values are reasonable to match the derivative. By applying the average values from interference tests first, it becomes easier to see what values of permeability and thickness are needed if an adjustments on the model is required to make a better match on the transients.

4.3.1.1   D-9

As mentioned above, one of the shut-in periods in the D-9 well was ideal as a starting point for time-lapse PTA because of its proximate radial flow regime. It should be noted that this period also indicates presence of a sealing fault. ***Figure 46*** below illustrates the initial case of the time-lapse PTA with the period from well D-9.

Parameters	
Total compressibility	1.729E-4 bar^{-1}
Permeability	34D
Sand thickness	29m
Distance to fault	1000 m
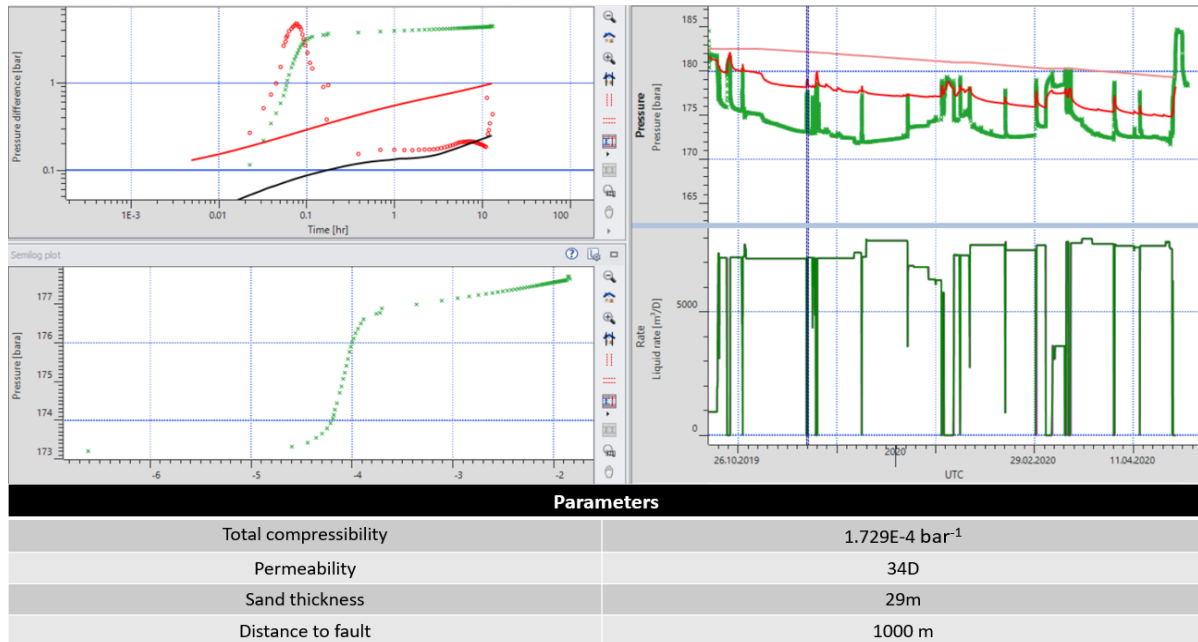
Figure 46 Shut-in period from well D-9 and a model with average values from interference test.

We observed that there is no match with the derivative from this period or the others, but the model behaves much the same as the pressure data. After modifying the permeability, increasing the sand thickness with 1 meter and adding skin into the model a very good match was obtained. The results are displayed in ***Figure 47,*** where also permeability and sand thickness values are shown. The reason why a small adjustment of sand thickness was implemented was to get a permeability value that correlated with the distance to the sealing fault. In a way we are finding kh based on this pressure transient, but with a little help from the interference tests.

Parameters	
Total compressibility	$1.729E{-}4$ bar^{-1}
Permeability	27D
Sand thickness	30m
Distance to fault	1000 m
Skin	9
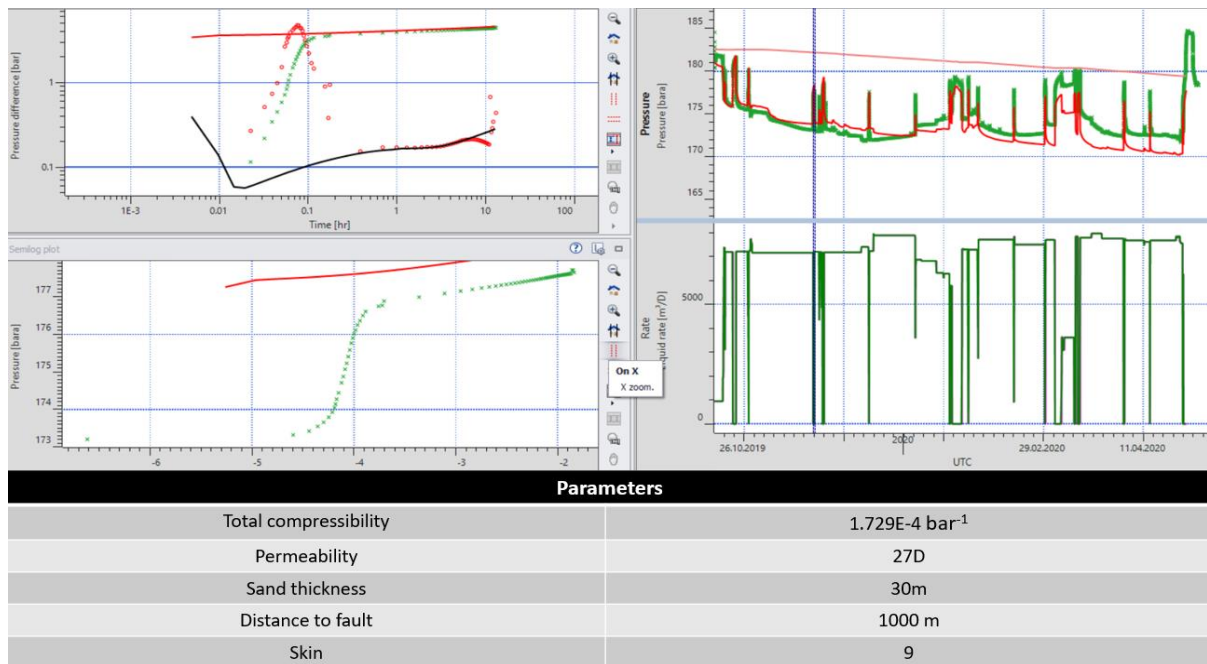
Figure 47 Same shut-in period and model, but modified permeability and sand thickness for better match.

We see that the model matches very well in the middle and end of the development. In the early time of the derivative, the wellbore storage effect is so high that it masks the early flow developments. However, the model's early derivative response makes sense in a theoretical perspective. *Figure 48* shows us how the model performs compared to other transient periods of well D-9. We see relatively good match in all the other periods also, which means there is a possibility that the permeability and sand thickness is around 27D and 30m. What is also observed from the model is that we are not able to match the end of the derivative in one period (top left). Another interesting observation of results is that it in reservoir pressure history, the model does not have the same reduction of reservoir pressure as the real data at the start. However, overtime the model shows a continuation of reduction of reservoir pressure while the data shows it is stabilizing.
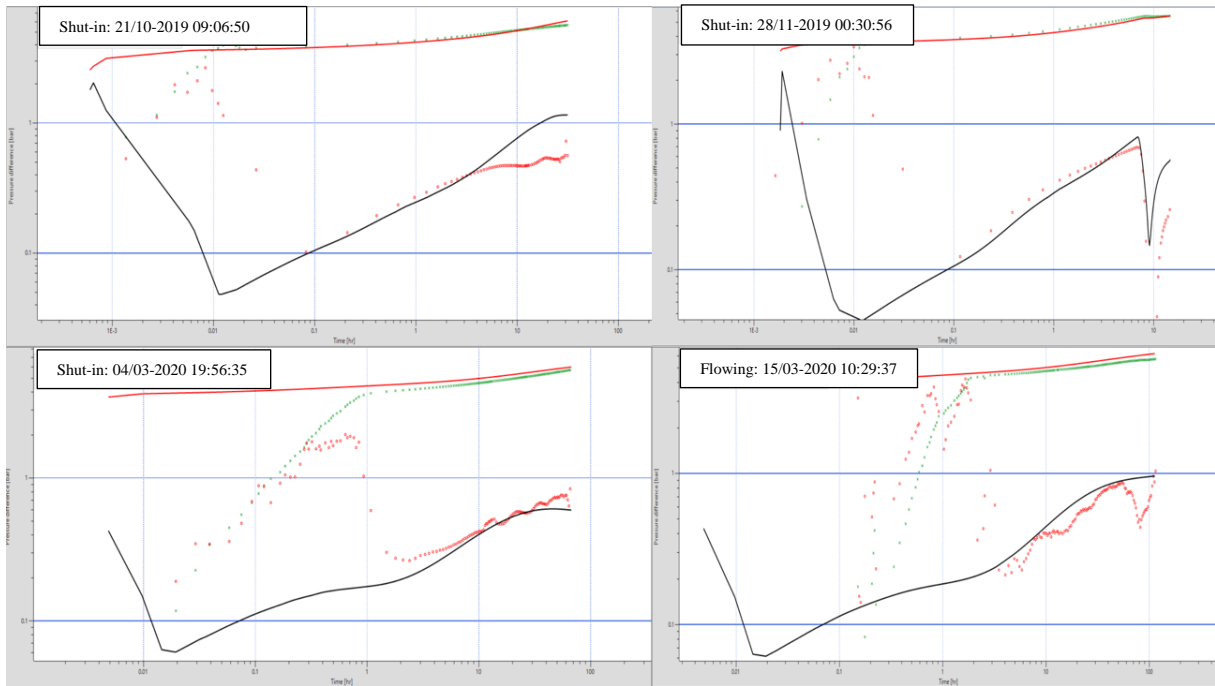
Figure 48 Other periods from well D-9 run with the updated model.

4.3.1.2 D-13

After time-lapse was conducted on well D-9, the values that were estimated in that model were then applied in well D-13. ***Figure 49*** shows us the results of the model for an early shut-in period and ***Figure 50*** show how the model responded in other time periods of the well.

Parameters	
Total compressibility	$1.729E\text{-}4$ bar^{-1}
Permeability	27D
Sand thickness	30m
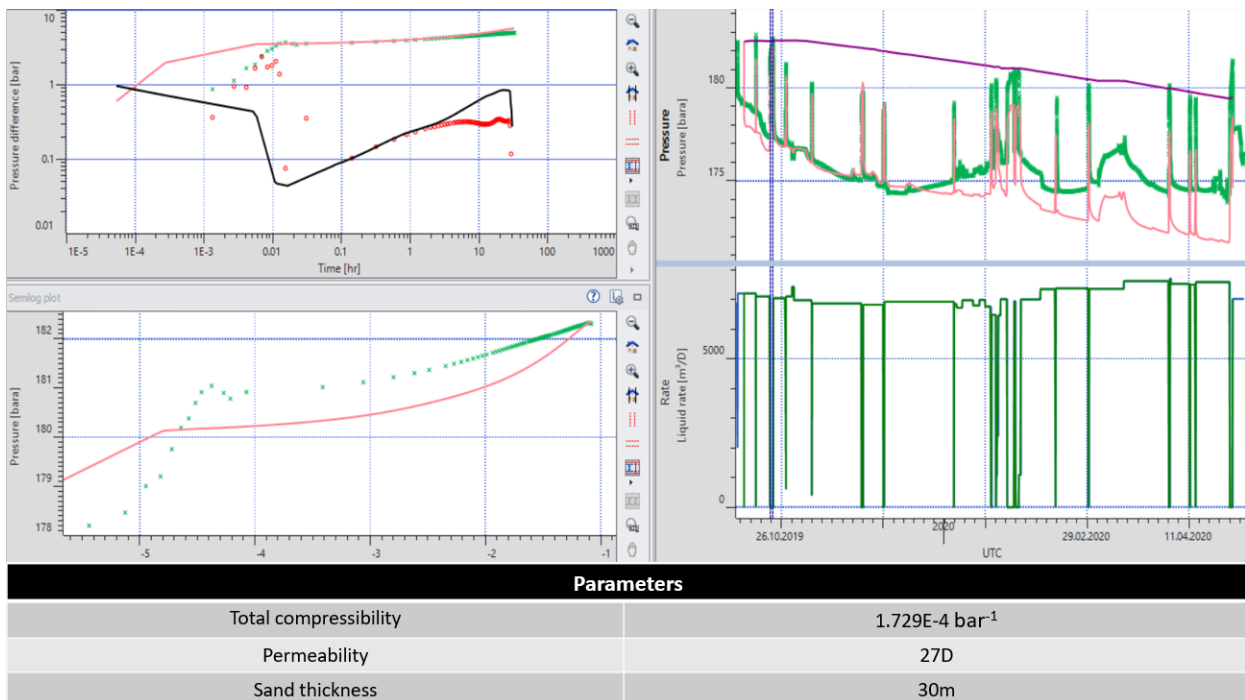
Figure 49 Shut-in period from well D-13 with the updated permeability and sand thickness values.
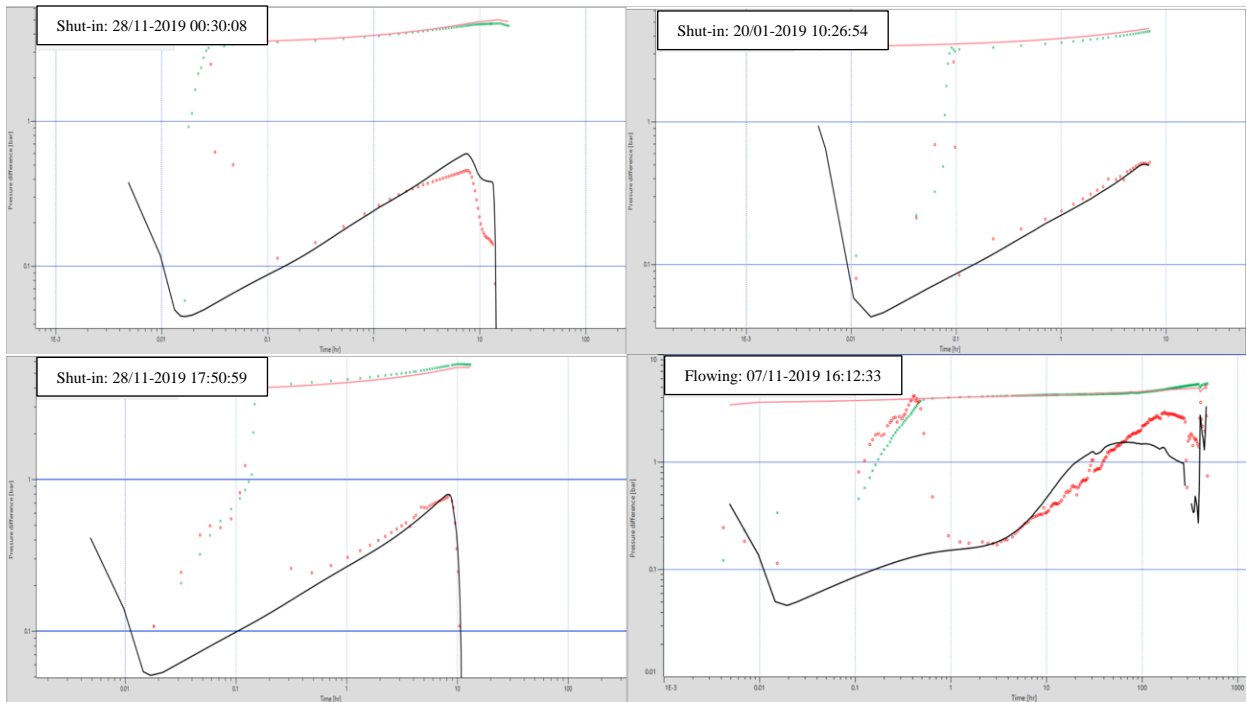
Figure 50 Other periods from well D-13 run with the same model.

Again, we observed in D-13 as in D-9 that there is a good match in the middle stretch of the derivative, but in later phases of the derivatives the model is partially off. Furthermore, we see in *Figure 49* that the model matches the reservoir history pressure better than D-9 initially, but also has a continuous pressure reduction while the data shows that it also stabilizes.

A further interesting observation is in the flowing period (right bottom picture) in *Figure 50*. There we see that the model has the same responses as the real pressure derivative.

4.3.1.3 D-14

The last well that was investigated with the model was D-14. **Figure 51** displays an early shut-in period with the response from the model and **Figure 52** shows us the models response in other periods.

Parameters	
Total compressibility	$1.729E{-}4$ bar^{-1}
Permeability	27D
Sand thickness	30m
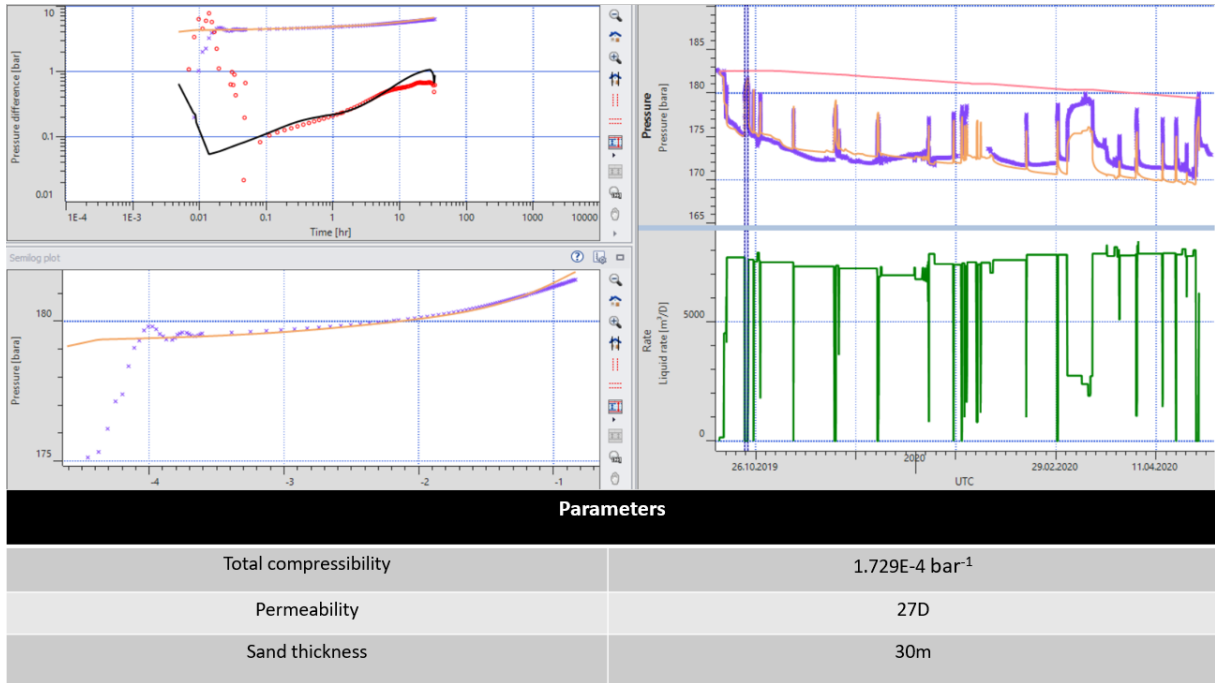
Figure 51 Shut-in period from well D-14.
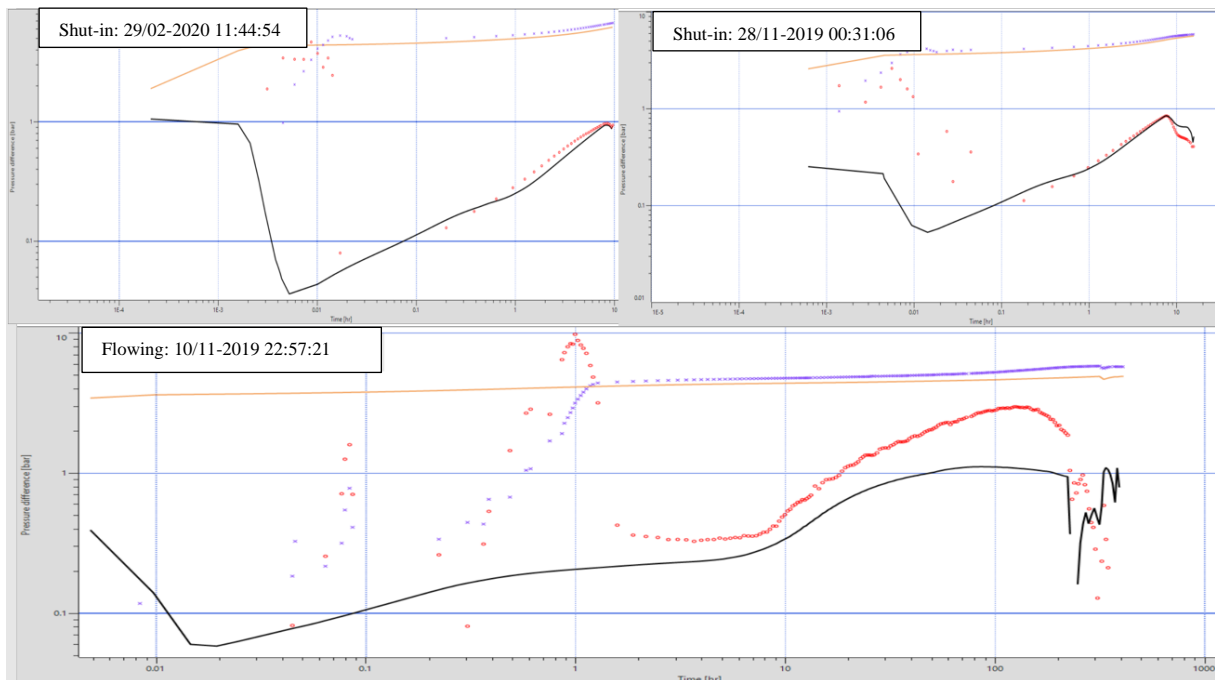
Figure 52 Other periods from well D-14 run with the same model.

What is interesting with the D-14 well is that the model does not match quite as well as in D-9 and D-13. It still has a relative satisfactory match in some of the periods. In contrast to the other wells the model matches the late response with the derivative in some of the periods, and the flowing period (bottom picture) in *Figure 52* shows us that the model successfully identify correct boundaries by having the same shape as the real data. Yet just as in D-13 the model is too low on the log-log scale compared to the derivative. We also see in the reservoir pressure history in *Figure 51* that the model matches halfway of the pressure history, but it also has an ongoing decrease of the reservoir pressure while the real data indicates it is stabilizing.

4.3.2 Sealing fault.

To confirm that the major fault west of the production wells is a sealing fault, a second time-lapse PTA was conducted to see how the model responds without a sealing fault. As we can see in *Figure 53*, the impact by not adding the sealing fault can been observed in both the log-log plot and in the pressure history. By not having the sealing fault to the west, the model is not able to match the late response in the derivative, and the reservoir pressure is not decreasing as fast when compared to real data.

Parameters	
Total compressibility	1.729E-4 bar^{-1}
Permeability	27D
Sand thickness	30m
Skin	9
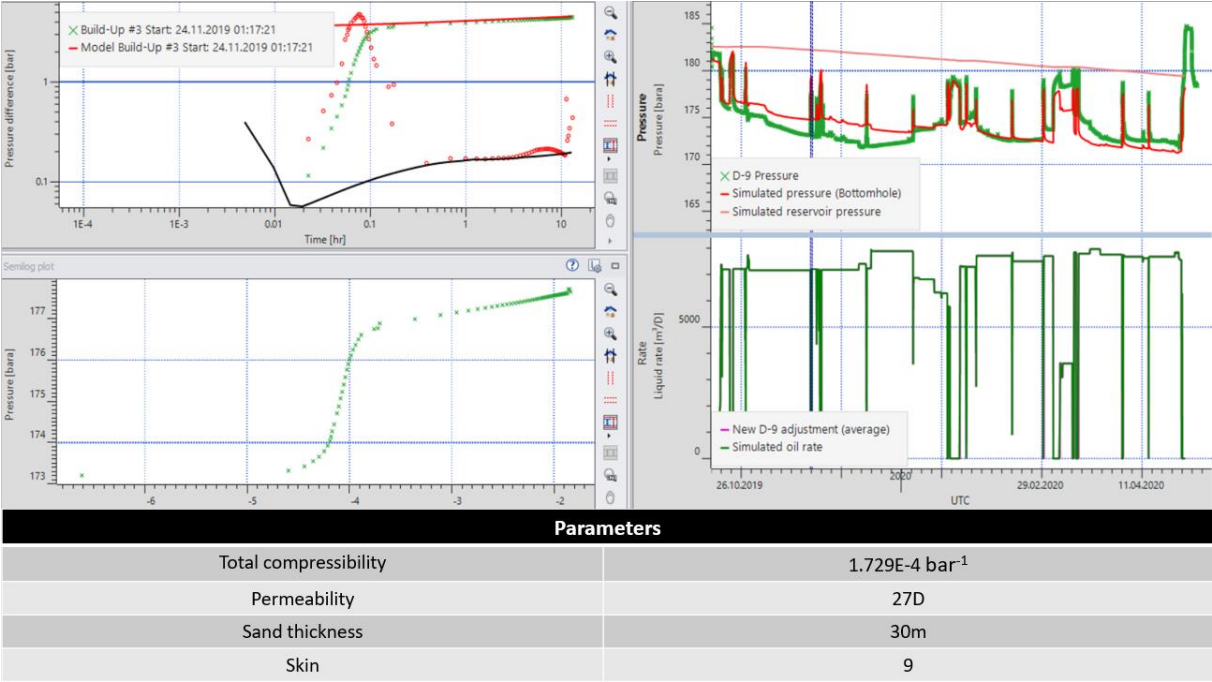
Figure 53 A second model without the sealing fault to the west.

4.3.2 Change in compressibility

When the compressibility changed from 1.729E-4 bar^{-1} to 2.35E-4 bar^{-1} in time lapse PTA, the only noticeable change that was observed was that the distance to the faults shifted. The sealing fault to the west was moved 100-200 meters further in towards the wells, while the leaky fault to the south was moved 100-200 meters further away from the wells. The values for permeability and sand thickness remained unchanged. *Figure 54* shows how moving the sealing fault from the west made the model match again with the pressure derivative. In *Figure 55* displays another period from well D-9 with the updated compressibility. It shows a better match is made with the pressure derivative compared to its first analysis (bottom right corner in *Figure 48*).
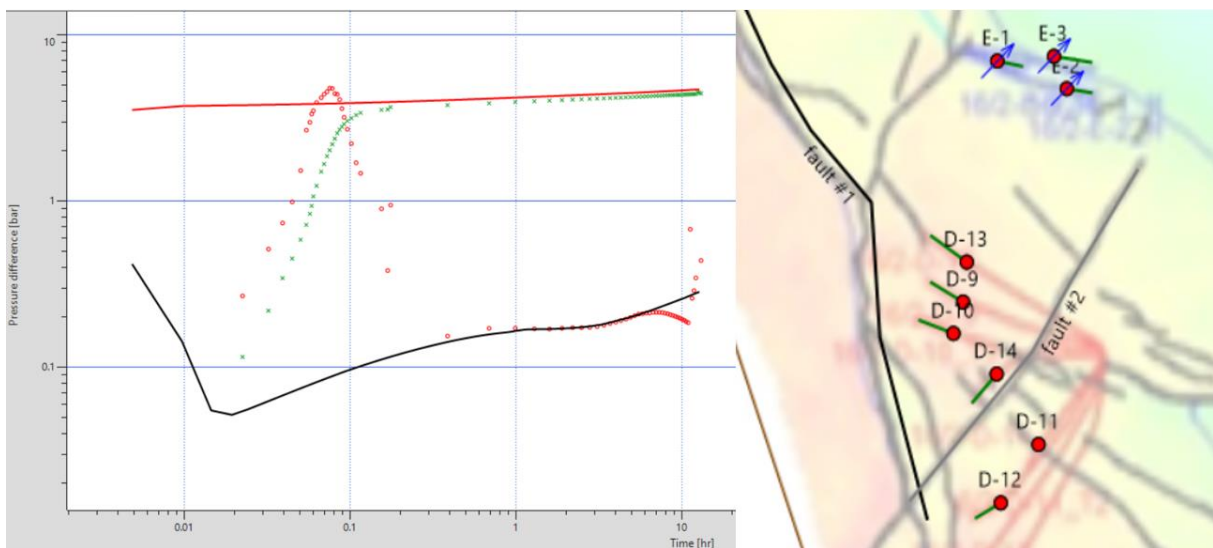
Figure 54 Shows how changing the distance to the sealing fault made the model still able to match the pressure derivative.
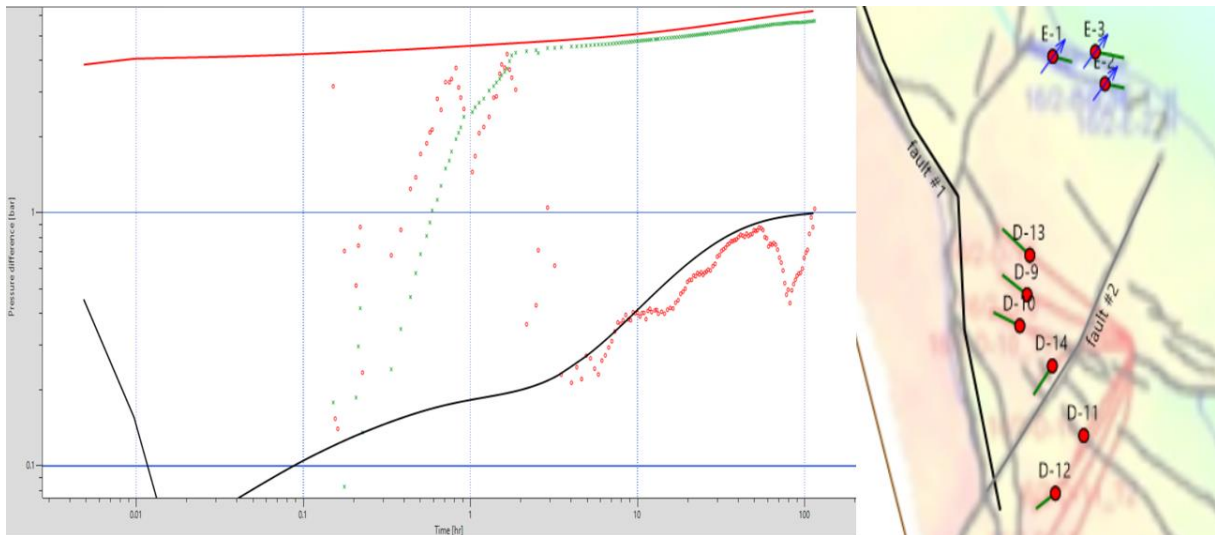
Figure 55 The flowing period of well D-9 shows how moving the sealing fault impacted the model.

In *Figure 56* we see how moving the leaky fault match better with shut-in period from well D-14 as the compressibility is increased. Compared with original shut-in analyse (*Figure 51*) the increase of compressibility lead to better match.
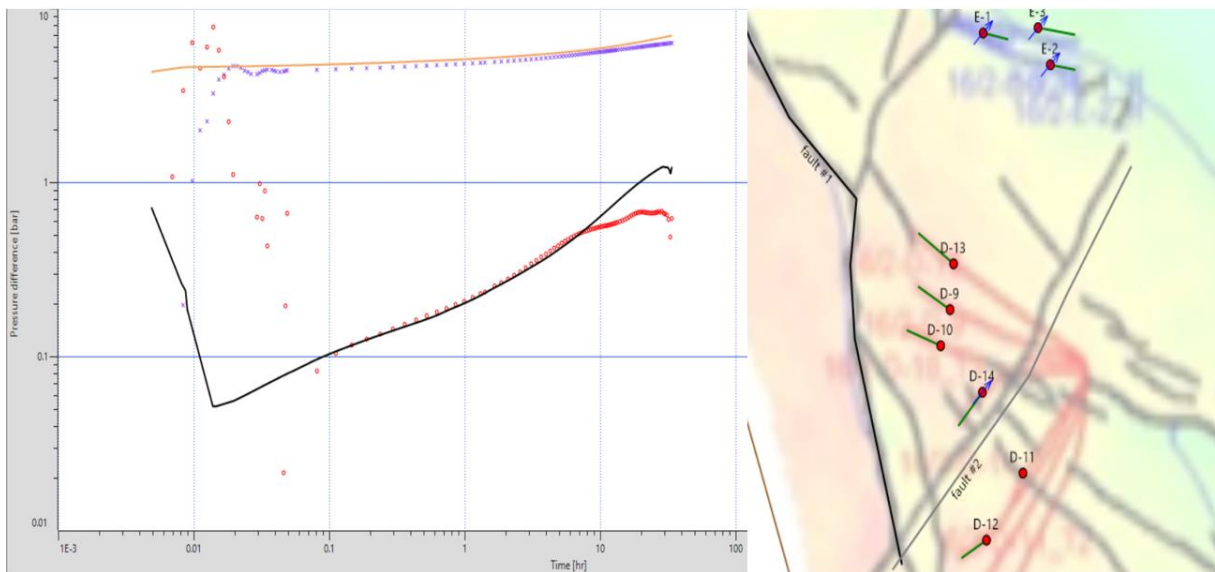
Figure 56 Illustrates how moving the leaky fault further away matched better with the pressure transient in D-14.

Chapter 5 Discussion

In the chapter 'Results' above, we see that the order of analyzing the different sources of pressure transient data is different from common field assessment workflow. Usually the DSTs are analysed first, then you look into interference testing or time-lapse PTA. However, the best data to estimate permeability and sand thickness came from the interference tests. So, the DSTs were analysed after the interference tests, to validate that the average estimates from the interference may be confirmed and finally, time-lapse PTA was applied mainly concentrated on well interference and boundary effects.

5.1 The selection and usage of the data

When starting to analyse the data set from the company, it was discovered early that a few of these wells did not have reliable long-lasting pressure transient responses with low noise level. This was observed both for the interference tests and time-lapse PTA. It was known by the company that the operator of the field did a sequential start of the production wells when the field was starting to produce. The purpose for this was to collect interference data to be analysed. However, when looking into the data from the start of the production there was no interference data sets that was interpretable due to much noise in the pressure data. Additionally, in some wells the step-wise rate changes during a short time, making it hard to observe pressure responses in another wells. Furthermore, the initial production period was looked with traditional PTA, but the data was not interpretable also due to too much noise in the data. *Figure 57* shows us some of the challenges with the initial production period in the most of the wells.
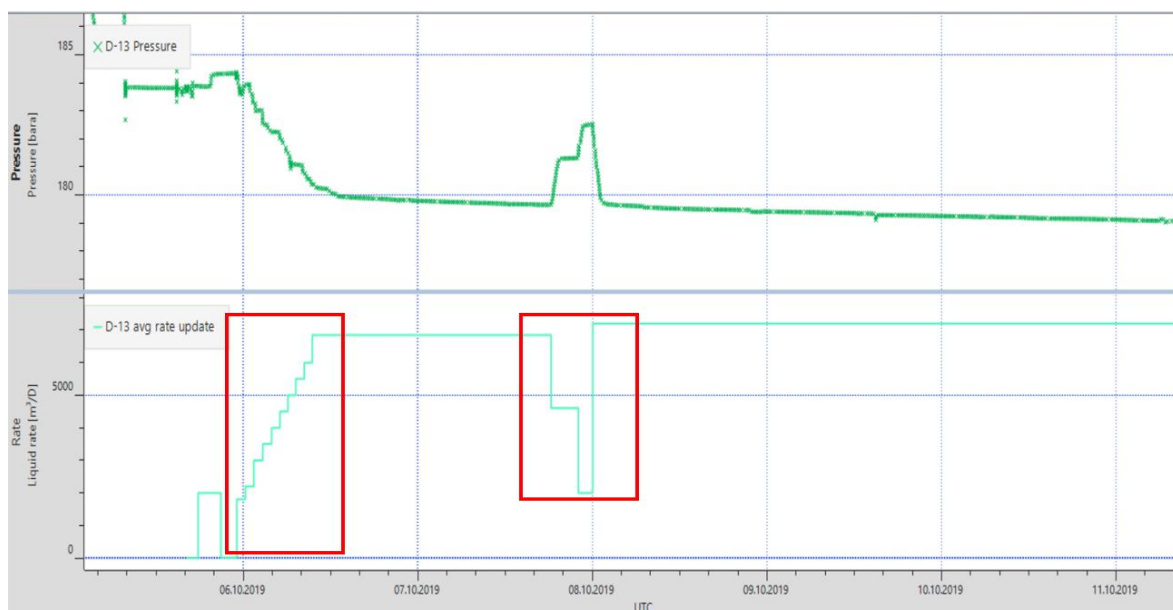
Figure 57 Rate and pressure data from well D-13 when it started to produce. Above is the pressure response and below the rate.

The highlighted periods in the figure are typical cases of the noisy pressure data. These rate changes where seen throughout the other wells when they also started production. Particularly the first highlighted area, which is a step by step increase of production. To be able to analyse an interference test, the rate of the well must change only once, and it has to be a large rate change. Otherwise it is difficult to get interpretable data for the test. In the chase of PTA, these small changes in rates should be accounted in superposition time equation, but since there are so many rate changes in a short time with instability of pressure transients the data was obscured. It should also be mentioned that when choosing a drawdown / flowing periods for time-lapse PTA, stable rate for some period before the analysed one is preferable. Otherwise you are at risk of miss calculation if the drawdown period is after just a small rate change like the second highlighted area in *Figure 57*.

Since the initial periods of the production wells were hard to interpret as an interference test and time-lapse PTA, it was decided to look through the whole production history of the wells and see which wells had the best data sets for interpretation. In the end, the production wells and injectors that were presented in the results chapter were the most suitable for both interference analysis and time-lapse PTA. However, it was important to consider other wells nearby when analyzing these periods, since neighboring wells could have an effect.

5.2   Challenges with estimating permeability and sand thickness

Results from time-lapse PTA with shut-in and flowing periods from all the production wells showed good indication of a linear flow regime. However, what was not observed from either the shut-in periods or the flowing periods was the early radial flow regime. Comparing the ideal reference case (*Figure 42*) with one shut-in (for example *Figure 46*) there is supposed to be indication of early radial flow regime in the pressure response. There is couple of reason why the early radial flow regime is not visible in the pressure responses from the production wells. The first reason is because of large wellbore storage (WBS) effect. We see for example in *Figure 46* that the initial period of the pressure response is dominated by a large WBS. A reason why the WBS is dominating so early and so long initially is because the gauge and the valve in the well is far from each other (showed in the field case), and the wells are producing at very large volumes. By starting or stopping the production from these wells means large quantities of compressible fluids with potential redistribution inside the well which creates WBS pressure responses that affect the gauges. An additional effect that increases the amount of time for WBS is that these wells are being gradually shut-in. Because of large volumes of liquid is being produced, the wells are being gradually shut-in or gradually started up to make sure the wells

do not experience to much force or strain from the oil flow. This of course also makes WBS longer.

The second reason why the early flow regime is not visible in the real well datasets is because of high permeability values compared to sand thickness values. The flow of liquids is traveling very fast in the reservoir. Thereby, the derivative in a pressure response goes straight into linear flow in a matter of few seconds. In our ideal case *Figure 42,* we see that the first radial flow comes in a couple of seconds before it turns into linear flow. Thereby, we are not able to see the early radial flow regime even without WBS.

Early radial flow regime is vital to estimate kh is because the presents of nearby wells is usually having an impact on the second radial regime. Since the flow of liquids is going so fast, the production wells are impacting each other. Thereby affecting the flow regimes. *Figure 45* in the result chapter shows us how the pressure travels in some of the wells and it demonstrates that we are usually not able to achieve second radial flow. Thereby, trying to estimate kh based on this flow regime could lead to inaccurate estimations. This provides a multitude of challenges when we are setting up our models for our analysis in time-lapse PTA and find one of our main goals with the thesis. Another thing that also would be impacted by not having the right kh values is the distance to the fault. By estimating the kh value wrong, the distance from a well to a boundary is wrong. Thereby making the model useless. Furthermore, estimation of skin and other parameters will also have an impact by estimating wrong kh.

Although it was not difficult to estimate kh with a certainty in time-lapse PTA, it was possible to estimate kh with interference tests. The advantages of using interference analysis is that it is not strongly impacted by WBS but dependent on having a radial flow regime to conduct an analysis. You only need a well to do a large rate change and a well close to it for observing the response. The interference test provides valuable information for further analysis in PTA because there were some data on what values of permeability and sand thickness was around the production wells. Rightfully so, it is not the most accurate way to use the average values from all interference analysis from a specific area and use it as initial starting point in time-lapse PTA to find the best match. However, when there are no possibilities to accurately find kh in any periods of a standard well test, other methods have to be used to be able to have some idea on what the values might be. It should be noticed though that one of the challenges with an interference test in a field with multiple wells is to find a period where only one well is doing a rate change during a long period while others wells are hold constant. Most times, several wells do rate changes at ones, making interference data obscured and not interpretable.

5.3 The results

When going through the results of both analyses of interference and time-lapse PTA, we can see that the sand thickness of around 30 meters provided reasonable match of the observed transients. However, there are some differences of permeability estimations between the interference analysis and time-lapse PTA.

5.3.1 The interference analysis

When first looking at the interference analyses including only active and observation wells (no other neighbor wells), the only analyses with consistent results were the ones that looked into the leaky fault. The rest of the analyses obtained different values for permeability. However, after conducting analysis with all production wells and injection wells in the interference tests, the spread of different permeability values was reduced. This proves that the neighbor wells may have an impact on the analysis. We see in *Figure 10* that the three production wells, D-9, D-10 and D-13 are in very close proximity to each other and interference analysis for these wells was impacted by inclusion of an additional well to the interfering pair. This could be a reason why the interference analysis results may vary depending on including other neighbor wells to the interfering well pair.

A second reason why the permeability values are different could be because the reservoir is heterogenous. As stated in the field case chapter, the reservoir consists mainly of unconsolidated sandstone. Parts of the area could have different permeabilities because the rock distribution is different in each area. However, there could be other factors that reduces the permeability.

5.3.1.1 The leaky fault

If a fault is present between active and observation wells, the interference test may be used to estimate cross-fault leakage, at the same time sealing fault prevents any interference. As shown in the result chapter, a fault identified from the seismic interpretation was looked into between the wells D-11, D-12 and D-14. Several attempts with an open fault between the wells were taken to see if there was a reasonable match within the limits of other geological data, particularly the pay thickness limitations. As shown in *Figure 20* and *Figure 21* this was not achieved and therefore there is some belief that a restriction of flow is happening across the fault. A good match was achieved after setting up a numerical model and adding a leakage factor on 0.25 across the fault (shown in *Figure 23*). To confirm that this model is reasonable, a second interference between D-14 and D-12 was analysed using the same model and parameters. A good match was achieved here as shown in *Figure 26*. It should be noted

however that the cross-section plot over this fault (***Figure 14***) shows a small throw and a large amount of sand between these wells. So, a leakage factor on 0.25 is perhaps too low. Although the model from the interference may contradict the illustration from the cross-plot, there could be other factors that prohibit the flow between the wells.

Another thing that was discovered subsequently was that well D-11 is a slanted well which goes down to a second sand formation underneath. This sand however has much lower permeability ranging in 1 – 10 D. As such, the model should have lower permeability to see the effect from the layer underneath. Nevertheless, it could have an effect on the interference test by making the leakage factor inaccurate. However, the D-12 production well is horizontal and there is no additional layer of sandstone underneath. Although the model managed to match this pressure response with a value of 0.25 leakage, it is recommended a further investigation of this fault with 3D simulations, e.g. in Kappa Rubis software, to evaluate importance of the layer underneath D-11.

5.3.2 Time-lapse PTA

Because of high permeability values in the field, it was observed in time-lapse PTA that nearby wells were interfering during the most of the transient periods. Two transition periods on top of ***Figure 48***, shows a sharp increase in both derivatives before they begin to flatten out. This is because in these periods all other neighboring wells were also closed in, which impacts the pressure response. In a standard flow regime development for a horizontal well, linear flow appears when the pressure transient impacts a top and a bottom layer. In this case however, the production wells are creating additional boundary effects on the pressure response. Hence, these wells are extending the linear flow when a multitude of them are shut-in at the same time. This effect demonstrates the importance of adding other wells. In some cases, neglecting neighboring wells have strong impact on estimated kh values.

When first starting to conduct the time-lapse PTA, it was a little surprising that the average values from the interference test gave us a model that looked like a potential good match. It was also surprising that not much adjustments were necessary on the permeability and sand thickness to get a good match with the periods in all the production wells that were in focus. Especially with a model that contains nine wells impacting the pressure response. It should be noted that it was fortuitous that the D-9 well had a long shut-in which indicated radial flow behavior (***Figure 46***). This created the ideal starting point to match the model (unlike other shut-in and flowing periods).

We see with the permeability of 27 Darcy and 30 meters of sand thickness that a relatively good match is achieved in most of the shut-ins and flowing periods in these wells. When comparing the values from time-lapse PTA with average values from interference test, there is a deviation with the permeability value. Ideally, we should see that both analysis techniques yield the same value. However, the deviation is around 20% which is acceptable. Nevertheless, the results from time-lapse PTA and interference tests indicates that the area of interest have permeability at around 27D-34D and a sand thickness around 29-30 meters.

An interesting observation from the time-lapse PTA model is that it does not manage to match the end of the derivative in a couple of shut-ins and flowing periods. We see this in all three wells from *Figure 48* to *Figure 52*. Particularly these long flowing periods from D-13 and D-14 (bottom right in *Figure 50* and bottom in *Figure 52*). The model managed to match the trend of the pressure responses, but not align with the data. This could be an indication that the permeability value is lower as the pressure wave is traveling further from these wells. In addition, there are observations of tidal effects in some of these periods. This is due to high permeability value and low pressure drop at production. However, we observe that the tidal effects do not corrupt the trends in the data and responses on the transients are smooth enough. Hence reducing (smoothing) of the tidal effect was not studied in the thesis.

What is also an interesting observation from the time-lapse PTA is the pressure history from each production well. We observe that the reservoir pressure initially decreases faster than the model but stabilizes one to two months after production has started, whereas the model continues to decrease. An explanation for why the model is not able to match the pressure history is because of the left-out production wells and injectors. If we take a look at *Figure 10* we see that there are two more production wells south of D-12 and a couple of more injectors even further down south of the reservoir. Due to the area of interest and scope of the thesis, these two wells and the injectors further south were excluded. Although they were not included, the model shows that these wells have an impact on the reservoir pressure around the area of interest. This proves that there is interference from the two last producers and the injectors down south.

5.3.2.1   *Sealing fault*

There was also a sensitivity analysis if the sealing fault to the west of the reservoir is sealing. As mentioned in the field case the cross plots only show the faults geometry, but it does not point out if it is sealing or not. Therefore, a sensitivity analysis was done to confirm this case even though there were clear indications from the cross plots that this fault should be sealing.

By comparing the model with a sealing fault in *Figure 47* and the other model without the fault in *Figure 53*, we see that without the sealing fault, the model is not able to match the end of derivative. In addition, we see that the model without a sealing fault does not decrease the reservoir pressure as fast as the model with fault, and the pressure history shows that the reservoir pressure decreases rapidly initially. Therefore, there is evidence that the fault to the west is sealing.

5.3.3 The DSTs

When reviewing the DSTs with the results from the interference, it was observed that the average values from the interference test helped to fit the pressure response in well 16/2-17S, and that the permeability from the interference tests also confirmed by matching DST of well 16/2-6T2. It indicates that the values from interference tests are viable. At the same time, by changing the permeability to 27D and increasing thickness to 37 meters provides an identical model as in *Figure 37*, and these values comply more with the time-lapse PTA. So, it is difficult to tell which values are closer to reality. Furthermore, results may indicate a presence of sealing fault to the west with well 16/2-17S. This means that this large fault west of the field, displayed in *Figure 10* is sealing all the way around the areas of interest and further south. It was investigated if other faults in the area could lead to same answer and it was found that it could be the case within the uncertainty range for permeability, pay thickness and compressibility, but it seems to be an extreme case.

When investigating well 16/2-6T2, it was challenging to explain the dip in the derivative. The form itself is indicative of a pressure support. However, it was hard to determine what causes it. Sætrom, Selseng, MacDonald, Kjølseth, & Kolbjørnsen, 2016 argued that the dip is caused by viscosity difference (oil / water at the oil-water contact), but the model indicates that the change from oil to water is happening at around 1300 meter. However, the map (*Figure 10*) shows the aquifer is at around 2000 meters. By using the first compressibility ($1.729E-4 \text{ bar}^{-1}$), the model can match the distance to a constant pressure boundary without changing the permeability.

Another possible cause for this dip may be conductivity of the faults around the well so they might provide hydraulic connection to the other areas of the reservoir (like aquifer) and pressure support. (Shchipanov, Kollbotn, & Berenblyum, 2017) studied a field case with faults between wells and showed similar derivative behavior (similar to constant pressure boundary effect) for conductive faults. This is a hypothetical case requiring further investigation of these faults and

their conductivity along with sensitivity analysis, e.g. with the total compressibility value, that could provide explanation for such a dip of the derivative.

5.4   The difference in compressibility

We observe that the compressibility has a significant impact on most of the analyses. In the interference test we observed that change in compressibility led to change in permeability and thickness, along with adjustments to the leakage factor. In the DSTs and time-lapse PTA, we observed that the distance to faults and skin is impacted by the compressibility change. Total compressibility is considered a very important parameter to all forms of well testing, because it establishes how fast the pressure pulse travels in the rock. When doing lab tests on this property it is usually a high certainty that the value from the experiments is relevant to the reservoir in focus. Yet, in our case some uncertainty with the rock compressibility was involved. We therefore investigated impact of two different values limiting the range of the uncertainty with total compressibility: 1.73E-4 and 2.35E-4 bar^{-1}.

The first total compressibility has yielded results from interference tests that make sense to the geologically proven range for sand thickness and to some degree permeability. It has also provided a kh value that matches the distances to observed faults in time-lapse PTA. However, when increasing the compressibility factor, kh and distances to faults do not match. Although a higher compressibility led a higher leakage factor that seems more realistic based on the cross plot over the fault. We also see that in one DST a better match was achieved by using the second compressibility and in the other DST it was better to use the first one.

In summary, it is difficult to firmly conclude which compressibility is more representative for the reservoir. When examining the results, the first compressibility seems to produce most matches. It provided a model that got obtained good matches in time-lapse PTA with a sealing fault to the west, and with a permeability and sand thickness values that suits with other geological data. However, future studies are recommended to see if the uncertainty in rock compressibility is the reason why some matches are not achieved or if there are other factors like reduced permeability or sand thickness in certain areas which are the cause.

Chapter 6   Conclusions

In this thesis an investigation has been conducted into estimating sand thickness and permeability for the Johan Sverdrup field. In addition, certain faults were examined to indicate if they were sealing or conductive. A comparison between two models with different compressibility was also undertaken. A series of interference tests and time-lapse PTA conducted over this field were reviewed to demonstrate strengths and weaknesses for both techniques. Few results came out of this investigation, the conclusions of which are as follows:

- The interference tests provided results that indicates a sand thickness around 29-30 meters. Concerning permeability, most of the tests provided different results. However, on average the permeability was around 34 D. Compared with other sources of data like core logs, these values seem reasonable. Using the average values from interference tests on nearby DSTs showed a reasonable match. It was also observed that other wells nearby the source well (active well) had an impact on the interference analysis.

- Time-lapse PTA was initially conducted using the average values of permeability and sand thickness from the interference test, since it's difficult to observe radial flow in the shut-in periods or flowing periods and well interference seems to drive the time-lapse pressure transients. After modifying permeability and sand thickness to 27 D and 30 meters we achieved a good match in most periods with the three production wells. However, the values used are slightly deviate from the results of the interference tests.

- A leaky fault was investigated with two interference analyses which provided a value for the leakage factor. It is recommended to undertake more analysis to this fault just to ensure that all possible impacts on the interference test are considered. Verification of a sealing fault west of the reservoir was also conducted with time-lapse PTA in production wells and standard PTA with one DST. All confirmed sealing conditions on the fault.

- We observe that it is easier to identify permeability and sand thickness with interference tests rather than with time-lapse PTA. However, time-lapse is better suited to identify faults around the wells and well interference over the whole life of the field. If a clear radial flow regime is identified in time-lapse pressure transients, it becomes an ideal tool to find kh, distances to faults and their conditions.

- Two compressibilites were tested to see how change in this property affects the results in the analyses. A comparison of results was also done between these compressibility's to identify which one gave a more realistic match with the pressure response. Compressibility of 1.729E-4 bar^{-1} gave most matches, but this does not mean this is the

right value. Further studies and lab testing on the rock compressibility are recommended.

- Time-lapse PTA with numerical reservoir model with multiple wells was able to match several transient periods. This indicates that there is communication between wells and major reservoir features has been implemented into the model.

References

Ahmad, S. B., BinAkresh, S., & Anisur Rahman, N. (2016). Application of Deconvolution Technique in PTA for Enhanced Reservoir Characterization. *SPE Kingdom of Saudi Arabia Annual Technical Symposium and Exhibition* (p. 11). Dammam, Saudi-Arabia: Society of Petroleum Engineers.

Al-Khamis, M., Ozkan, E., & Raghavan, R. (2005, 1 8). Analysis of Interference Tests with Horizontal Wells. *SPE Reservoir Evaluation & Engineering*(SPE-84292-PA), ss. 337-347.

Ambastha, A., McLeroy, P., & Grader, A. (1989, 6 1). Effects of a Partially Communicating Fault in a Composite Reservoir on Transient Pressure Testing. *SPE Formation Evaluation, 4*(2), 210-218.

Bourdet, D. (2002). *Well Test Analysis: The use of advanced interpretation models* (3 ed.). (J. Cubitt, Ed.) Elsevier Science.

Chaudhry, A. (2004). *Oil Well Testing Handbook.* Elsevier Science.

Cinco-Ley, H., Samaniego-V., F., & Viturat, D. (1985). Pressure Transient Analysis for High-Permeability Reservoirs. *SPE Annual Technical Conference and Exhibition* (p. 10). Las Vegas, Nevada: Society of Petroleum Engineers.

Dastan, A., & Horne, R. (2010). Significant improvement in the accuracy of pressure-transient analysis using total least squares. *SPE Reservoir Evaluation & Engineering, 13*(4), 614-625.

Feng, Q., Wang, S., Zhang, W., Song, Y., & Song, S. (2013). Characterization of high-permeability streak in mature waterflooding reservoirs using pressure transient analysis. *Journal of Petroleum Science and Engineering, 110*, 55-65.

Franco, F., Rincon, A., & Useche, M. (2018). Alternative Method for Pressure Transient Analysis. *Abu Dhabi International Petroleum Exhibition & Conference* (p. 17). Abu Dhabi, UAE: Society of Petroleum Engineers.

Glover, P. W. (2000). Petrophysics. *University of Aberdeen, UK*, 270.

Gringarten, A. (2012). Well Test Analysis in Practice. *The Way Ahead, 08*(02), 10-14.

Horne, R. N. (2007). Listening to the Reservoir—Interpreting Data From Permanent Downhole Gauges. *Journal of Petroleum Technology, 59*(12), 78-86.

Houzé, O., Viturat, D., & Fjaere, O. S. (2011). *Dynamic Data Analysis.* KAPPA.

Kuchuk, F., Goode, P., Brice, B., Sherrard, D., & Thambynayagam, R. (1990). Pressure-Transient Analysis for Horizontal Wells. *Journal of Petroleum Technology, 42*(08), 974-1031.

Larson, L. (2010). *Well Testing-Analysis of Pressure Transient Data.* Stavanger: University of Stavanger.

Ludvigsen, B., & Le, H. (2015). DST Matching and Interpretation Through Numerical Well Testing on the Johan Sverdrup Field. *SPE Annual Technical Conference and Exhibition* (p. 38). Houston, Texas: Society of Petroleum Engineers.

Mosaheb, M., & Zeidouni, M. (2017). Pressure Transient Analysis for Leaky Well Characterization and Its Identification from Leaky Fault. *SPE Health, Safety, Security, Environment, & Social Responsibility Conference - North America* (p. 13). New Orleans, Louisiana, USA: Society of Petroleum Engineers.

Oguntoye, P., Okpoiri, C., Akinyede, E., Afoama, E., & Ikwan, U. (2014). Divergent and Convergent Thinking Approach: A More Integrated Method to Pressure Transient Analysis and Interpretation. *SPE Nigeria Annual International Conference and Exhibition* (p. 23). Lagos, Nigeria: Society of Petroleum Engineers.

Onur, M., Ayan, C., & Kuchuk, F. (2011). Pressure-Pressure Deconvolution Analysis of Multiwell-Interference and Interval-Pressure-Transient Tests. *SPE Reservoir Evaluation & Engineering, 14*(06), 652-662.

Osman, Y., Retnanto, A., Samir, M., & Fraim, M. (2017). Enhancing Pressure Transient Analysis through the Application of Deconvolution Methods, Case Study. *SPE Middle East Oil & Gas Show and Conference* (p. 15). Manama, Kingdom of Bahrain: Society of Petroleum Engineers.

Sahni, A., & Hatzignatiou, D. G. (1995). Pressure Transient Analysis in Multilayered Faulted Reservoirs. *SPE Western Regional Meeting* (p. 14). Bakersfield, California: Society of Petroleum Engineers.

Schlumberger. (2002). *Well Test Intrepretation.* Schlumberger.

Shchipanov, A., Berenblyum, R., & Kollbotn, L. (2014). Pressure Transient Analysis as an Element of Permanent Reservoir Monitoring. *SPE Annual Technical Conference and Exhibition* (p. 13). Amsterdam, The Netherlands: Society of Petroleum Engineers.

Shchipanov, A., Kollbotn, L., & Berenblyum, R. (2017). Integrating Pressure Transient Analysis into Histroy Matching. *79th EAGE Conference & Exhibition 2017*, (p. 5). Paris.

Shchipanov, A., Kollbotn, L., & Prosvirnov, M. (2017). Step Rate Test as a Way to Understand Well Performance in Fractured Carbonates. *SPE Europec featured at 79th EAGE Conference and Exhibition* (p. 23). Paris, France: Society of Petroleum Engineers.

Stewart, G. (2011). *Well Test Design & Analysis.* PennWell Corporation.

Stewart, G., & Gutpa, A. (1984). The Interpretation of Interference Tests in a Reservoir With Sealing and Partially Communicating Faults. *European Petroleum Conference* (p. 17). London, United Kingdom: Society of Petroleum Engineers.

Sætrom, J., Selseng, H., MacDonald, A., Kjølseth, T., & Kolbjørnsen, O. (2016). Consistent Integration of Drill-Stem Test Data into Reservoir Models on a Giant Field Offshore Norway. *SPE Annual Technical Conference and Exhibition* (p. 18). Dubai, UAE: Society of Petroleum Engineers.

Tongpenyai, Y., & Raghavan, R. (1981). The Effect of Wellbore Storage and Skin on Interference Test Data. *Journal of Petroleum Technology, 33*(01), 151-160.

Yaxley, L. M. (1987). Effect of a Partially Communicating Fault on Transient Pressure Behavior. *SPE Formation Evaluation, 2*(04), 590-598.

Zeidouni, M. (2012). Analytical model of leakage through fault to overlying formations. *Water Resources Research, 48*(12).

Appendix

Appendix A

According to the paper from Sætrom, Selseng, MacDonald, Kjølseth, & Kolbjørnsen, 2016 the reason for sharp decline at the end of the derivative is because of the viscosity difference with water and oil. The water viscosity is 1/5 of the oil viscosity and because of the difference between them, it creates this dip response when the pressure wave travels through it. This observation was tested to see if we obtained the same response. The company gave us permeability and sand thickness values from their tests, displayed in *Table 3.*The rest of the parameters are the same as in well 16/2-17S.

Permeability	38 D
Sand thickness	6m

Table 3 Initial data from the company.

Here, the mobility and diffusivity ratio are able to match the late dip in the derivative. *Figure 58* displays the results. However, the compositional radius is too short compared to what the map indicates where there is a strong presence of aquifer (*Figure 10*). Other effect could be explained.

Although the model fits with the latter part of the derivative, it does not capture the middle part very well. The model was modified with a higher permeability, to more closely match the middle part and to see how this change would affect the viscosity ratio. *Figure 59* shows the modified model. An adjustment from 0.2 to 0.05 in the mobility and diffusivity ratios had to be done to match the end of the derivative. This could indicate that the viscosity difference may not be an accurate way for describing the dip because both analysis should have more or less the same values.
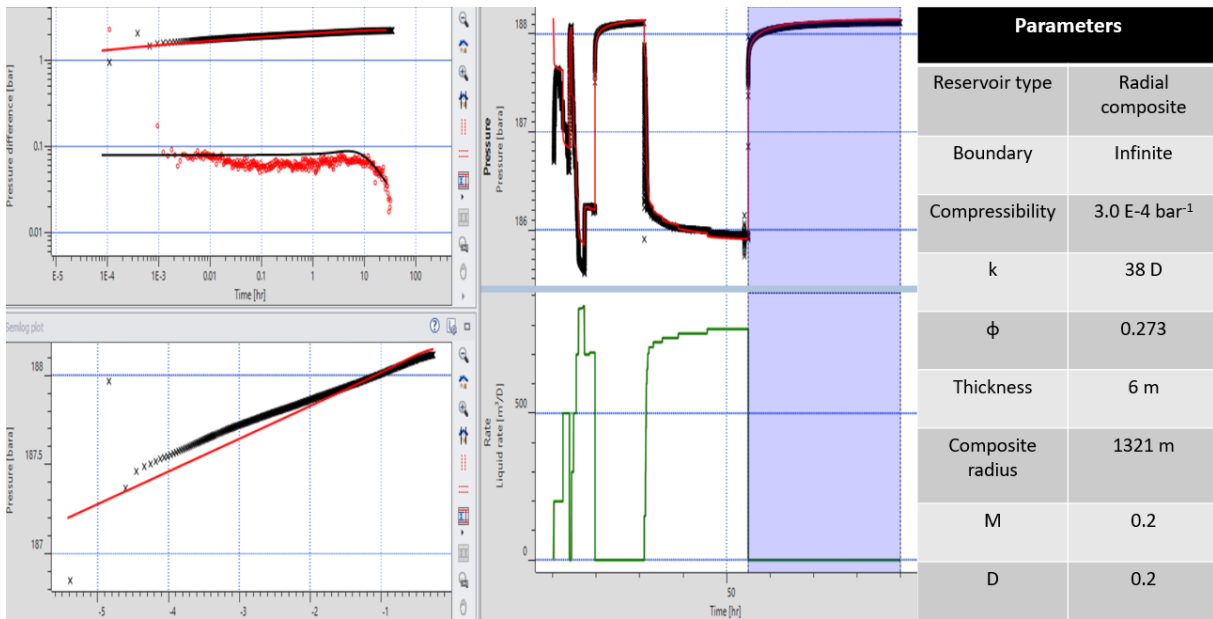
Figure 58 Model based on interpretation from (Sætrom, Selseng, MacDonald, Kjølseth, & Kolbjørnsen, 2016).
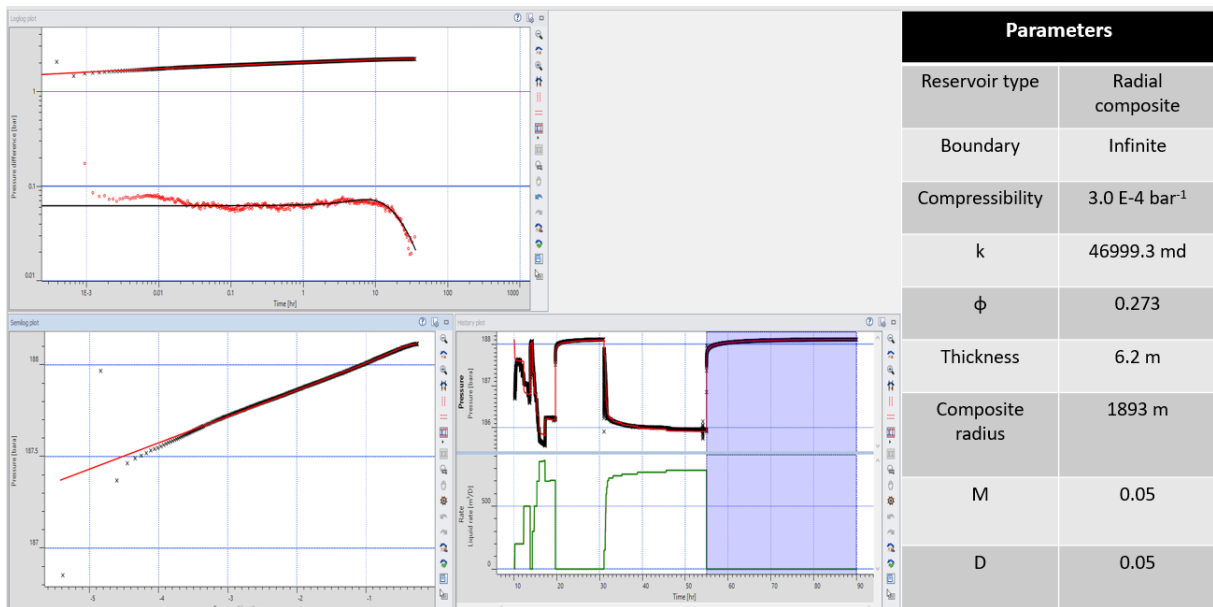
Figure 59 Same model as in figure 58 except a few parameters modified to get a better match.